UNIVERSIDADE DE SÃO PAULO
INSTITUTO DE FÍSICA DE SÃO CARLOS

CECILIA CAROLINA PINHEIRO DA SILVA

Supramolecular synthesis and characterization of new solid forms of the drugs 5-fluorocytosine and 5-fluorouracil

São Carlos
2015

CECILIA CAROLINA PINHEIRO DA SILVA

Supramolecular synthesis and characterization of new solid forms of the drugs 5-fluorocytosine and 5-fluorouracil

Thesis presented to the Graduate Program in Physics at the Instituto de Física de São Carlos, Universidade de São Paulo to obtain the degree of Doctor of Science.

Concentration area: Applied Physics
Option: Biomolecular Physics

Advisor:
Prof. Dr. Javier Alcides Ellena

Original Version

São Carlos
2015

Cataloguing data prepared by the Library and Information Service of the IFSC,
with the data supplied by the author

Silva, Cecilia Carolina Pinheiro da
Supramolecular synthesis and characterization of new solid forms of the drugs 5-fluorocytosine and 5-fluorouracil / Cecilia Carolina Pinheiro da Silva; orientador Javier Ellena -- São Carlos, 2015.
115 p.

Thesis (Doctorade - Graduate Program in Biomolecular Physics) -- Instituto de Física de São Carlos, Universidade de São Paulo, 2015.

1. Rational design. 2. Solid-state. 3. Cancer. I. Ellena, Javier , orient. II. Título.

SILVA, C .C. P. **Supramolecular synthesis and characterization of new solid forms of the drugs 5-fluorocytosine and 5-fluorouracil**. 2015. 115 p. Thesis (Doctor in Science) - Instituto de Física de São Carlos, Universidade de São Paulo, São Carlos, 2015.

ERRATA

Sheet	Line	Original text	Correction
19	**07**	**576 million**	**576 thousand**
26	**03**	**exhibit**	**observe**
27	**08**	**quite strong base**	**quite medium base**
37	**05**	**four conditions**	**five conditions**
40	**12**	**stoichiometric and nonstoichiometric 1:0.5, 2:1, 0.5:1 amounts**	**(1:0.5, 2:1, 0.5:1) amounts**
40	**18**	**stoichiometric and nonstoichiometric (1:0.5, 2:1, 0.5:1) amounts**	**1:0.5, 2:1, 0.5:1 amounts**

FOLHA DE APROVAÇÃO

Cecilia Carolina Pinheiro da Silva

Tese apresentada ao Instituto de Física de São Carlos da Universidade de São Paulo para obtenção do título de Doutora em Ciências. Área de Concentração: Física Aplicada - Opção: Física Biomolecular.

Aprovado(a) em: 16/09/2015

Comissão Julgadora

Dr(a). Javier Alcides Ellena

Instituição: IFSC/USP

Dr(a). Michael John Zaworotko

Instituição: University of Limerick/Irlanda

Dr(a). Paulo Cesar Pires Rosa

Instituição: UNICAMP/Campinas

Dr(a). Marcelo Barbosa de Andrade

Instituição: IFSC/USP

Dr(a). Renato Lajarim Carneiro

Instituição: UFSCar/São Carlos

With love, to my family

ACKNOWLEDGEMENTS

I would like to express my deep gratitude to:

- God, for sustaining and empowering me all the time.

- My parents, Alcir and Marta, for their love and unconditional encouragement, and for taking care and teaching Davi when I was not able to be with him.

- My husband Elvis, for giving me the best gift in the world, for holding my hand and walking with me every day in the joys and sorrows, in the victories and defeats, and sharing in the parenthood of our son.

- My son, Davi, for the privilege of becoming a mother. Every single smile from you gave me the necessary strength to be able to get here.

- My sister-in-law, Leticia, for her incredible help with Davi and with our home.

- My mother-in-law Luiza and my half brother "Tato", for encouraging me even not knowing exactly what I was researching.

- Prof. Dr. Javier Ellena, for sharing his experience and knowledge, for his guidance, and for his confidence in me. I am also extremely grateful because he allowed me to continue my research while also allowing me to be present in Davi's life. Lastly, I am also thankful for his friendship and for that of his family: Andrea, Micaela, Matias, and Mercedes.

- Prof.º Dr. Alejandro Ayala and Sara for all the collaboration during these years.

- People of room 25: Cristiane, Rebeka, and Larissa, for friendship. Paulo, Juan, Mariane, Talita and Richard, for companionship.

- The Crystallography Group of the IFSC, specially Augusto.

- The librarians, specially Neusa and Cris.

- The postgraduate service, specially Silvio, Ricardo, and Patrícia.

- Everyone who contributed to this project directly or indirectly. A special thanks to my friend Mariana B. Garcia, for always helping with my English corrections.

- CAPES for financial support.

The LORD will fulfill his purpose for me;
your steadfast love, O LORD, endures forever.
Do not forsake the work of your hands.
Psalm 138:8 – of David (English Standard Version)

ABSTRACT

SILVA, C .C. P. **Supramolecular synthesis and characterization of new solid forms of the drugs 5-fluorocytosine and 5-fluorouracil**. 2015. 115 p. Thesis (Doctor in Science) - Instituto de Física de São Carlos, Universidade de São Paulo, São Carlos, 2015.

For active pharmaceutical ingredients (APIs) exhibiting low solubility and/or stability and/or dissolution profiles, among other problems capable of affecting their therapeutic efficacy, Crystal Engineering approaches have been highlighted in recent decades as a satisfactory solution. In the solid state, APIs may exhibit polymorphs, salts, solvates, hydrates, cocrystals, amorphous and combinations of them. Associated to each solid form are physical and chemical properties which may or not vary in relation to the reference API. In this context, this research project aimed to rationally design, synthesize and characterize new solid forms of the prodrug 5-fluorocytosine (5-FC) and the antineoplastic drug 5-fluorouracil (5-FU), by considering that both exhibit physicochemical issues that difficult their application in solid dosage forms. Although used as a fungicide, 5-FC has become one of the most used prodrugs for cancer treatment by gene-directed enzyme prodrug therapy, as in the presence of the enzyme cytosine deaminase, 5-FC is converted into 5-FU inside cancer cells. For this purpose, suitable coformers were pre-selected from statistical analyses performed on the Cambridge Structural Database, based on the synthon competition approach. Briefly, crystallization protocols were designed following two techniques: slow evaporation from solution and mechanochemistry, in particular the solvent-drop grinding (SDG). Nine structures were obtained with 5-FC. All were analyzed by polarized light optical microscopy and by single-crystal X-ray crystallography. Six were characterized as cocrystals and three as salts. Pharmaceutical salts are preferred in formulations because they considerably improve the solubility/stability of APIs. Cocrystals have been increasingly explored because they promote improvements in the physicochemical properties of the API while not altering the API's nature. 5-FC salts were obtained with fumaric, oxalic, and maleic acids, and 5-FC cocrystals with adipic, terephthalic, malic, succinic, and benzoic acids. In addition, a multi-API cocrystal of 5-FC and 5-FU was obtained. These results, derived from the rational design of new solid forms, agreed well with the rule of three, implemented to variations in pKa values (pKa_{base} - pKa_{acid}). This rule allows for estimation of the salts/cocrystals formation during the crystallization process. The 5-FC salts were structurally and thermally analyzed. The 5-FC's cocrystals were structurally evaluated. The multi-API co-crystal was also synthesized by SDG as part of the ongoing efforts toward Green Chemistry application for drug scale-up production. The results obtained in this thesis offer a strong API candidate to be used as a coformer, namely the 5-FC, and introduce a multi-API co-crystal as a potential candidate for anticancer therapy.

Keywords: Rational design. Solid-state. Cancer.

RESUMO

SILVA, C. C. P. **Síntese supramolecular e caracterização de novas formas sólidas dos fármacos 5-fluorocitosina e 5-fluorouracila**. 2015. 115 p. Tese (Doutorado em Ciências) - Instituto de Física de São Carlos, Universidade de São Paulo, São Carlos, 2015.

Para os ingredientes farmacêuticos ativos (APIs) que exibem baixa solubilidade e/ou estabilidade e/ou perfis de dissolução, dentre outros problemas capazes de afetar a sua eficácia terapêutica, as abordagens da Engenharia de Cristais têm se destacado nas últimas décadas como uma solução satisfatória. No estado sólido, os APIs podem apresentar polimorfos, sais, solvatos, co-cristais, amorfos e combinações dos mesmos. Associadas a cada estado sólido estão propriedades físicas e químicas, que podem ou não variar em relação ao API de referência. Neste contexto, este projeto de pesquisa visou o planejamento racional, síntese e caracterização de novas formas sólidas do pró-fármaco 5-fluorocitosina (5-FC) e do fármaco antineoplásico 5-fluorouracila (5-FU), ambos exibindo problemas fisicoquimicos que dificultam sua aplicação em formas de dosagem sólidas. Apesar de ser usado como fungicida, recentemente o 5-FC se tornou um dos pró-fármacos mais utilizados na terapia antineoplásica por meio de terapia dirigida por gene-enzima-pró-fármaco, uma vez que na presença da enzima citosina-desaminase o 5-FC é convertido em 5-FU dentro das células cancerosas. Para esta finalidade, coformadores adequados foram pre-selecionados a partir de análises estatísticas, realizadas utilizando o banco de dados estruturais da Cambridge, com base na competição entre sintons. Na sequencia, protocolos de cristalização foram desenvolvidos de acordo com duas técnicas: evaporação a partir de solvente e mecanoquímica, em particular a moagem com gota-solvente (SDG). Nove estruturas foram obtidas com 5-FC. Todas foram analisadas por microscopia óptica de luz polarizada e por difração de raios X por monocristal. Seis foram caracterizadas como co-cristais e três como sais. Sais farmacêuticos são preferidos nas formulações porque melhoram consideravelmente a solubilidade dos APIs. Co-cristais farmacêuticos têm sido cada vez mais explorados porque promovem igualmente melhorias nas propriedades físico-químicas dos APIs sem alterar a natureza dos mesmos. Os sais de 5-FC foram obtidos com os ácidos fumárico, oxálico e maleico e os cocristais com os ácidos adípico, tereftálico, málico, succínico e benzóico. Além disso, obteve-se um co-cristal multi-API, de 5-FC e 5-FU. Estes resultados, obtidos por meio do desenho racional de novas formas sólidas, concordaram bem com a regra de três, implementada para variações nos valores pKa (pKa_{base} - $pKa_{ácido}$). Esta regra permite estimar a formação sais/co-cristais durante o processo de cristalização. Os sais de 5-FC foram analisados estrutural e termicamente. Os cocristais de 5-FC foram estruturalmente avaliados. O co-cristal multi-API também foi sintetizado por mecanoquímica, como parte dos esforços direcionados à aplicação dos princípios da Química Verde para a produção em larga escala de fármacos. Os resultados obtidos nesta tese oferecem um API como forte candidato a coformador, a saber a 5-FC, e introduz um co-cristal multi-API como potencial candidato para a terapia antineoplásica.

Palavras-chave: Planejamento racional. Estado sólido. Cancer.

LIST OF ABREVIATIONS AND ACRONYMS

5-FC	5-Fluorocytosine
5-FU	5-Fluorouracil
API	Active Pharmaceutical Ingredient
CCD	Charge Coupled Device
CCDC	Cambridge Crystallographic Data Centre
CD	Cytosine deaminase
CE	Crystal engineering
CSD	Cambridge Structural Database
DNA	Deoxyribonucleic acid
DPD	Dihydropyrimidine dehydrogenase
DSC	Differential Scanning Calorimetry
EBRT	External-beam radiotherapy
FDA	Food and Drug Administration
GDEPT	Gene-directed enzyme prodrug therapy
GRAS	Generally Regarded As Safe
HPLC	High performance liquid chromatography
IARC	International Agency for Research on Cancer
INCA	National Cancer Institute José Alencar Gomes da Silva
IR	Infrared Spectroscopy
MN	Malignant neoplasm
PLM	Polarized Light Optical Microscopy
PXRD	X-Ray Powder Diffraction
RCBP	Population-Based Cancer Registries
SC	Supramolecular chemistry
SC-PXRD	Single-Crystal X-ray Diffraction
SDG	Solvent-Drop Grinding
SES	Slow Evaporation of Solvent
SUS	Unified Health System
TGA	Thermal Gravimetric Analysis
TPLM	Thermal Polarized Light Microscopy
WHO	World Health Organization

CONTENTS

1 INTRODUCTION

Cancer has one of the highest mortality rates in Brazil and in the world.[1] Using cancer mortality statistics recorded by the World Health Organization (WHO), the International Agency for Research on Cancer (IARC) estimated 14,1 million new cases and 8,2 million deaths due to this disease worldwide in 2012.[2] By 2030 it is expected that the number of new cases will rise to above 75%, bringing the number of cancer cases close to 25 million.[3] In Brazil, the 2014/2015 estimate of cancer incidence published by the National Cancer Institute José Alencar Gomes da Silva (INCA) indicates the occurrence of 576 million new cases. [4] Prostate and lung cancers were the most commonly identified cancers in men, while breast and cervical cancers were the most common ones in women, second only to non-melanoma skin cancer (182,000 new cases).[4] It is evident that there is a need for investment in effective actions to control and treat cancer at all levels of expertise.

The application of solid-state technologies to the development of active pharmaceutical ingredients (API) with improved properties has been highlighted in recent years as one of the contemplated research lines of pharmacy.[5-6] Making use of these technologies, this thesis focused in the development of new solid forms of drugs utilized to treat cancer. The choice for solid forms was made by considering that dosages in the solid state are one of the most desirable delivery systems for cancer patients, ensuring them a better quality of life.[7]

The specific goals of this research project were rationally design and supramolecularly synthesize salts and/or cocrystals of the clinically used antineoplastic drug 5-fluorouracil and the prodrug 5-fluorocytosine. As vehicles to achieve these goals, supramolecular chemistry and Crystal Engineering techniques were applied in combination with statistical analysis of structural information performed in the Cambridge Structural Database (CSD), making it possible to select cocrystallizing agents (coformers) containing complementary chemical features and functional groups that maximize their interaction with the antineoplastic drugs' molecules. This rational strategy is being explored in the last decades once it enables a quite accurate crystal structure prediction based on structural information, which in turn directs the design of the experiments. In addition, the preselected non-APIs' coformers should be within libraries of pharmaceutically accepted compounds, in particular into the list of compounds generally regarded as safe for use in pharmaceutical formulations (GRAS). This GRAS list is published/updated by the Food and

Drug Administration (FDA), a federal agency of the United States of America responsible for protecting and promoting public health. [8-10]

Once the coformers were selected, different protocols were designed in the search for new solid modifications of the antineoplastic APIs. Combinations of the APIs and of the coformers with the APIs using different solvents were subjected to the crystallization protocols. The main crystallization technique implemented for such experiments was the slow evaporation of solvent (SES). Experiments were conducted under different temperatures and solvents (single or binary mixtures).[11-12] Moreover, following the principles of Green Chemistry, the solid-state grinding technique was also applied, in particular the solvent-drop grinding (SDG) method.[13] Finally, the resulting compounds were analyzed by several solid-state characterization techniques such as polarized light optical microscopy (PLM), thermal polarized light microscopy (TPLM), powder x-ray diffraction (PXRD), single crystal X-ray diffraction (SC-XRD), vibrational infrared spectroscopy (IR), Raman spectroscopy, thermal gravimetric analysis (TGA) and differential scanning calorimetry (DSC).

1.1 Cancer or malignant neoplasm

Cancer, the Latin word for crab, derives from the Greek *karkinos*. It is credited to the Greek physician Hippocrates (460-370 BC), who observed the finger-like spreading projections of this disease. Nowadays, the scientific definition of cancer is malignant neoplasm (MN, from the Latin *male* = evilly and *gnus* = born, and the Greek *neo* = new and *plasma* = formed, molded), referring to a newly formed part of the body, *i.e.*, a tumor, which is evil by nature. The MN is characterized by an uncontrolled growth of cells. Proliferating quickly and abnormally, these cells may spread to other parts of the body (metastasis), invading tissues and organs in a fashion that can lead to the organism's death.[14-18]

The disease is currently known to be genetic, resulting from the progressive accumulation of changes in the genetic material of a cell. In other words, MN can be considered a cellular illness. Each cell in the body has a function coordinated by its genetic material. In this way, the integrity of a given tissue results from a balance between cell proliferation and cell death, all mediated by a complex intra and extracellular signaling system. If a balance loss occur, cells may

have their activity changed, become no longer functional, and may exhibit particular behaviors if not eliminated by the apoptosis process. Among these behavior is uncontrolled replication, which could ultimately lead to the formation of a MN. [19-20]

Currently, cancer treatment is performed through surgery, radiation therapy, bone marrow transplantation, immunotherapy, hormonal therapy, and chemotherapy. The treatment type depends not only on location, tumor level, and stage of the disease, but also on the general health of the patient. [19-21] In theory, all cancers can be cured if entirely removed by surgery. However, this is not always an achievable goal; when the cancer has metastasized, complete surgical excision is usually impossible. Radiation therapy uses ionizing radiation to kill cancer cells and shrink tumors. It can be performed by external-beam radiotherapy (EBRT) or internally via brachytherapy. The effects of radiation therapy are local and confined to the region under treatment. Radiation acts on the genetic material of cancer cells, stopping their growth and replication.[21-22]

The bone marrow is one of the largest and most important organs of the body. It consists of a soft sponge-like material occupying the interior tissue of the bones, responsible for the continuous supply of platelets as well as red and white blood cells. It is essential for oxygenation, coagulation, and immunity in the body. For some diseases that affect blood cells, such as leukemia and lymphoma, bone marrow transplantation is a proposed treatment. The bone marrow transplantation can be considered a type of immunotherapy. New immune treatments have been established and all attempt to utilize the immune system to induce targeted antitumor responses. In addition, hormone therapy is being used to treat breast and prostate cancer, since these types of cancer respond to endocrine manipulation.[20,23-26]

Finally, chemotherapy is utilized to treat cancer through the use of chemicals able to destroy cancer cells (antineoplastic drugs or “against new growth” drugs).[21] As chemotherapeutic agents are the focus of this thesis, they are discussed in the next section.

1.2 Antineoplastic drugs

Cancer chemotherapy began with the discovery of mustards, synthesized in 1854 by the French chemists Cesar-Mansuete Despretz and Alfred Riche. First, a simple sulfur mustard gas

(Figure 1a), bis(2-cloroethyl)sulfide, was introduced during World War I as a chemical warfare agent. Once in contact with the body, even in very low concentrations, this gas caused severe irritation in the respiratory tract (if inhaled) and eyes, in addition to slow-healing chemical burns. At the time, autopsy observations revealed that mustard gas had provoked bone marrow aplasia and lymph node depletion. During the interwar years, several derivatives of mustard gas were synthesized and described. Medical research performed in the 1940's showed that nitrogen mustards (Figure 1b) were suitable candidates for clinical use as alkylating agents in the treatment of human cancer. In 1942 the first clinical trials with nitrogen mustards were performed, opening the doors to the modern era of chemotherapy.[21,27-29]

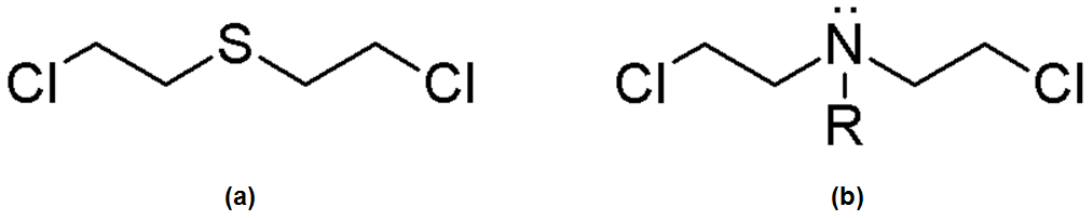

Figure 1 - Generalized chemical structure of (a) sulfur mustards and (b) nitrogen mustards.
Source: By the author

Most antineoplastic drugs interfere with the cell division process. The cell cycle (Figure 2) comprises two periods: nonproliferating (quiescence, G0) and proliferating (active). The latter is divided into four phases named G1 (growth 1), S (DNA synthesis), G2 (growth 2) and M (mitosis). The growth phases provide the necessary elements required for the following ones. The intersection between G1/S and G2/M are the major checkpoints in the cell cycle in which possible mutations can be detected and replaced (or not, in the case of cancerous cells). The checkpoints appear to be controlled by a number of extracellular hormones, cytokines, and growth factors, all regulated by signaling pathways. Cancer cells may overexpress these key components, resulting in higher replication rates when compared with normal cells and leading to a signaling cascade. In turn, these events provide a variety of targets for chemotherapy. Unfortunately, fast proliferating healthy cells are also attacked by the chemotherapeutic agents, due the drugs' low selectivity. This may generate several side effects, such partial or total loss of hair and impairment of the immune system. [21,30-31]

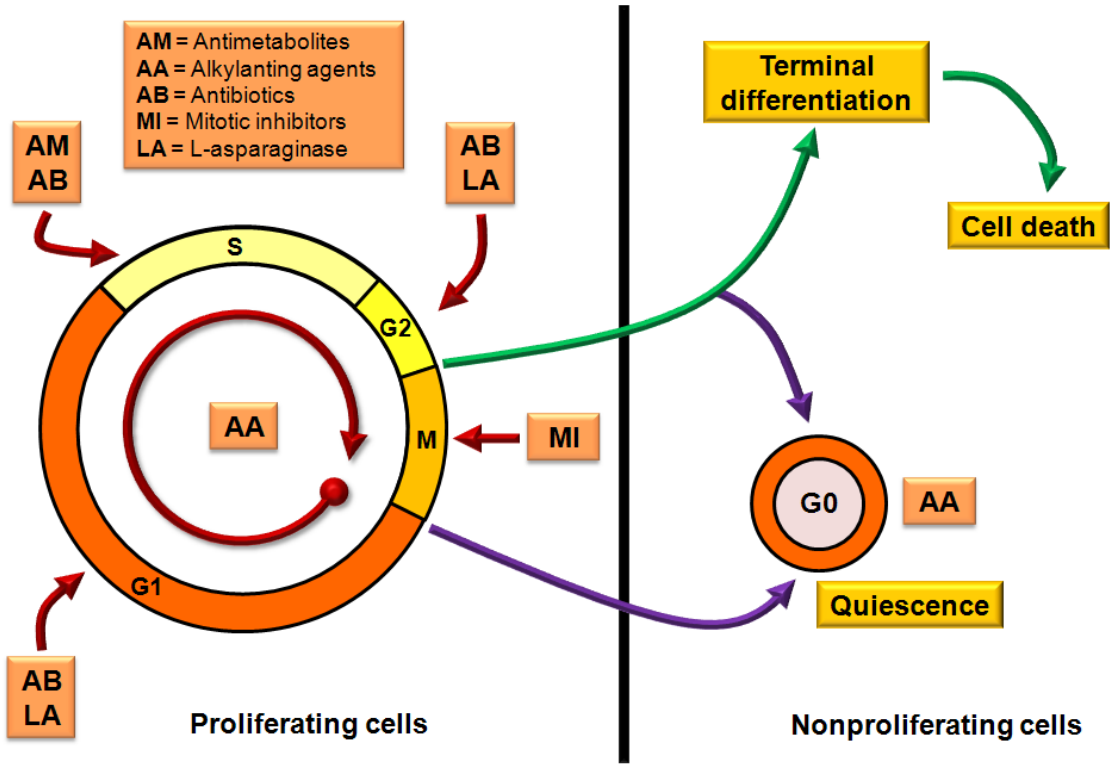

Figure 2 - Cell cycle evidencing the site of action of some different antineoplastic drugs.
Source: Adapted from CALLERY; GANNETT.[21]; LANORE; DELPRAT.[31]

Chemotherapeutic agents (Table 1) can be divided into several groups, according to their mode of action: (1) alkylating, which add alkyl groups especially to nucleic acids, preventing duplication in any stage of the cell cycle, (2) antimetabolites, which structurally mimic compounds naturally found in the body and affect the biosynthesis of essential constituents of nucleic acids, (3) antitumor antibiotics, substances with diverse chemical structure that inhibit nucleic acid or protein synthesis, (4) mitotic inhibitors, which paralyze mitosis at the metaphase, (5) topoisomerase inhibitors, which paralyze the separation of DNA strands, preventing them from being copied, (6) steroid hormones, which also help to prevent chemotherapy side effects such as nausea and vomiting, and (7) monoclonal antibodies, which identify and react with specific antigens produced by cancer cells. It is worth noting that there are some antineoplastic drugs that do not fit well into any of the groups, such as L-asparaginase (Figure 2), which is an enzyme. Often two or more types of drugs are co-administered (combined chemotherapy), allowing for the use of a drug cocktail that acts on different parts of the cells' metabolic

processes and increasing the likelihood of cancer cell extinction. Furthermore, toxic side effects of chemotherapy can be reduced by combining drugs with different toxicities, enabling each to be administered at a lower dose than that required if they were administered alone.[32-34]

Table 1 - Key antineoplastic drugs from each chemotherapeutic group.

Chemotherapeutic agents	Drugs
Alkylating	Mechlorethamine, Chlorambucil, Cyclophosphamide, Ifosfamide, Melphalan, Streptozocin, Carmustine, Lomustine, Busulfan, Dacarbazine, Temozolomide, Thiotepa, Altretamine, Cisplatin*, Carboplatin*, Oxalaplatin*
Antimetabolites	5-Fluorouracil (5-FU), 5-Fluorocytosine (5-FC)**, 6-Mercaptopurine, Capecitabine, Cladribine, Clofarabine, Cytarabine, Floxuridine, Fludarabine, Gemcitabine, Hydroxyurea, Methotrexate, Pemetrexed, Pentostatin, Thioguanine
Antitumor antibiotics	Daunorubicin, Doxorubicin, Epirubicin, Idarubicin, Actinomycin-D, Bleomycin, Mitomycin-C, Mitoxantrone
Mitotic inhibitors	Paclitaxel, Docetaxel, Ixabepilone, Vinblastine, Vincristine, Vinorelbine, Estramustine
Topoisomerase inhibitors	Topotecan, Irinotecan, Etoposide, Teniposide, Mitoxantrone
Steroids hormones	Anastrazole, Exemestane, Letrozole, Tamoxifen, Leuprolide, Goserelin, Flutamide, Bicalutamide, Prednisone, Methylprednisolone, Dexamethasone
Monoclonal antibodies	Rituximab, Trastuzumab, Bevacizumab, Alemtuzumab, Panitumumab, Tositomab, Gemtuzumab, Ibritumomab tiuxetan

***** *platinum drugs; ** this API is a 5-FU's prodrug*

Source: Adapted from AMERICAN…[34]

The majority of commercially available antineoplastic drugs are administered by parenteral route. A small portion, about 20, can be orally administered. It has been observed that only a fraction of the oral drugs' originally administered amount becomes available in the systemic circulation (bioavailability), so that their response is considered to be low (e.g. 5-20% for paclitaxel, docetaxel, doxorubicin). Regardless of their low bioavailability, oral delivery of antineoplastic drugs has gained major focus in the last decades, not only due to patient compliance, but because solid dosages are the most convenient, safe, and cheap way to deliver an API. [35] Of the orally administered antineoplastic drugs, two were chosen for this study: 5-FU and

the prodrug 5-FC (Table 1). These drugs were chosen mainly due their variable bioavailability profiles and physical stability, respectively.[36-37]

5-fluoro-2,4-(1H,3H)- pyrimidinedione, abbreviated as 5-FU (Figure 3), is a synthetic pyrimidine analog first synthezised in 1957.[38] It acts by inhibiting thymidylate synthase, which is essential for the production of thymine, one of the nitrogenous bases of DNA. It is probably one of the most used cancer treatment antimetabolites and can target several types of cancers, such as gastrointestinal, head and neck, breast, colorectal, and ovarian.[36] Despite its intense use, 5-FU's absorption is limited by the activity of the enzyme dihydropyrimidine dehydrogenase (DPD).[39] Literature reports its extensive ability of forming polymorphs, solvates, and cocrystals, having a total of 20 structures determined (Table 2).[40-56] This versatility can be attributed to the multiple N-H donors and C=O acceptors, which leads to a diversity of hydrogen bonding motifs and to the 5-FU's small size, which allows its incorporation into the crystalline lattices of other molecules. The first structure of anhydrous 5-FU (Form I) was determined in 1973, obtained after rapid dissolution of the drug in warm water yielding, after evaporation, large crystals crystallized in the triclinic $\bar{1}$ space group with a = 9.22(3) Å, b = 12.66(3) Å, c = 12.67(3) Å, α = 89.70(3)°, β = 43.90(3)° and γ = 98.60(3)°.[40]

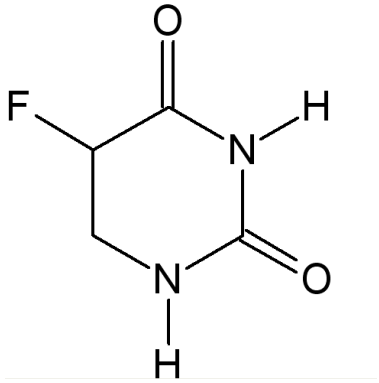

Figure 3 - Molecular structure of 5-FU.
Source: By the author.

Table 2 - Reported crystalline structures of 5-FU.

Year	Compound	Space group	Form
1967[41]	5-FU with 9-ethylhypoxanthine	$P2_1/c$	Cocrystal
1969[42]	5-FU with e cytosine	$\bar{1}$	Cocrystal
1969[43]	5-FU with 1-methylcytosine	Pbca	Cocrystal
1995[44]	5-FU with theophylline	$P2_1/c$	Cocrystal
2004[45]	5-FU with 1,4-dioxane	$\bar{1}$	Solvate
2004[46]	5-FU with dimethylformamide	$P2_1/n$	Solvate
2004[47]	5-FU with dimethyl sulfoxide	$P2_1/c$	Solvate
2005[48]	5-FU with 2,2,2-Trifluorethanol	$P2_1$	Solvate
2005[49]	Form II of 5-FU	$P2_1/c$	Polymorph
2006[50]	5-FU with thymine	C2/c	Cocrystal
2006[51]	5-FU with coper(II) complex and 1,10-fenantroline	$\bar{1}$	Cocrystal
2007[52]	5-FU with cytosine monohydrate	$\bar{1}$	Hydrated cocrystal
2008[53]	5-FU with benzonitrile	$P2_1/c$	Solvate
2008[53]	5-FU with formamide	$P2_1/m$	Solvate
2012[54]	Form III of 5-FU	$\bar{1}$	Polymorph
2013[55]	5-FU with acridine	$\bar{1}$	Cocrystral
2013[55]	5-FU with phenazine	$\bar{1}$	Cocrystal
2013[55]	5-FU with 4,4-bispyridylethene	$P2_1/c$	Cocrystal
2014[56]	5-FU with 4-hydroxybenzoic acid	$\bar{1}$ and $P2_1/c$	Cocrystal

Source: By the author

5-Fluorocytosine (5-FC, Figure 4), 4-amino-5-fluoro-1,2-dihydropyrimidin-2-one, was also synthesized in 1957 as an antimetabolite to be used in the antineoplastic therapy. However, at the time, 5-FC didn't exhibit cytotoxic activity against cancerous cells. In 1961, experiments revealed that 5-FC was active in killing *Candida* spp. and *Cryptococcus neoformans*. Seven years later it was released as an antifungal agent. Although 5-FC is still widely used to treat fungal infections, in combination with ketoconazole, fluconazole and itraconazole, special interest in this compound emerged as a result of its mechanism of action and advances in biotechnology. In fungal cells, 5-FC is deaminated by the enzyme cytosine deaminase (CD) into 5-FU. Thus, 5-FC can be considered a 5-FU's prodrug. In 1985, Nishyama and co-workers introduced 5-FC in combination with CD for cancer treatment expecting that "*if 5-FC is delivered to the tumor bed, in which CDase in immobilized form has previously been implanted surgically, ... then antineoplastic activity would develop at the local site with minimal systemic toxicity"*. The success in this first experiment combined with the development of gene-directed enzyme prodrug

therapy (GDEPT) turned 5-FC in one of the most used prodrug for cancer treatment, in particular for breast and prostate. In GDEPT, transgenes encoding enzymes capable of converting prodrugs into active metabolites are utilized. [57-63]

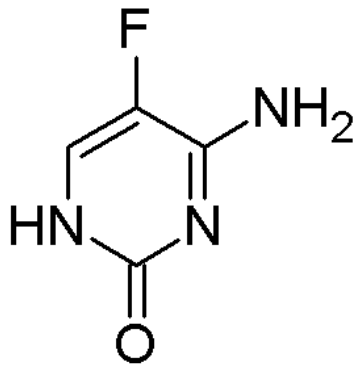

Figure 4 - Molecular structure of 5-FC.
Source: By the author

In 1982 the first crystal structure of 5-FC was reported, consisting of a monohydrate crystallized in the monoclinic space group $P2_1/c$, with cell parameters a = 7.562(8) Å, b = 9.390(8) Å, c = 21.361(12) Å and β = 125.13(10)º [64]. After that, a total of 33 structures were reported, including polymorphs, salts, co-crystals and solvates/hydrates (Table 3)[37,64-74]. 5-FC is a quite strong base (pKa = 3.26) and therefore its imine nitrogen tends to be protonated in the presence of acids, resulting in salt formation, which is not observed for 5-FU. Although 5-FC exhibits high water solubility and permeability, its development into a tablet product is not trivial considering that humidity variations can lead to interconversion between anhydrous and hydrate forms.[57-59, 37]

Table 3 - Reported crystal structures of 5-FC.

Year	Compound	Crystalline system	Form
1982[64]	5-FC, water	$P2_1/c$	Monohydrate
2001[65]	5-FC, salicylic acid	$P2_1/n$	Salt
2005[66]	5-FC, water	$P\bar{1}$	Hydrate
2006[67]	5-FC, water	$P2_1/c$	Monohydrate
2006[68]	5-FC	$P2_1/n$	Polymorph
2006[68]	5-FC	$P4_12_12$	Polymorph
2006[68]	5-FC, water	$P\bar{1}$	Monohydrate
2006[68]	5-FC, water	$P2_1/c$	Monohydrate
2006[68]	5-FC, water	$P2_1/c$	Hydrate
2006[68]	5-FC, trifluoroethanol	$P2_1/c$	Solvate
2006[68]	5-FC, methanol	$P2_1/n$	Solvate
2007[69]	5-FC, water, HCl	$P2_1/n$	Hydrated salt
2009[70]	5-FC, water	Cc	Hemihydrate
2009[70]	5-FC, dimethylacetamide	$P\bar{1}$	Solvate
2009[70]	5-FC, dimethylsulfoxide	$P2_1/c$	Solvate
2011[71]	5-FC, water, 5-nitrouracil	Cc	Hydrated cocrystal
2012[72]	5-FC, 2-aminopyrimidine	$P\bar{1}$	Cocrystal
2012[72]	5-FC, N-acetylcreatinine	$P\bar{1}$	Cocrystal
2012[72]	5-FC, 3-aminouracil	C2/c	Cocrystal
2012[72]	5-FC, water, 6-aminocytosine	$P\bar{1}$	Hydrated cocrystal
2012[72]	5-FC, 6-aminocytosine, N,N-dimethylfomamide	$P\bar{1}$	Solvated cocrystal
2012[72]	5-FC, 6-aminocytosine, N,N-dimethylformamide	$P\bar{1}$	Solvated cocrystal (polymorph-1)
2012[72]	5-FC, 6-aminocytosine, N,N-dimethylfomamide	$P\bar{1}$	Solvated cocrystal (polymorph-2)
2012[72]	5-FC, acyclovir	$P2_1/c$	Cocrystal
2012[73]	5-FC, biuret, dimethylsulfoxide acid	$P\bar{1}$	Solvated cocrystal
2012[73]	5-FC, 6-acetamidouracil, dimethylsulfoxide acid	$P\bar{1}$	Solvated cocrystal
2012[73]	5-FC, 6-aminocytosine	$P\bar{1}$	Solvated cocrystal
2012[73]	5-FC, water, 6-methylcytosine	$P\bar{1}$	Hydrated cocrystal
2013[37]	5-FC, methanol, saccharin	$P2_1/m$	Solvated salt
2013[37]	5-FC, nitric acid	$P2_1/c$	Salt
2013[37]	5-FC, hydroiodic acid	$P\bar{1}$	Salt
2013[37]	5-FC, hydrobromic acid	C2/c	Salt
2013[74]	5-FC, water, HCl	$P2_1/c$	Hydrated salt (polymorph)

Source: By the author.

1.3 Supramolecular Chemistry and Crystal Engineering applied to APIs

The concept of Supramolecular Chemistry (SC) was introduced by the French chemist Jean-Marie Lehn in the 1970's, driven by his attempt to understand the processes that occur in the nervous system. By considering molecular chemistry as the "*chemistry of the covalent bond*", Lehn defined SC as the "*chemistry beyond the molecule, bearing on the organized entities of higher complexity that result from the association of two or more chemical species held together by intermolecular forces*". His definition was tied to the processes of molecular recognition occurring in biological systems, where the binding of a substrate to its receptor yielded the so-called supermolecule. If properly handled, target molecules capable of interacting with high efficiency and selectivity with the receptors could be designed and synthesized.[75] In the early 1990's, structural chemists and crystallographers realized that "*a crystal of an organic compound is the perfect supermolecule, an assembly of literally millions of molecules self-crafted by mutual recognition at an amazing level of precision*".[76]

At the same time, worried about the need of a general and simple method for categorizing hydrogen-bond patterns in organic compounds, the chemist Margaret C. Etter introduced rules for hydrogen-bond formation of organic compounds and the graph-set notation, a notable analytical method later extended by the chemists Joel Bernstein, John C. MacDonald and Raymond E. Davis. Etter's work launched the first movements toward the possibility of predicting crystalline structures which is one of the most desired skills by pharmaceutical scientists. Briefly, Etter's introduced three rules for hydrogen-bond formation in neutral organic molecules: (1) All good proton donors and acceptors are used in hydrogen bonding, (2) Six-membered-ring intramolecular hydrogen bonds form in preference to intermolecular hydrogen bonds, and (3) The best proton donors and acceptors remaining after intramolecular hydrogen-bond formation form intermolecular hydrogen bonds to one another. Concerning the graph-set notation, this method allows the analysis of complex hydrogen-bond patterns that may be reduced to combinations of four simple motifs (Figure 5): intramolecular hydrogen bonds (S), infinite chains (C), rings (R), noncyclic dimers and other finite patterns (D). The graph set notation is specified by four

parameters and have the general form , with G being the pattern designator (*ie*, S, C, R or D), *d* being the number of donors, *a* the number of acceptors and *r* the degree, referring to the number of atoms involved in the hydrogen-bonding motif, including H atoms. When *d* or *a* are equal to 1, they can be omitted in the notation. The same applies when *n* is equal to 1 in designators assigned as D.[77-80]

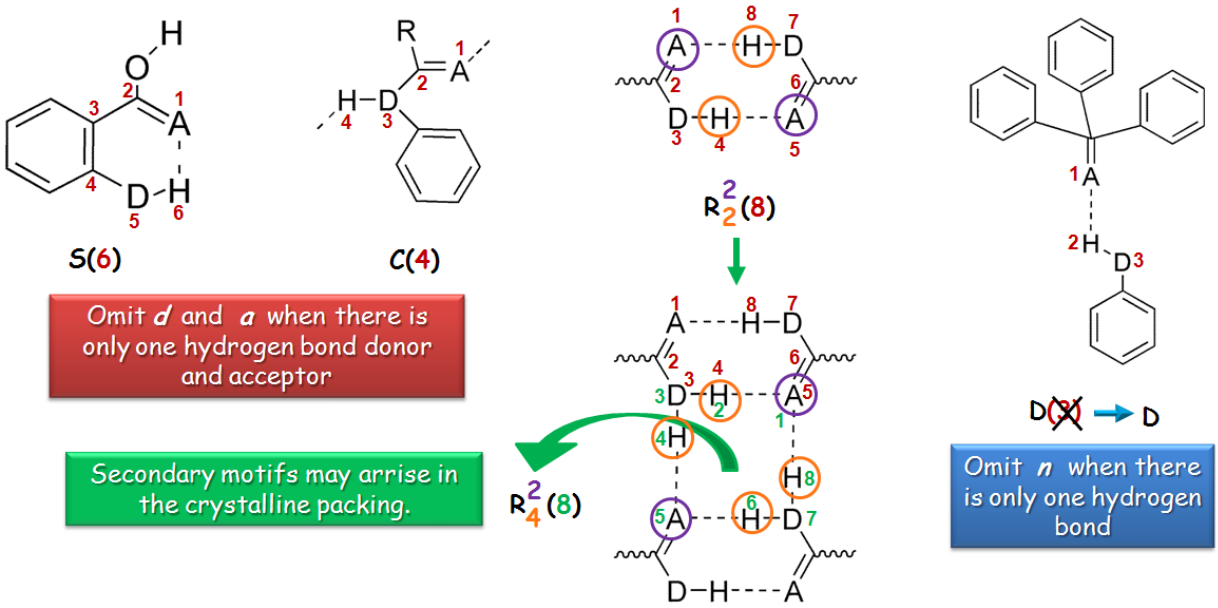

Figure 5 - Examples of motifs and the respective graph-set assignments
Source: By the author

A few years later, in 1995, by considering that Crystal Engineering (CE) dealed with "*the understanding of intermolecular interactions in the context of crystal packing and in the utilization of such understanding in the design of new solids with desired physical and chemical properties*", the Indian researcher Gautam R. Desiraju introduced the concept of "*supramolecular synthons*" (Figure 6). At the time, the American chemist Elias J. Corey had already introduced the term "synthon" as "…*structural units within molecules which can be formed and/or assembled by known or conceivable synthetic operations*". Extending the reasoning from a molecule to a supermolecule, Desiraju addressed the term to the fairly predictable spatial arrangement of the intermolecular interactions responsible for organizing the molecules in the crystal lattice. For the rational design of targets in organic synthesis, O-H•••O and N-H•••O

hydrogen bonding were commonly used as the supramolecular cement together with weaker forces such as C-H•••O, C-H•••N, C•••H, C•••C, halogen•••halogen, O•••halogen, N•••halogen.[76,81-82]

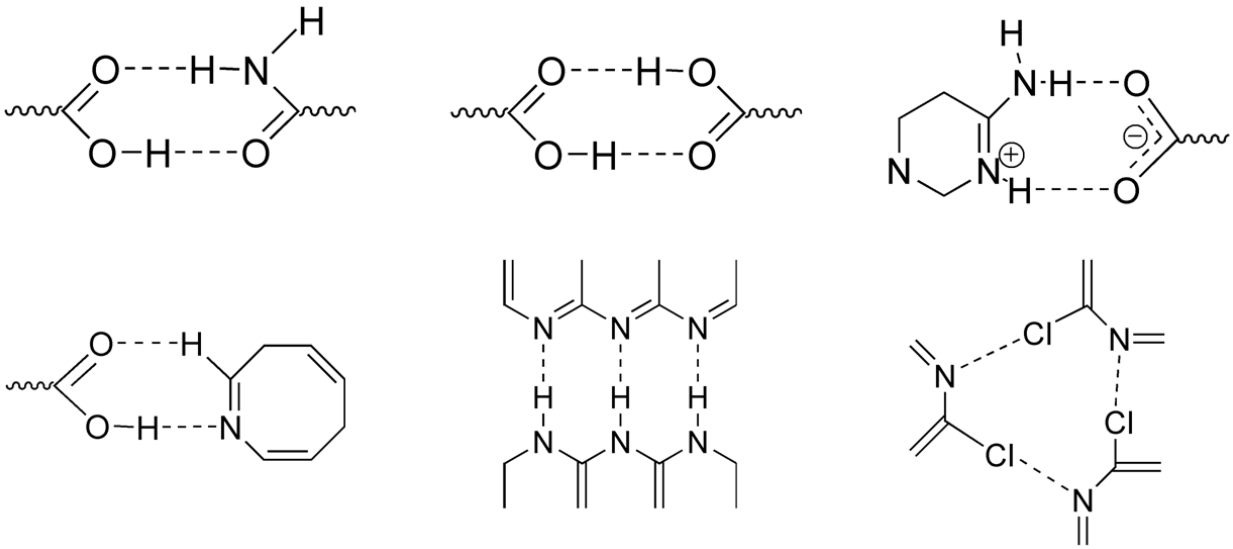

Figure 6 - Some supramolecular synthons.
Source: By the author

In the last 20 years, the growth of CE coincided with remarkable advances in the determination of crystal structures. The availability of these structural data, coupled with their effective collection and distribution via the CSD[9], has led to significant progress in the understanding and control of the interaction processes between molecules in the crystalline state.[83] Indeed, the access to a collection of molecular structures is a crucial requirement for application of the supramolecular synthon (also referred as motif or pattern) approach. In this sense, the Cambridge Crystallographic Data Centre (CCDC) launched in 2002 a tool named *Mercury*[84] which allows the visualization and investigation of the crystalline structures deposited in the CSD[9]. In 2008, updates in the program were performed and a new functionality was added, named *Materials Module*. This module allows the user to perform motif and crystal packing-feature searches, and identify similarities in the crystalline packing of structures containing the same compound. To utilize the *Materials Module*, knowledge about Etter's graph-set notation is

required. Researchers, such as Zawarotko and Wood developed the concepts of supramolecular chemistry in a quantitative way, by extracting information of the CSD[9], evidencing the relative quality of donors, acceptors, and synthons as coformers.[85-90] With all its beauty, however, it is worth mentioning that a major challenge in this area still lies on the improvement of the physicochemical properties of the crystalline solids, which depends of the molecular organization of the components in the crystal lattice as well as the molecular properties of these individual components. In this way is very clear that the CE has implications that exceed the materials sciences, pharmaceutical development and chemical synthesis and has become an indispensable tool for the design of APIs and non-APIs tailor-made materials.

In this context, before applying supramolecular chemistry and CE principles to the search for suitable coformers, it is advisable to analyze the behavior of the functional groups present in the target molecule. A list of the reported structures containing this target molecule and their respective refcodes can be imported from *ConQuest*, a primary program developed for searching and retrieving information from the CSD.[9] Once having these refcodes, all the analysis can be performed using the *Solid State Suite* tools within the *Materials Module*. Firstly, the *Hydrogen Bond Propensities* tool is used to provide what hydrogen bonds are likely and unlikely to occur in the solid form, thus allowing predicting the occurrence of a given hydrogen bond pattern. In sequence, the *Crystal Packing Feature* tool allows to investigate and analyze the relative geometric preferences of the intermolecular interactions occurring in the target molecule in order to use them in CE. Finally, the *Motif Search* tool can be used to search for suitable coformers, based on all previous results.

The search for coformers in the *Mercury* program can be performed using three methods available in the *Motif Search* tool: pre-defined motifs, generating new motifs and opening a motif query file. In this thesis, the first two methods were employed. In both, the search covered the entire CSD entries containing only organic compounds and allowed identifying structures containing the functional groups under research. The program provides the number of structures containing the pre-selected/designed motif and also provides the frequency of occurrence. This frequency is calculated considering the number of instances in which the motif is observed divided by the number of structures containing the selected functional groups. If the aim is to find suitable coformers, then a useful strategy is to limit the search filtering structures that contain more than one distinct molecular component in the crystal lattice and have the functional groups

on different molecules. For or other ring motifs, it is possible to choose homosynthons (synthons formed between similar functional groups) or heterosynthons (synthons formed between different functional groups) and also specify if they may or may not occur among parent molecules.

Once suitable coformers are found, the next step is to evaluate the nature of these compounds, with a critical view to their safety, chemical properties, and biological applications. This is a critical step to ensure the success of the final product for clinical use and thus requires careful consideration. It is advisable that the pre-selected coformers belong to some of the libraries of pharmaceutically accepted compounds, in particular the GRAS, which is released by the FDA and is internationally recognized [10]. This proceeding eliminates molecules that may be hazardous to public health. If the coformer is another API, then it is necessary to verify whether the co-administration of both is feasible or whether there is a risk of undesirable drug interactions such as additive, synergistic, or antagonistic effects, pharmacological incompatibility, competitive inhibition, etc. The main physicochemical properties (melting point, pKa, solubility, stability, etc) and features (size, molecule geometry, etc) of the coformers must be known and compared with those of the cocrystallizing API. For example, if the pre-selected coformers exhibit solubility profiles much less than the one of the APIs, it is likely that in solution it will crystallize first. Finally, the API issues and the biological application must be clear enough so the best coformers can be selected, i.e., if the API has stability issues and presents ionizable groups, then choosing an acidic or basic coformer is a good strategy considering that salt formation may overcome this issue. If the administration of a given API causes inflammatory effects, then cocrystallizing it with an anti-inflamatory API can be a good strategy.[91-92]

By considering the functional groups present in the antineoplastic drugs (Figure 7), searches pointed, among others, to hydrogen-bonds involving carboxylic groups. In particular, dicarboxylic acids stood out from structures containing this group. Indeed, carboxylic acids are good proton donors, most of them belong to the GRAS list and perhaps are "*the longest and most widely studied functional group in terms of our understanding of hydrogen bonding in both solution and the solid state*".[88]

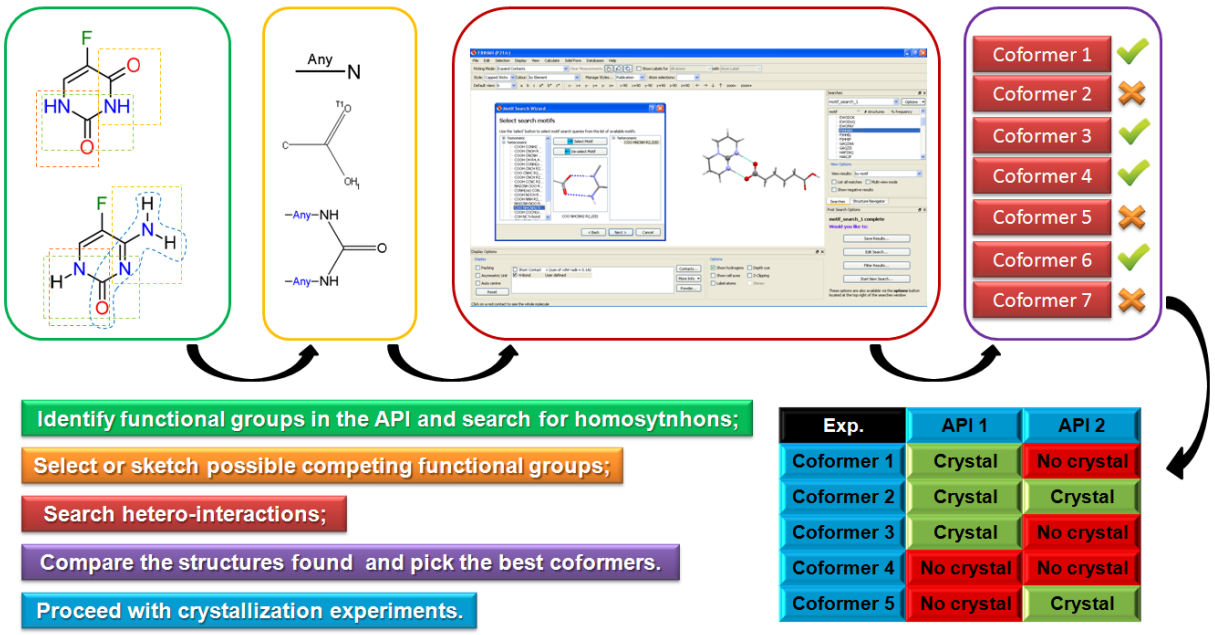

Figure 7 - Steps for new solid state supramolecular synthesis based on synthon competition.
Source: By the author

1.4 Pharmaceutical Salts and Cocrystals

Most antineoplastic drugs are administered intravenously, mainly because of their low aqueous solubility and/or low intestinal permeability profiles when orally administered, although stability and hygroscopicity are also inherent issues.[7,37,39] One of the strategies of CE to circumvent this problem is the rational design, development and production of new solid forms of these drugs aiming enhanced pharmacokinetic properties. Solid forms of APIs comprise polymorphs, solvates, salts, cocrystals, amorphous and combinations of them, such as solvated salts, for example. This thesis focused on the rational supramolecular synthesis of salts and cocrystals of antineoplastic drugs.

Salt selection is a common strategy employed to modify the physicochemical properties of ionizable APIs. Salts can be rationally prepared using adequate bases or acids in order to protonate the API. The choice for a salt is usually done when the API (free base/acid) has one or more undesired properties such as very low solubility in water, apparently not crystallizable, melting point below 80ºC, high hygroscopicity, low chemical stability, etc. On the other hand, cocrystals are an alternative to salts when the APIs do not have ionizable groups or are very weak

bases or acids. The main difference between salts and co-crystals is the proton transfer, whose prediction can be estimated applying the ΔpKa rule and whose confirmation if a salt or a cocrystal was formed should be carefully evaluated by physical techniques: single-crystal X-ray diffraction, infrared and Raman spectroscopy. Both solid forms are attractive for the pharmaceutical industry, however, co-crystals show three main advantages over salts: (1) they do not alter the nature of the API, (2) they are not limited to a binary combination (acid-base motif), i.e., are able to address multiple functional groups simultaneously, constituting tertiary and/or quaternary compounds, and (3) the number of pharmaceutically acceptable co-crystal coformers is larger than the number of counter-ions utilized for salt screening. Definitions of pharmaceutical salts and cocrystals as well as the ΔpKa rule are detailed in the research articles transcribed in the PAPERS section. [91]

Finally, one of the greatest advantages of pharmaceutical salts and co-crystals is that they open the doors not only for the possibility of engineering new properties but also for achieving patent protections and adding new commercial values for the API. By considering that both solid forms fulfill the three criteria for patentability (novelty, utility and non-obviousness), they may be applicable for use in formulations as an API in either immediate or extended release. [91,93-94]

2 MATERIALS AND METHODS

2.1 Selection of coformers and solvents

As depicted earlier, the coformers were selected from analyzes utilizing statistical methods in the CSD. Tables 4 and 5 depict examples of these analysis. Table 4 lists the first search performed for the 5-FU and 5-FC molecules using the tool *Crystal Packing Feature*; the synthon search was performed using as starting points the cocrystallizing molecules reported in the literature for each API. Four conditions were evaluated: number of homo-interactions, defined as the interaction when the synthon under research occurs among the same molecule, number of hetero-interaction, defined as the interaction when the synthon occurs among different molecules, number of structures containing any of the APIs, number of excluded structures, and number of structures containing dicarboxylic acids. Table 5 shows two motif searches performed using the *Motif Search* tool, option *pre-defined motif(s)*. Considering all the motif searches performed for both compounds, some supramolecular preferences emerged, in particular interactions with carboxylic, acetamido, and formimidamide groups. Among the compounds containing carboxylic groups, it was found that crystallization with dicarboxylic acids were recurrent (Table 4). Following these indications, several dicarboxylic acids and one carboxylic acid were selected as coformers for the design of the crystallization protocols (Table 6). In addition, these compounds have pKa values ranging from very weak to strong acids. Thus the use of these compounds as coformers allowed us to perform experiments on a wide range of pH. Consulting the GRAS list, most of the selected acids were assigned as safe. The only carboxylic acid not included in the GRAS list was the terephthalic one, but it was used in the crystallization tests due its intermediate pKa value (Table 6).

Table 4 - Example of synthon search performed for the 5-FU and 5-FC molecules.

Synthon	Refcode	Hits	Number of homo-interactions	Number of hetero-interactions	Number of structures containing any of the APIs	Number of excluded structures	Number of structures containing dicarboxylic acids
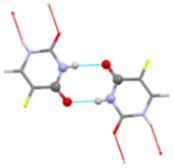	FURACL02 5-FU	1320	1300	---	14	---	1
	BOLMAR 5-FU	3	---	2	1	---	---
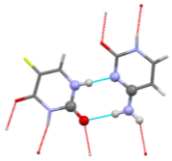	CITFUR 5-FU	101	6	17	2	76	---
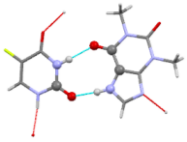	ZAYLOA 5-FU	11	8	2	1	---	---
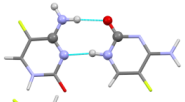	BIRMEU 5-FC	93	19	4	25	45	
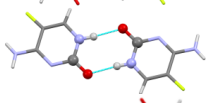	BIRMEU03 5-FC	1133	1124	---	6	3	4
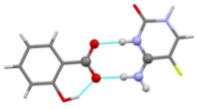	EDATOS 5-FC	53	5	47	1	---	14
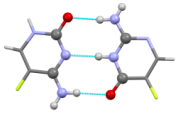	PANLAS 5-FC	29	12	8	9	---	---

Source: By the author.

Table 5 - Example of frequencies for pre-selected motifs.

Motif	Number of structures	Frequency	Dicarboxylic acids
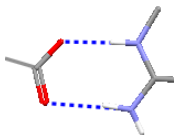	608	76%	Fumaric (25), malic (5), oxalic (12), L-tartaric (15), maleic (20), malonic (17), adipic (14), succinic (18), trimesic (6), terephtalic (10), glutaric (8), phtalic (18), benzoic (16), citric (2)
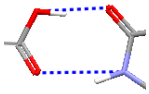	122	23.1%	Oxalic (8), maleic (2), fumaric (1), succinic (1), adipic (1), pimelic (1), glutaric (3), trimesic (3), tartaric (5), malonic (2)

Source: By the author.

Table 6 - List of selected coformers for the design of crystallization protocols.

Coformers	Molecular Structure	pKa in water[95]
Oxalic acid	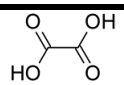	1.25, 3.81
Maleic acid	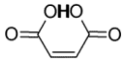	1.92, 6.23
Malonic acid	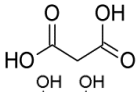	2.83, 5.69
L-Tartaric acid	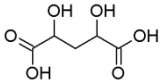	2.98, 4.34
Fumaric acid	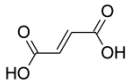	3.02, 4.38
Trimesic acid	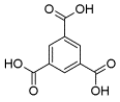	3.12, 3.89, 4.70
Malic acid	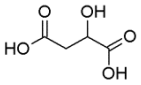	3.40, 5.11
Terephtalic acid	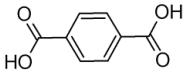	3.54, 4.34
Succinic acid	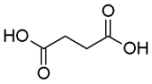	4.21, 5.64
Benzoic acid	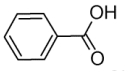	4.20
Adipic acid	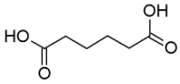	4.41, 5.41
5-fluorocytosine	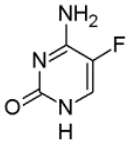	3.26

Source: By the author.

The solvents to be used in the design of the crystallization protocols were pre-selected using as starting point the related literature. These solvent were: deionized water, acetonitrile, 1,4-dioxane, ethanol, methanol, chloroform and isopropanol.

2.2 Design of the Crystallization protocols

The crystallization protocols were initially planned and designed using as starting point the ΔpKa's rule of three. The protocols involved all the pre-selected solvents as well as binary combinations of them (water plus other solvent, for example). For the experiments, it was used 5 mg or 10 mg of each API. The decision about the amount was based on the resulting coformer's amount: if < 3 mg, then 10 mg of the API was added. This small amount of raw material for each experiment was chosen specially because of the availability of the drugs: 2G for 5-FC and 5G for 5-FU.

Firstly, stoichiometric and nonstoichiometric (1:0.5, 2:1, 0.5:1) amounts of the APIs and coformers were added to a single solvent solution which was heated until complete dissolution of the reagents and maintained semi-covered to allow for the slow evaporation of the solvent. Whenever the dissolution was observed before heating, the system was stored immediately without any further preparation. The experiments were stored at room and low temperatures (20ºC, 5ºC and -4ºC). In a second bunch of experiments, the designs of the protocols were extended to involve stoichiometric and nonstoichiometric (1:0.5, 2:1, 0.5:1) amounts of the APIs and coformers being added to binary mixtures of solvents in proportions 1:1, 5:1 and 10:1, always having water as one of the solvents. Again, the systems were heated until complete dissolution of the reagents (if necessary), and stored semi-covered under different temperatures. Cocrystallization experiments were also conducted aiming the production of multi-API structures. To achieve this, stoichiometric and nonstoichiometric amounts of the APIs were dissolved in all the solvents and mixtures of them. The systems were equally stored semi-covered under different temperatures. Figure 8 depicts experiments with resulting suitable crystals.

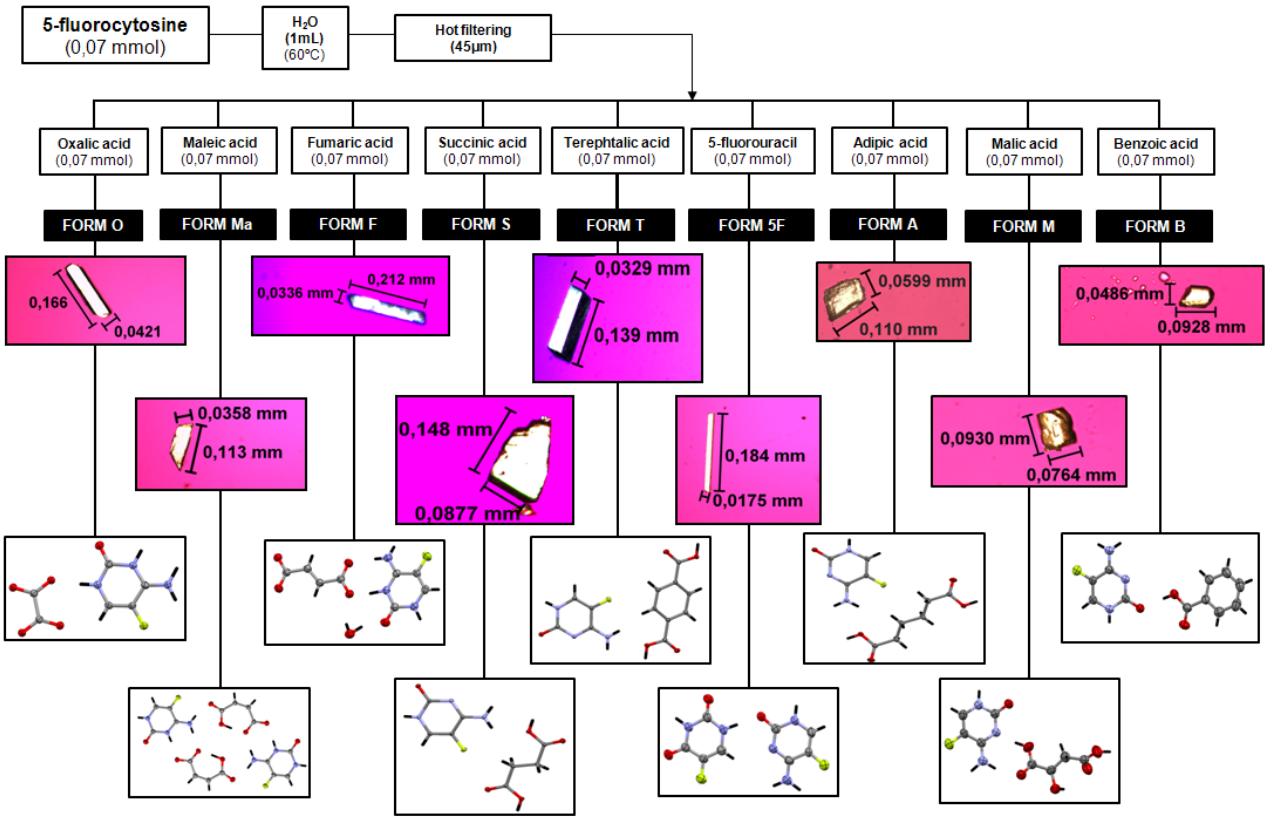

Figure 8 - Proceedings utilized to prepare the crystalline modifications with 5-fluorocytosine and 5-fluorouracil. Source: By the author

Considering that Pharmaceutical Green Chemistry has became an emerging issue in medicine production *vs* environmental impact, mechanochemical experiments were also conducted, in particular for the cocrystallization among the APIs. In particular, solvent-drop grinding (SDG) was utilized because it provides further benefits such as higher yield and crystallinity over neat grinding.[13] For this, stoichiometric amounts of the APIs were added to a 25 mL volume stainless steel milling jar containing two 7 mm diameter stainless steel balls. The system was milled under different frequencies and different times until the best cocrystallization protocol be achieved. The milling experiments were all performed in an oscillatory ball mill Mixer Mill MM400 RETSCH.

2.3 Solid-State Characterization

The solid forms obtained from the crystallization protocols were analyzed by the following techniques:

- **Polarized Light Optical Microscopy** – (All samples) Performed on an Olympus SD-ILK microscope equipped with a 40x objective and polarizers. Allows primary analysis of crystals' quality in terms of size, shape and crystallinity.
- **X-ray crystallography** – (All samples) Some of the single crystal X-ray diffraction data collection were performed in an Enraf-Nonius Kappa-CCD and others in an APEX II DUO diffractometer. This technique allows the analysis of the arrangement of the molecules in the crystalline lattice and provides information of the intermolecular interactions responsible for holding the crystalline packing. In addition, powder X-ray diffraction experiments were performed in a Rigaku-Denki diffractometer to evaluate the purity and stability of the obtained solid forms.
- **Spectroscopic analysis** – (Salts of 5-FC). Infrared (IR) and Raman spectroscopy provide information about vibrational modes of the molecules. These techniques were used for the characterization of the sample as well as in the evaluation of extension of proton transfer of the new solid forms. The data were collected on a Bruker VERTEX 70 (IR) and a Jobin Yvon LabRam HR (Raman) spectrometers, installed at the Physics Department of the Universidade Federal do Ceará (UFC), in collaboration with Prof. Dr. Alejandro Pedro Ayala.
- **Thermal analysis** – (Salts of 5-FC and the multi-API cocrystal). The thermal experiments were performed on a Shimadzu DSC TA-60 WS, a Shimadzu TGA-50/50H and on a Linkam T95-PE hot/cold stage connected to a Leica DM2500P microscope. The DSC experiments provide the thermal behavior of the solid forms allowing, for example, to identify the melting point or the presence of phase transformations if the samples. The TGA experiments provide information about the weight loss associated with the decomposition process of the compound. The hot/cold stage allows visualizing the external morphology and the behavior of the crystal in function of the temperature.

3 PAPERS

A total of two papers are presented here, both related to the nine new crystalline structures obtained with 5-FC.

In the first paper, the salt formations of 5-FC with fumaric, maleic, and oxalic acids are depicted and discussed. Over the last few years one of the most impactful crystal engineering challenges can be attributed to the ability of predicting the formation of salts or co-crystals of APIs. Furthermore, the ΔpKa of these structures are inside the continuum, where the power of prediction is still problematic. These results allowed us to conclude that, at least for this case, but eventually for other APIs with similar features, it is the nature of the main compound that dictates whether a salt or a cocrystal will be obtained in the continuum, i.e. compounds like 5-FC that tend to be basic or acidic would tend to form salts in the continuum.

In the second paper, by considering that the achievement of the controlled supramolecular synthesis of crystal-engineered assemblies is one of the most desired skills by pharmaceutical scientists worldwide, cocrystals were obtained with 5-FC and adipic, succinic, terephtalic, benzoic, and malic acids. In particular, the co-crystal of 5-FC with malic acid (ΔpKa = –0.1) is featured as a transition structure among salts and co-crystals, as it exhibits supramolecular synthons similar to both co-crystals and salts. Finally, as a consequence of all these findings, we successfully designed and conducted the supramolecular synthesis of a co-crystal of 5-FC and 5-fluorouracil, an antineoplastic drug. This experiment can be considered the first step toward the application of 5-FC as a co-former in new controlled synthesis experiments for the design of new tailor-made drugs.

The Supporting Information File of each paper can be seen in the Appendix A and B, respectively.

PAPER 1:

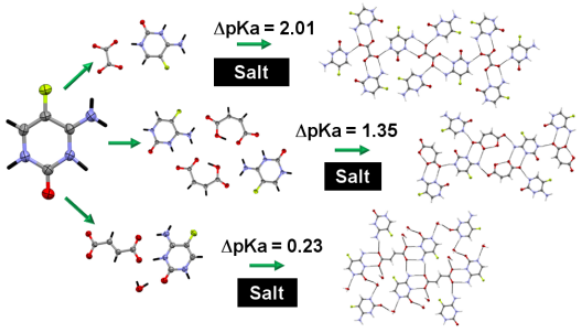

DA SILVA, C.C.P.; PEPINO, R.O.; TENORIO, J.C.; HONORATO, S.B.; AYALA, A.P.; ELLENA, J. The Continuum in 5-Fluorocytosine. Towards Salt Formation, *Cryst. Growth Des.*, **2013**, *13*(10), 4315–4322.

PAPER 2:

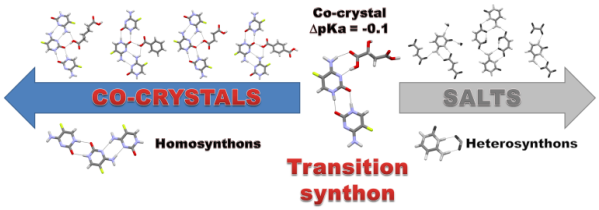

DA SILVA, C.C.P.; PEPINO, R.O.; DE MELO, C.C.; TENORIO, J.C.; ELLENA, J. Controlled synthesis of new 5-fluorocytosine co-crystals based on pKa rule, *Cryst. Growth Des.*, **2014**, *14*(9), 4383–4393).

CRYSTAL GROWTH & DESIGN

Article

pubs.acs.org/crystal

The Continuum in 5-Fluorocytosine. Toward Salt Formation

Cecília C. P. da Silva,[†] Rebeka de Oliveira,[†] Juan C. Tenorio,[†] Sara B. Honorato,[‡] Alejandro P. Ayala,[‡] and Javier Ellena*[,†]

[†]Instituto de Física de São Carlos, Universidade de São Paulo, CP 369, 13560-970, São Carlos, São Paulo, Brazil

[‡]Departamento de Física, Universidade Federal do Ceará, CP 6030, 60455-970 Fortaleza, Ceará, Brazil

Supporting Information

ABSTRACT: 5-Fluorocytosine (5-FC) was crystallized with complementary dicarboxylic acids, aiming to achieve a controlled synthesis of structures based on the ΔpK_a rule proposed in the salt−cocrystal continuum study and to provide structural information helpful in the comprehension of its supramolecularity. Although 5-FC tends to be basic, pK_a = 3.26, only three salts are reported. In this way, new 5-FC salts were obtained, the fumaric, maleic and oxalic ones, all crystallizing in the monoclinic space group $P2_1/c$. In the 5-FC oxalate and fumarate cases, the acid molecules are placed on an inversion center in a fashion that each half molecule exhibits one terminal donor−acceptor site, leading to the constitution of a 5-FC−acid−5-FC heterodimer. Such a heterodimer is observed in only one donor−acceptor site of the maleate of 5-FC, whose acid molecule exhibits a closed chain architecture. Infrared and Raman spectra recorded for the three compounds complement the salt characterization on the basis of the extent of proton transfer. Thermal analysis evidence that the salt formation decreases the melting point of the new compounds, ranking this molecule as a coformer candidate to improve the physical properties of other drugs.

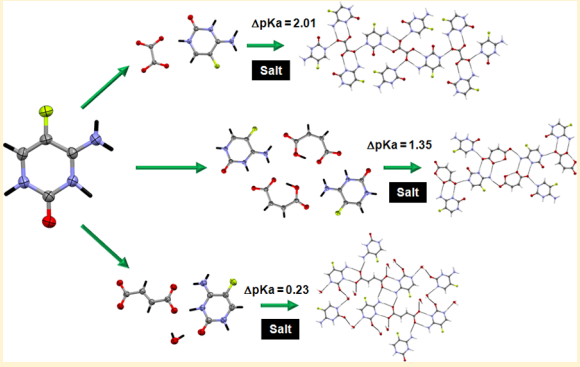

1. INTRODUCTION

Pharmaceutical salts are composed of at least one molecular cationic or anionic active pharmaceutical ingredient (API) and one molecular or monatomic counterion, having the charge balance to possess a definite stoichiometry.[1] They have been preferred for the pharmaceutical industry for a long period because they offer preferential properties in comparison with their parent molecules such as increased chemical stability, solubility, and dissolution rates.[2] In the past few years, the term pharmaceutical cocrystal has emerged in scientific publications worldwide, referring to crystalline structures composed by neutral molecular components, usually involving an API and one cocrystal former, also exhibiting a definite stoichiometry ratio, often leading to a hydrogen-bonded molecular complex. The main distinction between salts and cocrystals is based on the charge transfer ratio occurring among the API and the guest molecule: if the proton involved in the hydrogen-bonding interaction is transferred from the donor to the acceptor, a salt is formed and, on the contrary, a cocrystal is generated.[1,3]

However, when acid−base complexes exhibit similar values of pK_a, a problem emerges, and the decision if the new compound is a salt or a cocrystal is not possible. In an attempt to predict the influence of the crystal contents on the ionization states of the molecules, i.e., to evaluate the extend of proton transfer in the solid state aiming to establish if a salt or a cocrystal will be formed, Childs et al.[4] performed a study involving a total of 20 complexes with theophylline, proposing modifications in the ΔpK_a rules. The proposed guideline is known by "rule of three" and states that salts are expected if the ΔpK_a ($pK_{a-(base)} - pK_{a(acid)}$) is greater than 2 or 3 units. Nangia et al.[5] noted that if the ΔpK_a was smaller than 0, cocrystal formation was expected. Therefore, ΔpK_a ranging between 0 and 2 or 3 are considered to be in a salt−cocrystal continuum, having the extension of proton transfer between the compounds decided on the basis of C−O bond distances. Recently, an extensive work based on salt−cocrystal design considered that there is poor predictive power on the salt−cocrystal continuum and that it is different among systems.[6] On the other hand, Perumalla et al.[7] were able to control the synthesis of two protonated states of cytosine and 5-fluorocytosine structures by manipulating the pK_a and the concentration of the acids used for the salt formation.

5-Fluorocytosine (4-amino-5-fluoro-1,2-dihydropyrimidin-2-one, 5-FC, Scheme 1) is an antimetabolite widely used as an antifungal agent, acting by the deamination of 5-FC into 5-fluorouracil (5-FU) by the enzyme cytosine deaminase (CD) present in the fungal cells.[8] 5-FU is a potent, but highly toxic, antineoplastic agent used for topical treatment of superficial basal cell carcinomas and injected to treat some types of cancer such as gastric, breast, head, neck, rectal, etc.[9,10] In 1985, 5-FC

Received: April 30, 2013
Revised: August 20, 2013
Published: September 3, 2013

   dx.doi.org/10.1021/cg400662n | *Cryst. Growth Des.* 2013, 13, 4315−4322

Scheme 1. Molecular Structure of 5-FC

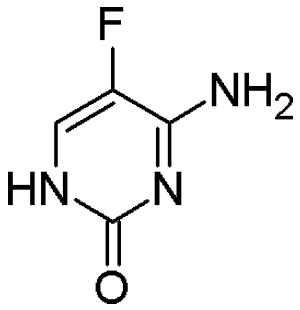

was introduced in combination with CD for cancer treatment.[8,11] The activation of 5-FC in tumor tissues is accomplished by gene-directed enzyme prodrug therapy (GDEPT). In this technique, the CD gene is delivered into the tumor cells and expressed on it, enabling systematically administered 5-FC to be converted into 5-FU inside these cells, killing the tumor.[12]

Although 5-FC tends to be basic (pK_a = 3.26), only three protonated structures were reported, a salicylate and two chloride monohydrates,[7,13,14] against two polymorphs,[15] seven hydrates,[15−19] four solvates,[15,17] and thirteen cocrystals (including eight solvated cocrystals).[20−22] In an effort to contribute with the salt−cocrystal continuum study and attempting to provide information helpful toward the comprehension of the chemical features that lead 5-FC to form salts or cocrystals, particularly in the continuum, we worked with dicarboxylic acids exhibiting pK_a values in such a way that the ΔpK_a ranged from close to 0 until close to 2: oxalic (pK_a = 1.25), maleic (pK_a = 1.91), and fumaric (pK_a = 3.03) acids.

2. EXPERIMENTAL SECTION

5-FC was purchased from Sigma-Aldrich Brazil and used without further purification. Reagents were purchased from commercial vendors and also used without purification. Milli-Q water, acetonitrile, and 2-propanol were used as solvents. The resulting salts were analyzed by single crystal X-ray diffraction, X-ray powder diffraction, hot-stage microscopy, thermal analysis, and spectroscopic studies.

2.1. Synthesis of the Crystals. 5-FC was dissolved, under stirring using a magnet, with oxalic, fumaric, and maleic acids in an equimolar ratio (0.07 mmol) in 1 mL of hot water (60 °C) until the complete dissolution of the solids. Next, the hot mixtures were filtered through a 0.45 μm filter (Milipore), and the resulting solutions were maintained at room temperature, semicovered by Parafilm until complete slow evaporation of the solvent. After 24 h, colorless, plate-shaped crystals of 5-FC with oxalic acid started to grow inside the solution. The complete evaporation of the solvent occurred after 14 days, and crystals were collected for the experiments. For the 5-FC experiments with the fumaric and the maleic acids, the crystals grew only after 12 and 15 days, respectively, i.e., after the complete evaporation of the solvent. The crystallization experiments were repeated at 4 °C. Others crystallization conditions were also used, like solutions of water/acetonitrile (1:1) and water/2-propanol (1:1). These experiments were performed at room temperature as well as at 4 °C.

The above proceedings were adopted as an attempt to analyze the dependence of salt−cocrystal formation under different experimental conditions. It is worth mentioning that lower temperatures were not considered for the experiments to avoid problems with the water freezing.

2.2. Powder X-ray Diffraction (PXRD). bulk samples were analyzed using a Rigaku−Denki powder diffractometer. Experimental conditions: Cu Kα radiation, λ = 1.5418 Å; 50 kV; 100 mA; step scan with a step width of 0.01° in an interval of 10−50° in 2θ; time per step 3 s. Experimental and calculated PXRD patterns were compared in order to confirm if the composition of each bulk material was consistent with that used in the single crystal X-ray diffraction analysis.

2.3. Single Crystal X-ray Structure Determination. X-ray diffraction data collection (φ scans and ω scans with κ offsets) were performed on an Enraf−Nonius Kappa−CCD diffractometer (95 mm CCD camera on κ-goniostat) using graphite-monochromated Mo Kα radiation (0.71073 Å). Intensity data were collected at 100.0(2)K, using the Oxford Cryosystem cryogenic device. The software COLLECT[23] and Denzo−Scalepack package of softwares[24] were applied for acquisition, indexing, integration, and scaling of Bragg reflections. The final cell parameters were obtained using all reflections. No absorption correction was applied. The structures were solved by direct methods, and the models obtained were refined by full-matrix least-squares on F^2 (SHELXL-97[25]) using the WinGX v1.70.01[26] program packages. Hydrogen atoms were stereochemically positioned and refined with fixed individual displacement parameters [U_{iso}(H) = 1.2U_{eq}] according to the riding model (C−H bond lengths of 0.93 Å), except for the N^+−H and O−H ones, which were located on the difference Fourier maps and refinement of their positions with fixed isotropic thermal parameters was performed (U_{iso}(H) = 1.2U_{eq}(N) or 1.5U_{eq}(O)).

The programs MERCURY (version 2.3)[27] and ORTEP-3[28] were used within WinGX v1.70.01[26] to prepare the crystallographic information files (CIF) and artwork representations for publication. The CIFs of the three 5-FC structures were deposited with the Cambridge Structural Data Base under the codes CCDC 915469, 915470, and 915471, for oxalate of 5-FC, maleate of 5-FC and fumarate monohydrate of 5-FC, respectively. Copies of these files may be solicited free of charge from The Director, CCDC, 12 Union Road, Cambridge CB2 1EZ, UK; fax, + 441223-336033; e-mail, deposit@ccdc.cam.ac.uk or http:www.ccdc.cam.ac.uk.

2.4. Hot-Stage Polarized Optical Microscopy. Microscopy was performed on a Leica DM2500P microscope connected to the Linkam T95-PE hot-stage equipment. Data were visualized with the Linksys 32 software for hot stage control. One crystal of each sample was placed on a 13 mm glass coverslip, placed on a 22 mm diameter pure silver heating block inside of the stage. The sample was heated at a ramp rate of 10 °C/min up to a final temperature of 300 °C but discontinued on melting of all material.

2.5. Thermal Analysis. Differential scanning calorimetry (DSC) curves were obtained using a Shimadzu TA-60WS thermal analysis system, where the samples were loaded in aluminum pans (2−5 mg) and heated from room temperature up to 296 °C, at 10 °C·min^{-1}, under nitrogen flow (50 mL min^{-1}). Thermogravimetric (TG) curve for the fumarate monohydrate of 5-FC was obtained using a Shimadzu TGA-50, where 4.6 mg of sample was loaded in an alumina pan and heated from room temperature up to 180 °C, at 10 °C·min^{-1}, under nitrogen flow (50 mL min^{-1}).

2.6. Vibrational Spectroscopy. Fourier transform infrared (FT-IR) spectra were recorded at a spectral resolution of 4 cm^{-1} using a Bruker VERTEX 70 spectrometer. Samples of oxalate of 5-FC, fumarate monohydrate of 5-FC, and maleate of 5-FC were analyzed by the transmission technique as KBr pellets prepared using a hydraulic press (mixtures comprising 200 mg of KBr and 1 mg of each sample). Raman spectra were recorded in a Jobin Yvon LabRam HR spectrometer equipped with a liquid nitrogen refrigerated CCD detector. A HeNe laser was used as excitation source.

2.7. Quantum Mechanical Calculations. Quantum chemistry theoretical calculations of the potential energy surface (PES) scan were performed to explore the influence of the proton displacement between the 5-FC (nucleic base) and the carboxylic acids on the energy of the ionic pair. The electronic structure and optimized geometry were computed within the density functional theory employing a hybrid of Becke's nonlocal three-parameter exchange functional and the Lee−Yang−Parr correlation functional (B3LYP)[29−31] and Hartree−Fock HF level of theory[32] using Gaussian 03.[33] The spent energy of proton displacement was evaluated by using the 6-311++G and the 6-31++G basis set, calculated by 20 steps varying in intervals of 0.1 Å.

dx.doi.org/10.1021/cg400662n | Cryst. Growth Des. 2013, 13, 4315−4322

3. RESULTS

3.1. Structural Description. To simplify the discussion concerning the new 5-FC crystalline structures, the following nomenclature will be applied: form O (oxalate of 5-FC), form Ma (maleate of 5-FC), and form F (fumarate monohydrate of 5-FC). The crystallographic data for the structures are summarized in the Table 1.

Table 1. Crystallographic Data for the 5-FC Forms O, Ma, and F

form O $C_4H_5FN_3O^+$, $^1/_2C_2O_4^-$	form Ma $2C_4H_5FN_3O^+$, $2C_4H_3O_4^-$	form F $C_4H_5FN_3O^+$, $^1/_2C_4H_2O_4^-$, H_2O
space group $P2_1/c$	space group $P2_1/c$	space group $P2_1/c$
a (Å) = 5.2610(2)	a = 9.3450(5)	a = 3.550(5)
b (Å) = 15.1970(6)	b = 11.8620(6)	b = 9.093(5)
c (Å) = 7.8840(3)	c = 18.9540(8)	c = 24.527(5)
β = (Å) 92.206(3)	β = 113.573(3)	β = 91.737(5)
V (Å^3) = 629.87(4)	V = 1925.73(16)	V = 791.4(12)
Z = 4	Z = 4/Z' = 2	Z = 4
ρ_{calc} = 1.836 g/cm^3	ρ_{calc} = 1.691 g/cm^3	ρ_{calc} = 1.722 g/cm^3
1287 unique reflns	3907 unique reflns	1600 unique reflns
$R_{(int)}$ = 0.0298	$R_{(int)}$ = 0.0570	$R_{(int)}$ = 0.0178
θ_{max} = 26.42°	θ_{max} = 26.37°	θ_{max} = 26.29°
$R_{1[I>2\sigma(I)]}$ = 0.0466	$R_{1[I>2\sigma(I)]}$ = 0.0545	$R_{1[I>2\sigma(I)]}$ = 0.0346
wR_2 = 0.1214	wR_2 = 0.1162	wR_2 = 0.0965
S = 1.046	S = 1.045	S = 1.053

All 5-FC salts crystallize in the monoclinic space group $P2_1/c$ (see Table 1), protonated at the N3 ring position (Figure 1). In Supporting Information Table 2, the main hydrogen-bond geometries for each crystal structure are listed.

3.1.1. Oxalate of 5-FC. The asymmetric unit of form O (Figure 1) exhibits one $(5\text{-FC})^+$ and one $(\text{oxalate})^{-2}$, being the anion placed on a crystallographic 2-fold axis (Figure 1). The main motif $R_2^2(8)$ (Figure 2a) is assembled via complementary N41−H41A···O4 and $N3^+$−H3···$O3^-$ hydrogen bonds between the 5-FC molecule and a half $(\text{oxalate})^-$ ion. Taking into account the presence of an inversion center on the $(\text{oxalate})^{-2}$ ion, we will consider the resulting three-component supermolecule (5-FC−oxalate−5-FC, Figure 2a) as a unit, referring to it as the heterodimer or dimeric unit for the discussion in succession. In this way, the adjacent dimeric units of form O are connected through secondary N1−H1···O4 hydrogen bonds to form a planar layer perpendicular to the *ac* plane. These dimeric units are disposed in a zigzag fashion. A secondary $R_2^2(10)$ motif, constituted by self-complementary N41−H41B···F51 hydrogen bonds (Figure 2a), is observed between the 5-FC molecules belonging to the stacked dimeric units. Finally, the 3D packing of form O is completed by $\pi\cdots\pi$ stacking interactions occurring among adjacent layers, perpendicular to the *ac* plane (Figure 2b), the interlayer distance being of 3.13(2)Å.

3.1.2. Fumarate of 5-FC Monohydrate. The asymmetric unit of form F (Figure 3a) exhibits one $(5\text{-FC})^+$, one $(\text{fumarate})^{-2}$, and one molecule of water, where the anion is placed on a crystallographic 2-fold axis. (Figure 1). As the $(\text{fumarate})^{-2}$ ion also exhibits an inversion center, the heterodimer unit observed in form O is preserved in form F. Thus, the main motif $R_2^2(8)$ (Figure 3a) formed by complementary N41−H41A···O4 and $N3^+$−H···$O3^-$ hydrogen bonds is retained in the crystal packing of form F. Secondary

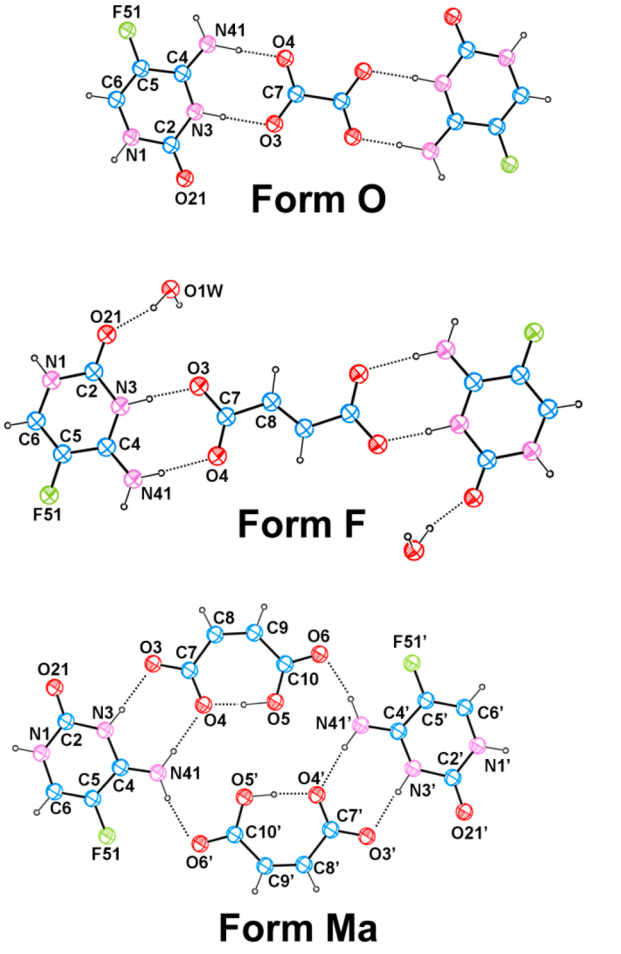

Figure 1. ORTEP-3[20] type view of the asymmetric unit of all 5-FC salts. Thermal ellipsoids are at the 50% probability level. Hydrogen atoms are drawn as spheres of arbitrary radii. Hydrogen bonds are shown as a dashed line.

N41−H41B···O4 hydrogen bonds (Figure 3a) connect adjacent heterodimers to form infinite planar 1D tapes of dimeric units along the *b* axis. The main and secondary H-bond interactions generate a four-component supermolecule ($R_4^2(8)$) as is shown in Figure 3a. The 1D tapes are connected via H-bonds performed by water molecules. Two hydrogen bonds, N1−H1···O1W and O1W−H1W···O21, connect the water molecule with two 5-FC molecules of adjacent 1D tapes (see Figure 3a), forming a layer perpendicular to the *ac* plane (see Figure 3b). One O1W−H2W···O3 hydrogen bond connects the water molecule with a $(\text{fumarate})^{-2}$ ion belonging to the 1D tape of the adjacent layers (Figure 3b). In the layer, it can be observed that the adjacent 1D tapes are disposed in a zigzag fashion and no classical intermolecular interactions occur between them, just one weak C6−H6···O21 hydrogen bonding. In the [100] direction, the adjacent layers generate columns of 1D tapes. Therefore, the water molecules play an important role in the maintenance of the crystalline arrangement of form F. Beyond the presence of water molecules, the 3D packing of form F is completed by $\pi\cdots\pi$ stacking interactions occurring among 1D tapes of the same column, perpendicular to the *ac* plane (Figure 3b), the column interlayer distance being 3.247(4)Å.

3.1.3. Maleate of 5-FC. The asymmetric unit of form Ma exhibits two $(5\text{-FC})^+(\text{maleate})^-$ ionic pairs (Figure 1). The

dx.doi.org/10.1021/cg400662n | Cryst. Growth Des. 2013, 13, 4315−4322

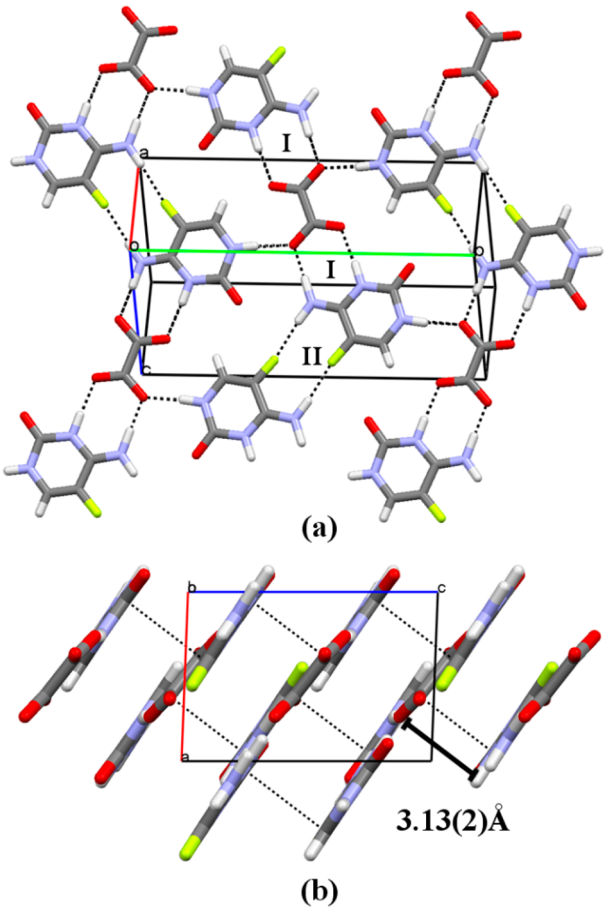

Figure 2. (a) Crystal packing diagram of form O. Dashed lines indicate hydrogen bonds, (I) refers to the $R_2^2(8)$ motif, and (II) refers to the $R_2^2(10)$ motif. (b) Three-dimensional hydrogen-bonded network of form O.

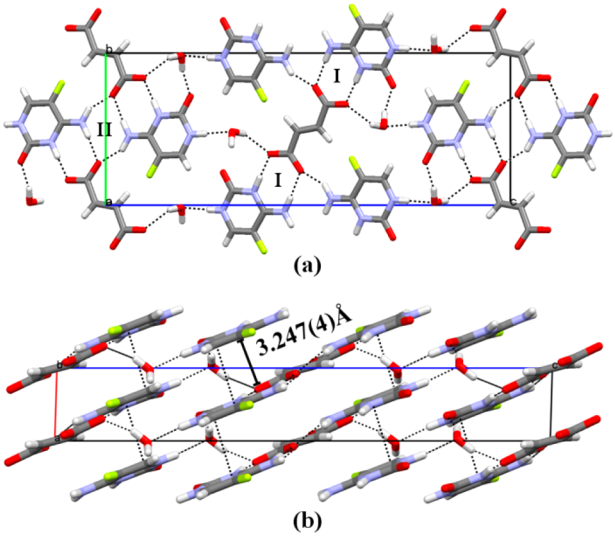

Figure 3. (a) Crystal packing diagram of form F. Dashed lines indicate hydrogen bonds, (I) refers to the $R_2^2(8)$ motif, and (II) refers to the $R_4^2(8)$ motif. (b) Three-dimensional hydrogen-bonded network of form F.

heterodimer of this salt, unlike observed in the forms O and F, is composed by one molecule of 5-FC and one molecule of the $(maleate)^-$ ion, once the ion exhibits no inversion center due to the presence of an intramolecular O−H···O hydrogen bond. Nevertheless, the main motif $R_2^2(8)$ (Figure 4a) is still preserved

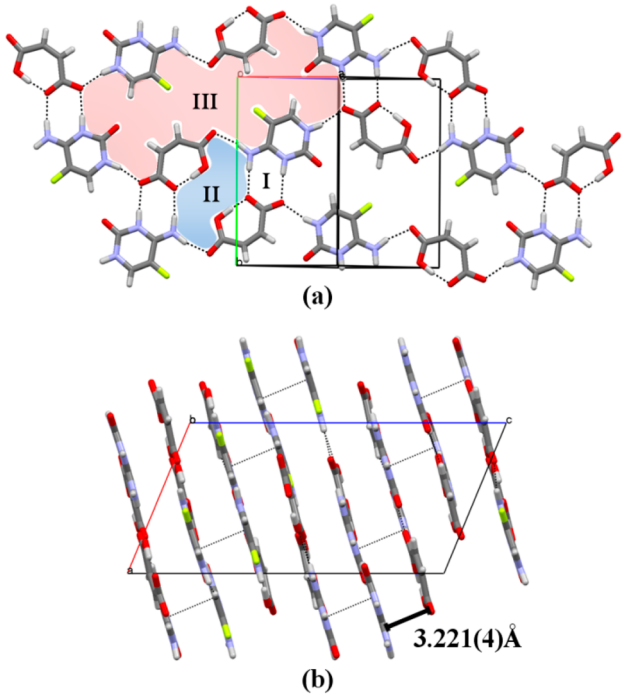

Figure 4. (a) Crystal packing diagram of form Ma. Dashed lines indicate hydrogen bonds, (I) refers to the $R_2^2(8)$ motif, (II) refers to the $R_6^4(16)$ motif, and (III) refers to the $R_8^6(48)$ motif. (b) Three-dimensional hydrogen-bonded network of form Ma.

in one side of the $(maleate)^-$ ion, which exhibits the same complementary N41−H41A···O4 and $N3^+$−H···$O3^-$ hydrogen bond patterns among the 5-FC and the acid (Figure 4a). Two secondary N−H···O hydrogen bonds occur with the $(maleate)^-$ ion and the 5-FC molecules and act in order to form planar layers along the *ab* plane. One of them involves the free hydrogen atom H41B of the amine group of the 5-FC molecule and the oxygen atom O6 of the $(maleate)^-$ ion. Together with the N41−H41A···O4 and the intramolecular O−H···O hydrogen bonds, this secondary hydrogen bond constitutes a ring, composed by the molecules of the asymmetric unit of form Ma, which we will denominate heterotetramer, exhibiting a $R_6^4(16)$ graph-set motif (detached area II in the Figure 4a). The other secondary hydrogen bond involves the N1−H1···O3 atoms and is responsible for connecting adjacent heterotetramers. Every four connected heterotetramers lead to the formation of a bigger ring motif ($R_8^6(48)$) detached area III in the Figure 4a. The absence of water molecules in the crystalline arrangement of form Ma generates a 3D crystal packing similar to the one observed for form O, where $\pi\cdots\pi$ stacking interactions occur between adjacent layers, also perpendicular to the *ac* plane (Figure 4b), with an interlayer distance of 3.221(4)Å.

4. DISCUSSION

5-FC is a rigid molecule, adopting a planar conformation (rms deviation for forms O, F, and Ma molecules A and A′, respectively = 0.0224 Å, 0.0078 Å, 0.0156 Å, and 0.0099 Å for all non-H atoms). When compared to the cytosine pK_a value (pK_a = 4.6),[34] the 5-FC is a weakly basic compound (pK_a = 3.26) due the presence of a most electronegative fluorine atom in its constitution. This substitution attracts the π electrons of

dx.doi.org/10.1021/cg400662n | *Cryst. Growth Des.* 2013, 13, 4315−4322

the N3 nitrogen atom, interfering in its protonation. The fluorination of organic compounds is being increasingly explored in the clinical use, once evidences of improvements in the pharmacokinetic properties of the drugs are being observed. Although halogens are expected to be excellent hydrogen bond acceptors due their high electronegativity, in reality and in particular for the fluorine atom, the propensity to form hydrogen bonds is poor, in a fashion that the organic fluorine acts as an extremely weak base. For this reason, N−H···F intermolecular/intramolecular interactions are rare to occur and only a few examples are found in the literature. Nevertheless, intramolecular N−H···F interactions are observed in all the three salts and an intermolecular N−H···F interaction is observed in the form O. On the basis of the available structural information and on the performed theoretical studies, it is believed that these interactions occur as stabilizing forces inside the crystalline packing and not as a result of close packing. In particular, the intermolecular N−H···F interaction observed in the form O acts as a connector among the heterodimeric units, thus contributing to the stabilization of this salt.[35,36]

By considering that dicarboxylic acids are a class of compounds which exhibit a large range of pK_a values, dicarboxylic acids with opened and closed chains were used in the crystallization experiment in order to evaluate the behavior of the hydrogen bonding patterns in the 5-FC molecule and its potential to form salts or cocrystals. For this purpose, the acids were chosen according to their pK_a values, considering that the ΔpK_a between the acid and the 5-FC were inside the range of the salt−cocrystal continuum, i.e., $0 < \Delta pK_a < 2$. It is worth mentioning that in a first approach, all crystallization experiments were conducted in water solutions to ensure proximity of the intrinsic pK_a value of each compound. Then, variations in the pK_a were promoted by using acetonitrile and 2-propanol, both mixed with water (1:1), to evaluate the behavior and dependence of the 5-FC salt formation in relation to the ΔpK_a. Storage temperature was also considered in this evaluation.

The distinction between salts and cocrystals for carboxylic acids as the crystallizing molecule can be made based on the C−O distance, D_{C-O}.[5] If a $(carboxylate)^-$ is formed, i.e., if a salt is formed, then the C−O distances possesses similar values (1.25 Å[37]) and the ΔD_{C-O} is smaller than 0.03 Å. On the other hand, if there is no ionization, i.e., if a cocrystal is formed, then the neutral carboxyl groups possess different C−O values (1.20 Å[37] and 1.30 Å[37]) and the ΔD_{C-O} is larger than 0.08 Å. By calculating the ΔD_{C-O} for the carboxyl groups of the acid molecules present in the forms O (ΔD_{C-O} = 0.0091(22) Å), F (ΔD_{C-O} = 0.051(16) Å), and Ma (ΔD_{C-O} = 0.0134(28) Å and 0.0102(30) Å), it can be verified that for two of the three salts, the ΔD_{C-O} remains smaller than 0.03 Å, indicating that salts are indeed formed. For form F (ΔpK_a = 0.23), however, the ΔD_{C-O} value indicates that the complex could be a salt or a cocrystal. Although the hydrogen atoms positions are somewhat uncertain when determined from the electron density maps obtained by X-ray diffraction, the proton transfer is observed in the electron density map of form F, being the smaller symmetry in the $(carboxylate)^-$ attributed to the interaction between its oxygen atom and the water molecule trapped into the lattice. This causes a rearrangement of the charge density around the oxygen involved in this interaction that lead to an increase of one of the carboxylic C−O distance to 1.292(2)Å, when it was expected to assume an intermediate bond length of ca. 1.25 Å.[37] The other oxygen−carbon bond of the $(carboxyl)^-$ anion assumes a C−O distance of 1.241(2) Å, which is in agreement with the formation of the anion.

The above results seem to indicate that for the 5-FC case the use of water as the crystallization solvent lead preferentially to the formation of salt in the continuum. However, unpredictable ionization states in the continuum region could occur if, for example, the solvent was changed once the pK_a value changes with different solvents. Nevertheless, even changing the solvents during the crystallization experiments performed with the 5-FC molecules, the salts were still formed, indicating that at least for this molecule, the salt formation in the continuum seems to be a tendency that depends more of the chemical features of the molecule than of the ΔpK_a, which in turn plays an important role in the selection of acid−base pairs and their potential to form salts. In an attempt to state this tendency, quantum mechanical calculations of the energy surface of an isolated acid/5-FC dimeric unit were performed by scanning the $N3^{\delta+}-H\cdots O3^{\delta-}$ interaction to evaluate the energy involved in the proton transition between the carboxylic group and a 5-FC unit. The calculation performed on the forms O and Ma showed that the energy surfaces present their minimum values when the proton is near to the imine nitrogen atom of the 5-FC base-unit when the chemical species are ionized (see Supporting Information). As the proton distance increases, i.e., when the proton gets closer to the carboxylic group, the energies increase linearly reaching its maximum values between 12 and 16 kcal/mol. This values indicate the cocrystal formation is the higher energy state, being the salt forms more stable than the cocrystal forms.

4.1. Supramolecular Analysis. By comparing the supramolecular synthons observed in the 5-FC salts depicted here with the salicylate of 5-FC[14] and with similar synthons found in the Cambridge Structural Database (CSD),[37] a structural preference emerge: the formation of heterosynthons with a $R_2^2(8)$ graph-set motif. According to Allen and Desiraju et al.,[38,39] the $R_2^2(8)$ motif is one of the most recurrently synthons among the crystalline structures. It is expected for complementary compounds, such as carboxylic acids which present donor−acceptor terminal groups and the 5-FC molecule that exhibits two acceptor−donor hydrogen bonding sites, N3:N41 and O21:N1. The heterosynthons are observed in all the salts depicted here and in the 5-FC salt with salycilic acid,[13] involving the same acceptor−donor hydrogen bonding site of the 5-FC molecule, the N3:N41, where the N3 nitrogen atom is protonated in a fashion that the hydrogen atom of the carboxylic group is linked to this atom characterizing the salt formation. In this way, the CSD (version 5.33, with August 2012 updates) motif search,[40] considering the statistics associated with the supramolecular heterosynthon formed with this 5-FC site, was carried out in two steps, within the Materials Mercury tool:[27] one considering the predefined COO···NHCNH2 motif, denominated as raw data in the Figure 5, and another one considering the structures containing exclusively the carboxylic acid group interacting with the 4-aminopyrimidine group, constituting salts, denominated refined data in the Figure 5. Although homosynthons with a $R_2^2(8)$ graph-set motif, composed by carboxylic acid−carboxylic acid or by 4-aminopyrimidine−4-aminopyrimidine groups are also expected to occur, the heterosynthon dominates in the crystalline structures containing similar $R_2^2(8)$ motifs, stated on the basis that 74% of the structures containing both functional groups exhibit the heterosynthon arrangement

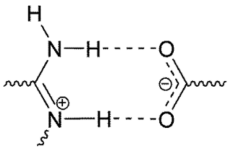

Raw data:

614 entries both COO^- and $HNCNH_2$

454 (74%) entries COO^- ••• $HNCNH_2$ supramolecular heterosynthon

Refined data:

111 entries both COO^- and $(4\text{-aminopyrimidine})^+$

52 (47%) entries COO^- •••$(4\text{-aminopyrimidine})^+$ supramolecular heterosynthon

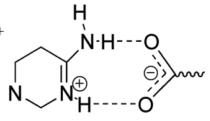

Figure 5. CSD[22,26] statistics associated with the preference of the intermolecular $COO^-/NHCNH_2$ and the $COO^-/(4\text{-aminopyrimidine})^+$ interactions to form heterosynthons.

(Figure 5). For the two chloride monohydrate of 5-FC,[7,13] such a heterosynthon is not observed once it is one halide (Cl) which protonates the N3 atom of the 5-FC molecule. However, in one of the chloride monohydrate structures,[13] the hydrogen bonding pattern shows intermolecular interactions between the 5-FC molecules similar to the CG Watson and Crick base pairing, evidencing a third acceptor−acceptor−donor hydrogen bonding site available in the 5-FC molecule for salt formation, the O21−N3−N41.

4.2. Thermal Analysis. The DSC thermal curve of the raw 5-FC shows a sharp endothermic peak at T_{onset} = 297.81 °C, which is in agreement with its reported melting point[15] (see Figure 6a). This event is followed by an intense exothermal effect, attributed to the drug decomposition process. This same thermal behavior is observed in the DSC curves of the forms F, O, and Ma (Figure 6b,c,d, respectively). The forms O and Ma exhibit only one peak, at 253.73 and 198.29 °C, respectively, associated to the fusion/decomposition of the compound. The form F, on the other hand, exhibits two peaks, one at 98.29 °C, associated to a not reversible process of water loss (confirmed by TGA, see Supporting Information) and another one at 236.44 °C, associated the fusion/decomposition of the compound. Commonly, salt formation is applied to improve stability of APIs by increasing its melting point, but according to the DSC experiments (Figure 6), the salt formation of the 5-FC molecule is decreasing its melting point. For forms F and Ma, the melting point decreases more than 55 °C. In the form O, however, where the acid molecule exhibits the smaller pK_a value, thus forming the strongest salt, the melting point is about 25 °C below the one observed for the free base and the behavior during the decomposition process is closer to sublimation instead of boiling as observed in the forms F and Ma decomposition.

4.3. X-ray Diffraction Analysis. X-ray powder diffractograms of the forms F, Ma, and O were made for two reasons in this work: to verify the sample purity after the crystallization process and to verify the stability of the form F after the water loss. All the calculated and experimental X-ray powder diffractograms are in good agreement (see Supporting Information Figure 7), stating the purity of the compounds, which is one of the most important features that must be achieved during the synthesis of a new solid form of an API. Concerning the form F, once the molecules of water are strongly linked into the crystalline lattice, trapped by O−H···O and N−H···O hydrogen bonds, the diffractogram shows that this compound suffers a partial amorphization process after the water loss. However, even with an amorphous phase emerging, it still preserves some peaks, indicating that a small amount of crystallinity is preserved (see Supporting Information Figure 7).

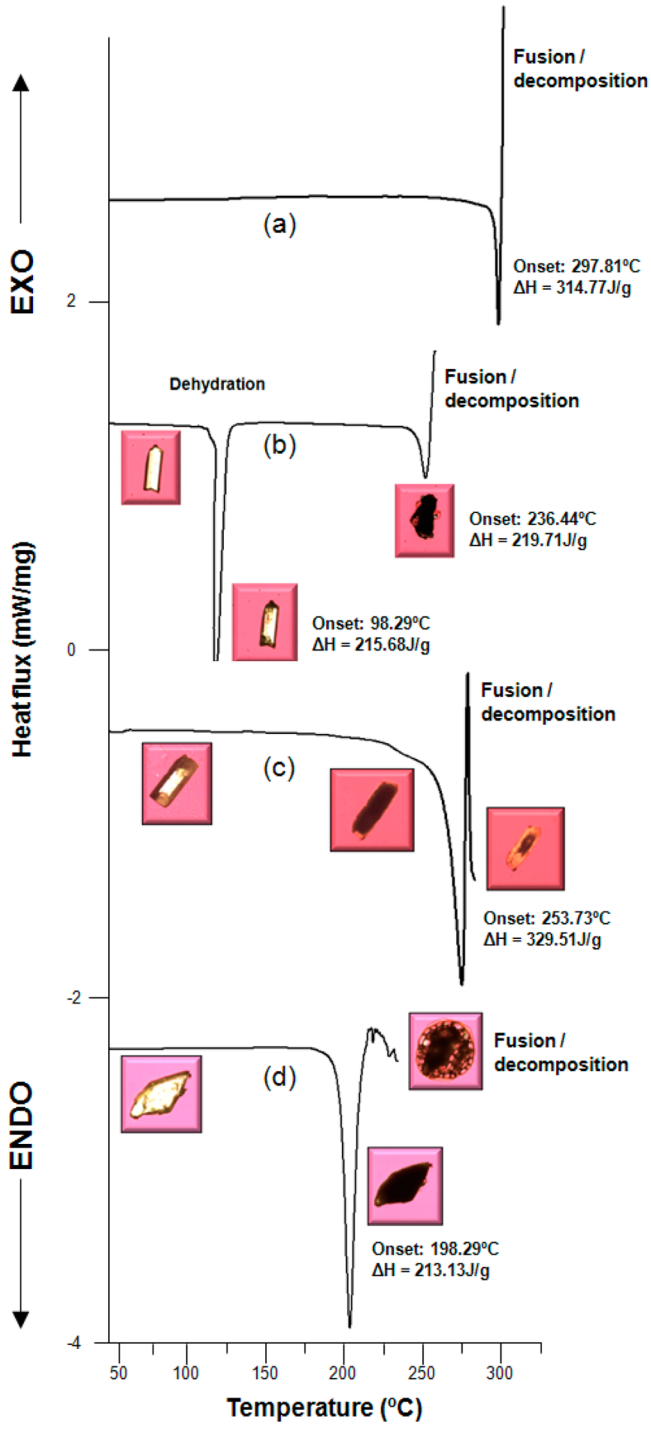

Figure 6. DSC curves and crystal behavior visually checked by hot-stage microscopy of the (a) free base, (b) form F, (c) form O, and (d) form Ma.

Nevertheless, the peaks recorded after the water loss suggest the formation of a new phase, probably a dehydrated one, once the peaks do not overlap neither with the fumaric acid nor with the 5-FC powder diffractograms by themselves. Until the present, we were unable to synthesize the dehydrated form of the form F, which would allow us to confirm our hypothesis.

4.4. Vibrational Analysis. To support the intermolecular interactions determined by single crystal X-ray diffraction, FT-IR and Raman scattering experiments were conducted (see Supporting Information Figure 8). A detailed discussion of the

dx.doi.org/10.1021/cg400662n | Cryst. Growth Des. 2013, 13, 4315−4322

vibrational spectra of 5-FC was reported by Seshadri et al.[41] and Jaworski et al.[42] The main spectral features of the 5-FC molecule can be easily identified in the three salts. For example, the breathing mode of the aromatic ring is clearly identified at 780 cm^{-1} and the in-plane deformation of the C−H and N−H are observed between 1200 and 1400 cm^{-1}. However, differences in the molecular environment and intermolecular interactions lead to univocal features which can be associated to the new crystal forms. The carbonyl group usually fingerprints the intermolecular interactions due to its participation in hydrogen bonds. That is the case of the crystalline structure of 5-FC[28] and, as a consequence, the ν(C2O21) stretching is shifted toward lower wavenumbers (1675 cm^{-1}). On the other hand, this moiety does not play a relevant role in the crystal packing of the 5-FC salts, which exhibit the ν(C2O21) at a higher wavenumber (~1715 cm^{-1}). However, the 5-FC carbonyl bands are overlapped with those of the carboxylic acid and it is not possible to perform an accurate assignment. Another interesting signature of the 5-FC spectra is the ν(C6H) stretching (3091 cm^{-1}), which is observed at different wavenumbers in forms O (3095 cm^{-1}) and F (3087 cm^{-1}), whereas it is split in form Ma (3061/3070 cm^{-1}) due to the two 5-FC molecules in the asymmetric unit. The C6H group is not involved in the main hydrogen bond pattern but exhibit single (5-FC and form Ma) and bifurcated (form O and form F) short contacts (see Supporting Information Table 2). In particular, the lower wavenumbers observed in form Ma is well correlated with the shortest C6H···X intermolecular distance among the 5-FC salts reported in this contribution. Finally, the ν(NH) stretching modes need to be considered because the corresponding bonds are essential in stabilizing the crystalline structure. These modes are spread between 3100 and 3450 cm^{-1}, mainly due to the red-shift induced by the hydrogen bonds. In the case of form O, a very sharp band is observed at 3450 cm^{-1}, which could be associated to the ν(N41−H41B) because it is weakly bonded to fluorine atoms (see Supporting Information Table 2). In the remaining structures, including the one of 5-FC,[15] N41H41B is linked to strongest acceptors, increasing the red-shift and inducing wider bands. Our results show that vibrational spectroscopy was successful to provide distinctive spectral signatures, confirming the intermolecular interactions characteristic of the 5-FC salts.

5. CONCLUSION

According to the salt−cocrystal study, salts are formed when the ΔpK_a among the API and the molecules crystallized with it are higher than 2. When the $0 < \Delta pK_a < 2$, the charge transfer analysis is difficult to predict and it is often performed on the basis of the C−O bond lengths differences, for carboxylic acids in particular. In this study, salts of the API 5-FC were obtained with fumaric, maleic, and oxalic carboxylic acids, first in water solutions, with the system exhibiting ΔpK_a values of 0.23, 1.35, and 2.01, respectively. The experiments were repeated varying the storage temperature and the solutions, leading all of them to the same salts formation results. These results, together with theoretical calculations performed over the free molecule and over the new salts, points to a tendency of this drug do form salts in the continuum. For this particular case, this tendency depends more on the chemical features of the 5-FC molecules than on the ΔpK_a. In this way, together with the consideration about the ΔpK_a, it is believed that tendencies for a given molecule in the continuum might be assigned when complementary experimental and/or theoretical physicochemical studies are considered and explored.

All the salts reported here show a similar hydrogen-bond pattern interactions, complementary to those of 5-FC, protonating its N3 nitrogen atom and forming a $R_2^2(8)$ motifs formed essentially by the same N−H···O hydrogen bond among the acid and the API. According to the DSC experiments, the salt formation reduced the melting point of the solid. This effect suggests that the presence of protonated 5-FC into a crystalline arrangement could improve the physicochemical properties of compounds with dissolution rate/solubility problems.

■ ASSOCIATED CONTENT

Ⓢ Supporting Information

Crystallographic data of 5-FC salts, differential scanning calorimetry and thermogravimetric curves, powder X-ray diffraction pattern, quantum mechanical calculations. This material is available free of charge via the Internet at: http://pubs.acs.org/.

■ AUTHOR INFORMATION

Corresponding Author

*Phone: +55 16 3373 8096. Fax: +55 16 3373 9881. E-mail: javiere@ifsc.usp.br.

Notes

The authors declare no competing financial interest.

■ ACKNOWLEDGMENTS

The authors thank CAPES (C.C.P.S. and J.C.T.), CNPq (J.E., R.O and A.P.A.) and FAPESP for the financial support.

■ REFERENCES

(1) Bond, A. D. In *Pharmaceutical Salts and Cocrystals*; Wouters, J., Quéré, L., Eds.; Royal Society of Chemistry: Cambridge, UK, 2012, Chapter 2, pp 9−28.
(2) Aateka, P.; Stuart, A. J.; Albert, F.; Nilesh, P. *Br. J. Cardiol.* **2009**, *16* (6), 281−286.
(3) Clarke, H. D.; Hickey, M. B.; Moulton, B.; Perman, J. A.; Peterson, M. L.; Wojtas, Ł.; Almarsson, Ö.; Zaworotko, M. J. *Cryst. Growth Des.* **2012**, *12* (8), 4194−4201.
(4) Childs, S. L.; Stahly, G. P.; Park, A. *Mol. Pharmaceutics* **2007**, *4* (3), 323−338.
(5) Bhogala, B. R.; Basavoju, S.; Nangia, A. *CrystEngComm* **2005**, *7*, 551−562.
(6) Ebenezer, S.; Muthiah, P. T. *Cryst. Growth Des.* **2012**, *12* (7), 3766−3785.
(7) Perumalla, S. R.; Pedireddi, V. R.; Sun, C. C. *Cryst. Growth Des.* **2013**, *13* (2), 429−432.
(8) Vermes, A.; Guchelaar, H.-J.; Dankert, J. *J. Antimicrob. Chemother.* **2000**, *46* (2), 171−179.
(9) Kim, K.-H.; Kim, J.-Y.; Lee, K.-H.; Noh, M.-J.; Kim, Y.-C.; Park, H.-J. *Bioorg. Med. Chem. Lett.* **2002**, *12* (3), 483−486.
(10) Longley, D. B.; Paul Harkin, D.; Johnston, P. G. *Nature* **2003**, *3*, 330−338.
(11) Nishiyama, T.; Kawamura, Y.; Kawamoto, K.; Matsumura, H.; Yamamoto, N.; Ito, T.; Ohyama, A.; Katsuragi, T.; Sakai, T. *Cancer Res.* **1985**, *45* (4), 1753−1761.
(12) Xu, G.; McLeod, H. L. *Clin. Cancer Res.* **2001**, *7* (11), 3314−24.
(13) Prabakaran, P.; Murugesan, S.; Muthiah, P. T.; Bocelli, G.; Righi, L. *Acta Crystallogr., Sect. E: Struct. Rep. Online* **2001**, *57* (10), o933−o936.
(14) Portalone, G.; Colapietro, M. *J. Chem. Cryst.* **2007**, *37* (2), 141−145.

(15) Hulme, A. T.; Tocher, D. A. *Cryst.Growth Des.* **2006**, *6* (2), 481−487.
(16) Portalone, G.; Colapietro, M. *Acta Crystallogr., Sect. E: Struct. Rep. Online* **2006**, *62* (3), o1049−o1051.
(17) Tutughamiarso, M.; Bolte, M.; Egert, E. *Acta Crystallogr., Sect. C: Cryst. Struct. Commun.* **2009**, *65* (11), o574−o578.
(18) Hulme, A. T.; Tocher, D. A. *Acta Crystallogr., Sect. E: Struct. Rep. Online* **2005**, *61* (7), 02112−o2113.
(19) Louis, T.; Low, J. N.; Tollin, P. *Cryst. Struct. Commun.* **1982**, *11*, 1059−1064.
(20) Portalone, G. *Chem. Cent. J.* **2011**, *5* (51), 1−8.
(21) Tutughamiarso, M.; Wagner, G.; Egert, E. *Acta Crystallogr., Sect. B: Struct. Sci.* **2012**, *B68* (4), 431−443.
(22) Tutughamiarso, M.; Egert, E. *Acta Crystallogr., Sect. B: Struct. Sci.* **2012**, *B68* (4), 444−452.
(23) *COLLECT*; Data Collection Software; Nonius: Delft, The Netherlands, 1998.
(24) Otwinowski, Z.; Minor, W. In *Methods in Enzymology: Macromolecular Crystallography*; Carter, C. W., Jr., Sweet, R. M., Eds.; Academic Press: New York, 1997, Part A, Vol. *276*, pp 307−326.
(25) Sheldrick, G. M. *Acta Crystallogr., Sect. A: Found. Crystallogr.* **2008**, *A64*, 112−122.
(26) Farrugia, L. J. *J. Appl. Crystallogr.* **2012**, *45*, 849−854.
(27) Macrae, C. F.; Bruno, I. J.; Chisholh, J. A.; Edgington, P. R.; McCabe, P.; Pidcock, E.; Rodriguez-Monge, L.; Taylor, R.; van de Streek, J.; Wood, P. A. *J. Appl. Crystallogr.* **2008**, *41*, 466−470.
(28) Farrugia, L. J. *J. Appl. Crystallogr.* **1997**, *30*, 565.
(29) Parr, R. G.; Yang, W. *Density Functional Theory of Atoms and Molecules*; Oxford University Press: New York, 1989.
(30) Lee, C. T.; Yang, W. T.; Parr, R. G. *Phys. Rev. B* **1988**, *37*, 785−789.
(31) Becke, A. D. *J. Chem. Phys.* **1993**, *98*, 5648−5652.
(32) Møller, C.; Plesset, M. S. *Phys. Rev.* **1934**, *46*, 618−622.
(33) Frisch, M. J.; Trucks, G. W.; Schlegel, H. B.; Scuseria, G. E.; Robb, M. A.; Cheeseman, J. R.; Montgomery, J. A., Jr.; Vreven, T.; Kudin, K. N.; Burant, J. C.; Millam, J. M.; Iyengar, S. S.; Tomasi, J.; Barone, V.; Mennucci, B.; Cossi, M.; Scalmani, G.; Rega, N.; Petersson, G. A.; Nakatsuji, H.; Hada, M.; Ehara, M.; Toyota, K.; Fukuda, R.; Hasegawa, J.; Ishida, M.; Nakajima, T.; Honda, Y.; Kitao, O.; Nakai, H.; Klene, M.; Li, X.; Knox, J. E.; Hratchian, H. P.; Cross, J. B.; Adamo, C.; Jaramillo, J.; Gomperts, R.; Stratmann, R. E.; Yazyev, O.; Austin, A. J.; Cammi, R.; Pomelli, C.; Ochterski, J. W.; Ayala, P. Y.; Morokuma, K.; Voth, G. A.; Salvador, P.; Dannenberg, J. J.; Zakrzewski, V. G.; Dapprich, S.; Daniels, A. D.; Strain, M. C.; Farkas, O.; Malick, D. K.; Rabuck, A. D.; Raghavachari, K.; Foresman, J. B.; Ortiz, J. V.; Cui, Q.; Baboul, A. G.; Clifford, S.; Cioslowski, J.; Stefanov, B. B.; Liu, G.; Liashenko, A.; Piskorz, P.; Komaromi, I.; Martin, R. L.; Fox, D. J.; Keith, T.; M. A. Al-Laham, Peng, C. Y.; Nanayakkara, A.; Challacombe, M.; Gill, P. M. W.; Johnson, B.; Chen, W.; Wong, M. W.; Gonzalez, C.; Pople, J. A. *Gaussian 03*, revision C.02;Gaussian Inc.: Wallingford, CT, 2004.
(34) Bossche, H. V.; Willemsens, G.; Marichal, P. *Crit. Rev. Microbiol.* **1987**, *15*, 57−72.
(35) Sunil, S. L.; Nayak, S. K.; hathwar, V. R.; Chopra, D.; Row, T. N. In *Pharmaceutical Salts and Cocrystals*, Wouters, J., Quéré, L., Eds.; Royal Society of Chemistry: Cambridge, UK, 2012, Chapter 3, pp 29−43.
(36) Desiraju, G.; Steiner, T. The Weak Hydrogen Bond. *Structural Chemistry and Biology*; Desiraju, G., Steiner, T., Eds.; Oxford University Press Inc.: New York, 1999, Chapter 3, pp 202−215.
(37) Allen, F. H. *Acta Crystallogr., Sect. B: Struct. Crystallogr. Cryst. Chem.* **2002**, *58*, 380−388.
(38) (a) Allen, F. H.; Raithby, P. R.; Shields, G. P.; Taylor, R. *Chem. Commun.* **1998**, *9*, 1043−1044. (b) Allen, F. H.; Motherwell, W. D. S.; Raithby, P. R.; Shields, G. P.; Taylor, R. *New J. Chem.* **1999**, *23*, 25−34.
(39) Desiraju, G. R. *Angew. Chem., Int. Ed. Engl.* **2003**, *34*, 2311−2327.
(40) Shan, N.; Zaworotko, M. *Drug Discovery Today* **2008**, *13* (9/10), 440−446.
(41) Seshadri, S.; Gunasekaran, S.; Muthu, S.; Kumaresan, S.; Arunbalaji, R. *J. Raman Spectrosc.* **2007**, *38* (11), 1523−1531.
(42) Jaworski, A.; Szczesniak, M.; Szczepaniak, K.; Kubulat, K.; Person, W. B. *J. Mol. Struct.* **1990**, *223*, 63−92.

CRYSTAL GROWTH & DESIGN

Article

pubs.acs.org/crystal

Controlled Synthesis of New 5-Fluorocytosine Cocrystals Based on the pK_a Rule

Cecília C. P. da Silva, Rebeka de O. Pepino, Cristiane C. de Melo, Juan C. Tenorio, and Javier Ellena*

Instituto de Física de São Carlos, Universidade de São Paulo, CP 369, 13560-970, São Carlos, São Paulo, Brazil

Supporting Information

ABSTRACT: 5-Fluorocytosine (5-FC) was investigated for the controlled synthesis of cocrystals by applying the pK_a rule. Five cocrystals were designed and developed with adipic, succinic, terephtalic, benzoic, and malic acids, all exhibiting negative ΔpK_a values ranging from close to zero up to roughly −1. The synthesized cocrystals were analyzed by single crystal X-ray diffraction, and the observed supramolecular synthons were compared to the reported structures containing 5-FC. In the first four cocrystals, the intermolecular interactions between adjacent 5-FC molecules form two different homodimers showing $R_2^2(8)$ motifs and assembled via complementary N−H···O and N−H···N hydrogen bonds, respectively. However, in the cocrystal with malic acid (ΔpK_a = −0.1), an intermediate supramolecular synthon pattern between salts and cocrystals is observed. In this crystal packing, the homodimer of 5-FC molecules held by the N−H···O interactions is preserved, but a new heterodimer is formed between 5-FC and the acid molecule, such as the ones observed for 5-FC salts. These differences were analyzed using UNI Force Field Calculations to establish the intermolecular potentials of the synthons. As an application, we synthesized a cocrystal of 5-FC with 5-fluorouracil. This can be considered the first step toward the application of 5-FC for the design of new tailor-made drugs.

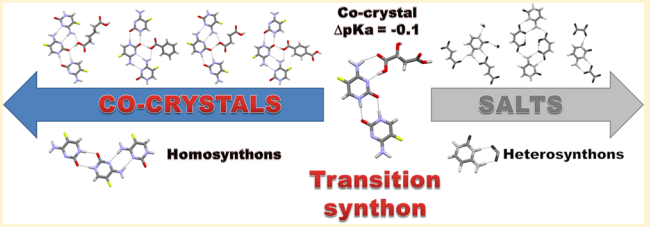

1. INTRODUCTION

Crystal engineering and supramolecular chemistry are emerging issues in active pharmaceutical ingredients (APIs). Achieving the ability to explore and predict the occurrence of noncovalent interactions among APIs and other molecules, such as solvents, acids, bases, and other substances recognized as safe (GRAS), for the rational design of pharmaceutical products in the solid state, exhibiting improved physical and chemical properties, is a challenge to scientists. Among the solid forms that an API may exhibit, the class of pharmaceutical cocrystals is noteworthy, i.e., solid pharmaceutical compounds containing at least one molecular API and at least one solid nontoxic cocrystal former (usually a GRAS compound) interacting with one another through unique binding interactions; it is a hard task to predict how the API(s) and the coformer(s) will interact to each other. This class has presented increasing interest in the last few years due to its immense ability to form new compounds that do not alter the pharmacological activity of the API but may improve its physical properties, not being restricted to binary compounds, once ternary and quaternary cocrystals may be designed.[1−7]

By considering that cocrystal formation is not obvious (it is a result of a supramolecular study and synthesis), beyond the fact that pharmaceutical cocrystals have utility (may improve the physical properties of an API) and are considered a novel compound (possesses a new chemical composition and an unpredictable chemical bonding), they are subject to patents. This possibility opens the door to new commercial opportunities for an API, offering to the pharmaceutical industries the benefits of generating a new and exclusive patent upon a new chemical compound or even of maintaining and extending its exclusivity, by covering, beforehand, new solid forms. In this sense, the patent can encompass not only the initial chemical compound but also its cocrystals through the creation of a solid-form patent portfolio. As advantage, the path to patent a cocrystal can be abbreviated in some aspects, considering that issues such as toxicology and discovery do not need to be extensively evaluated.[8,9]

5-Fluorocytosine (4-amino-5-fluoro-1,2-dihydropyrimidin-2-one, 5-FC, Scheme 1) was synthesized in 1957 as an antimetabolite drug to be used as an antitumor agent. It was found to exhibit activity against fungal infections and was released for this use in 1968. By the discovery of its mechanism of action, i.e., conversion into 5-fluorouracil (5-FU) by deamination performed by the enzyme cytosine deaminase (CD)—natural in fungal cells—5-FC is being recently

Scheme 1. Molecular Structure of 5-FC

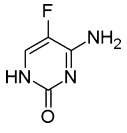

Received: April 11, 2014
Revised: July 3, 2014
Published: July 14, 2014

Table 1. Crystallographic Data for the 5-FC Solid Forms S, T, A, M, B, and 5-F

Form S	Form A	Form T
$C_4H_4FN_3O$, 1/2 $C_4H_6O_4$	$C_4H_4FN_3O$, 1/2 $C_6H_{10}O_4$	$C_4H_4FN_3O$, 1/2 $C_8H_6O_4$
space group $P\bar{1}$	space group $P\bar{1}$	space group $P\bar{1}$
a (Å) = 4.9209(3)	a (Å) = 5.2742(5)	a (Å) = 3.6265(3)
b (Å) = 8.6115(5)	b (Å) = 6.6650(7)	b (Å) = 9.5274(8)
c (Å) = 9.4689(6)	c (Å) = 12.8441(13)	c (Å) = 13.7902(12)
α (°) = 72.466(3)	α (°) = 86.411(6)	α (°) = 107.812(5)
β (°) = 75.129(3)	β (°) = 80.757(6)	β (°) = 92.036(4)
γ (°) = 89.747(3)	γ (°) = 71.970(6)	γ (°) = 96.844(4)
V (Å^3) = 368.64(4) Å^3	V (Å^3) = 423.72(7) Å^3	V (Å^3) = 449.09(7) Å^3
Z = 2	Z = 2	Z = 2
ρ_{calc} = 1.695 g/cm^3	ρ_{calc} = 1.585 g/cm^3	ρ_{calc} = 1.569 g/cm^3
2572 unique reflns	1624 unique reflns	2602 unique reflns
$R_{(int)}$ = 0.0219	$R_{(int)}$ = 0.0280	$R_{(int)}$ = 0.0302
θ_{max} = 25.00°	θ_{max} = 25.80°	θ_{max} = 27.50°
$R_{1[I>2\sigma(I)]}$ = 0.0381	$R_{1[I>2\sigma(I)]}$ = 0.0476	$R_{1[I>2\sigma(I)]}$ = 0.0449
wR_2 = 0.1153	wR_2 = 0.1322	wR_2 = 0.1131
S = 1.103	S = 1.122	S = 1.078
Form M	**Form B**	**Form 5F**
$C_4H_4FN_3O$, $C_4H_6O_5$	$C_4H_4FN_3O$, $C_7H_6O_2$	$C_4H_4FN_3O$, $C_4H_3FN_2O_2$
space group $C2/c$	space group $P2_1/n$	space group $P2_1/c$
a (Å) = 20.8980(4)	a (Å) = 9.0565(2)	a (Å) = 15.0176(3)
b (Å) = 14.8590(9)	b (Å) = 5.4318(2)	b (Å) = 3.5604(1)
c (Å) = 7.244(1)	c (Å) = 22.8887(8)	c (Å) = 27.3113(4)
β (°) = 107.178(3)	β (°) = 92.870(1)	β (°) = 138.282(1)
V (Å^3) = 2149.1(4) Å^3	V (Å^3) = 1124.55(6) Å^3	V (Å^3) = 971.78(4) Å^3
Z = 8	Z = 4	Z = 4
ρ_{calc} = 1.639 g/cm^3	ρ_{calc} = 1.484 g/cm^3	ρ_{calc} = 1.772 g/cm^3
2451 unique reflns	2306 unique reflns	1628 unique reflns
$R_{(int)}$ = 0.0547	$R_{(int)}$ = 0.0252	$R_{(int)}$ = 0.0284
θ_{max} = 27.49°	θ_{max} = 25.242°	θ_{max} = 66.685°
$R_{1[I>2\sigma(I)]}$ = 0.0729	$R_{1[I>2\sigma(I)]}$ = 0.0482	$R_{1[I>2\sigma(I)]}$ = 0.0312
wR_2 = 0.1853	wR_2 = 0.1212	wR_2 = 0.0841
S = 1.010	S = 1.035	S = 1.069

employed in gene-directed enzyme prodrug therapy (GDEPT) to treat cancer. Concerning pharmacokinetics, toxicity, and drug interactions, 5-FC is a BCS class I drug of small size, high solubility in water, and high permeability (bioavailability of 76% − 89%). It exhibits minor side effects, although hepatotoxicity and bone marrow depression may occur. Nevertheless, normal mammalian cells do not express CD and are resistant to this drug, such that over 90% of it is eliminated unchanged in the urine.[10−12]

The first crystal structure of 5-FC deposited in the Cambridge Structural Database (CSD)[13] was a monohydrate reported in 1982.[14] Since then, 30 five crystal structures were reported in the literature, including two polymorphs,[15] six hydrates,[15−18] four solvates,[15,17] 10 salts[19−22] and 13 cocrystals.[23−25] Nineteen of them crystallize in the monoclinic crystalline system, 12 in the $P2_1/c$ (four hydrates, four salts, one solvate, and three cocrystals), four in the $P2_1/n$ (two salts, one solvate, and one polymorph), two in the Cc (one hydrate and one cocrystal), and one in the $C2/c$ (one cocrystal) space groups. Twelve crystallize in the triclinic $P\bar{1}$ space group (two hydrates, one solvate, and nine cocrystals), and one in the tetragonal $P4_12_12$ space group (polymorph). From these numbers, it is possible to observe that neutral state is predominant for this fluoropyrimidine. Furthermore, it is worth noting that three salts and eight cocrystals have solvents introduced into the crystalline arrangement.[20−22,24,25]

In our previous work,[22] we discussed salt formation by the 5-FC molecules on the basis of a salt/cocrystal continuum study.[26,27] As a follow-up to these studies, here we discuss the supramolecular synthesis of five cocrystals of 5-FC containing adipic, succinic, benzoic, tereftalic, and malic acids as coformers, aiming to add information to the salt−cocrystal continuum study, to improve understanding of 5-FC drug−receptor interactions and, especially, to understand the controlled synthesis of cocrystals. On the basis of the supramolecular patterns established by these 5-FC cocrystals, we were able to design and synthesize a cocrystal involving two APIs, 5-FC and 5-FU, an antineoplastic drug.

2. EXPERIMENTAL SECTION

All reagents were used without additional purification.

2.1. Cocrystals Supramolecular Synthesis. Stoichiometric amounts of 5-FC (Sigma-Aldrich Brazil) with succinic, adipic, benzoic, terephtalic, and malic acids and 5-FU were employed, using water as the solvent. The solutions were filtered through a 0.45 μm filter (Milipore) and maintained at room temperature, semicovered by Parafilm until complete slow evaporation of the solvent. The resulting crystals were selected for single crystal X-ray diffraction experiments.

2.2. Single Crystal X-ray Structure Determination. The crystallographic data for the cocrystals of 5-FC with adipic, succinic, and terephtalic acids were collected on a Bruker Super-Duo APEX II CCD diffractometer using MoKα radiation (0.71073 Å). For the cocrystal of 5-FC with 5-FU, Cu Kα radiation was used (1.54178 Å) in

dx.doi.org/10.1021/cg500502j | Cryst. Growth Des. 2014, 14, 4383−4393

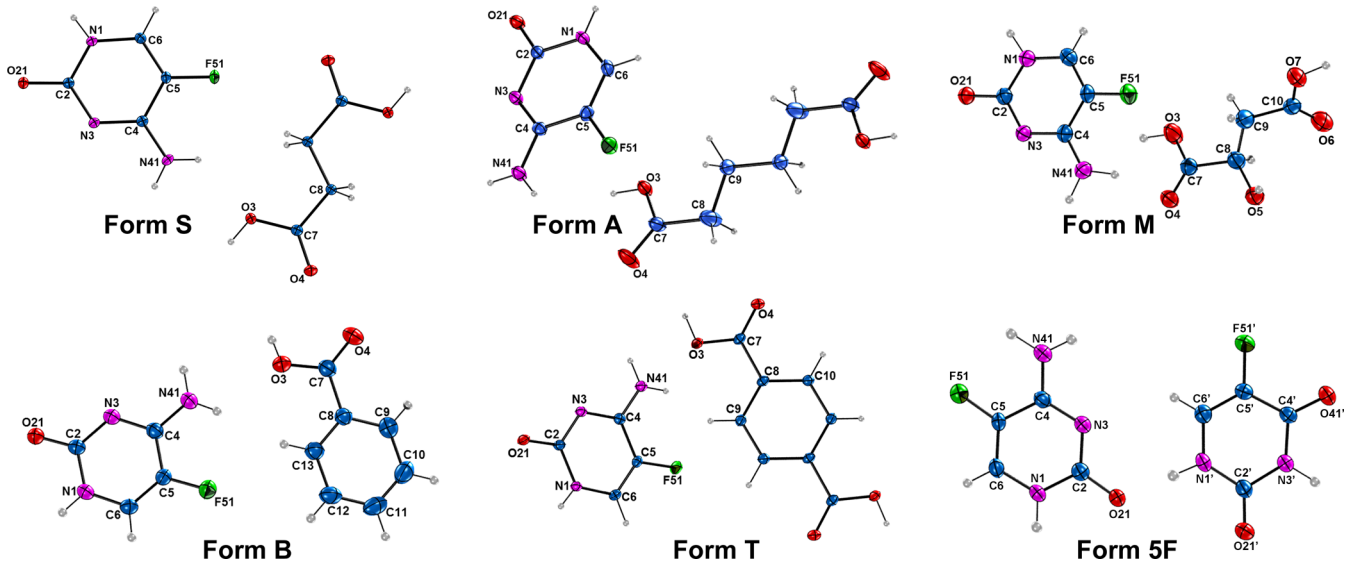

Figure 1. ORTEP-3[36] type view of the 5-FC cocrystals. Thermal ellipsoids for forms S, A, and T are at the 50% probability level and for forms M, B, and 5F at the 30% probability level. Hydrogen atoms are drawn as spheres of arbitrary radii.

the same equipment. X-ray diffraction data collection (φ scans and ω scans with κ offsets) for the cocrystals of 5-FC with malic and benzoic acids were performed on an Enraf-Nonius Kappa-CCD diffractometer (95 mm CCD camera on κ-goniostat) using graphite-monochromated Mo$K\alpha$ radiation (0.71073 Å). For refinement details[28−34] see the Supporting Information.

In all cases, the programs MERCURY (version 2.3)[35] and ORTEP-3[36] were used also within WinGX v1.70.01[32] to prepare the crystallographic information file (CIF) and artwork representations for publication.

The CIFs of the three 5-FC cocrystals were deposited in the Cambridge Structural Data Base under the codes CCDC 933072 (cocrystal of 5-FC with adipic acid), CCDC 933073 (cocrystal of 5-FC with succinic acid), CCDC 933074 (cocrystal of 5-FC with terephtalic acid), CCDC 991413 (cocrystal of 5-FC with 5-FU), CCDC 991431 (cocrystal of 5-FC with malic acid) and CCDC 991584 (cocrystal of 5-FC with benzoic acid). Copies of these files may be solicited free of charge from The Director, CCDC, 12 Union Road, Cambridge, CB2 1EZ, UK, fax: + 44123−336−033; e-mail: deposit@ccdc.cam.ac.uk or http:www.ccdc.cam.ac.uk.

3. RESULTS

3.1. Structure Determination. We adopt the following nomenclature for the cocrystals depicted herein: form S (cocrystal of 5-FC with succinic acid), form T (cocrystal of 5-FC with terephtalic acid), form B (cocrystal of 5-FC with benzoic acid), form M (cocrystal of 5-FC with malic acid), form A (cocrystal of 5-FC with adipic acid), and form 5F (cocrystal of 5-FC with 5-FU). Table 1 exhibits the crystallographic data for the structures.

3.2. Structural Description. A detailed description of the structures is depicted below. The main hydrogen-bond metrics for each cocrystal are listed in Table S1 (Supporting Information). In Figure 1, an ORTEP-3[36] view of the asymmetric unit of each cocrystal is shown. The structure and data for form 5F will be depicted in a separate section.

Cocrystal of 5-FC with Succinic Acid. The asymmetric unit of form S (Figure 1) exhibits one 5-FC molecule as well as a succinic acid, the latter sitting on a crystallographic inversion center giving just half of this molecule per asymmetric unit. Bifurcated hydrogen bonds (N41−H41A···O3 and O3−H3···O21) occur among the acid and two 5-FC molecules (Figure 2a). These interactions lead the 5-FC molecules to interact with each other forming a $R_2^2(8)$ motif[37a,b] (Figure 2a) assembled via complementary N41−H41···N3 hydrogen bonds and also promote the formation of a nonclassical C6−H6···O4 (bond

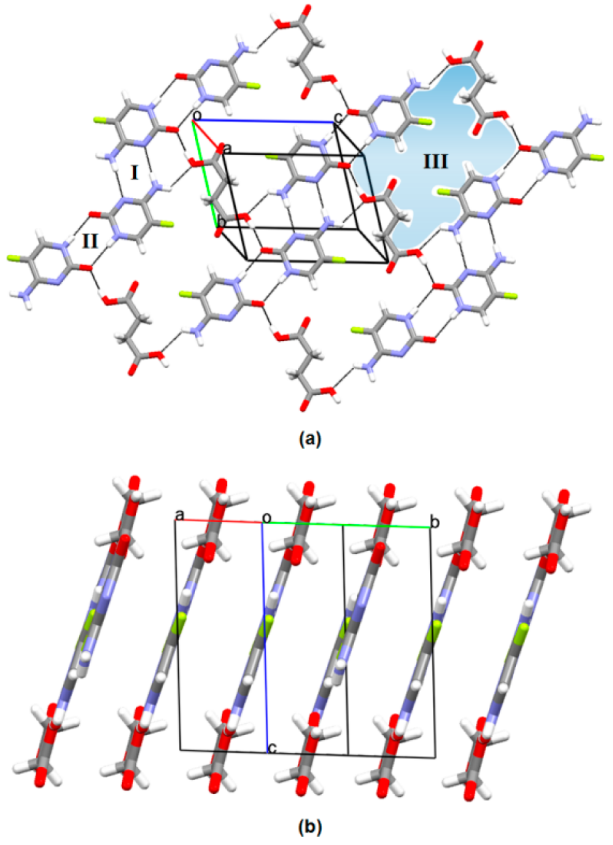

Figure 2. (a) Crystal packing diagram of form S. Black dashed lines indicate hydrogen bonds, (I) refers to the $R_2^2(8)$ motif[37a,b] involving the N−H···N 5-FC homodimers, (II) to the $R_2^2(8)$ motif[37a,b] involving the N−H···O 5-FC homodimers, and (III) to the $R_6^4(40)$ motif,[37a,b] (b) three-dimensional hydrogen-bonded network of form S.

dx.doi.org/10.1021/cg500502j | Cryst. Growth Des. 2014, 14, 4383−4393

length of 2.071 Å) one. A second $R_2^2(8)$ motif is observed between the 5-FC molecules, involving complementary N1−H1···O21 hydrogen bonds, leading to the formation of 1-D tapes which run parallel on both sides of the acid molecule. This arrangement of the molecules in the crystal lattice gives rise to the formation of cavities with graph set $R_6^4(40)$ and constitutes flat layers offset stacked along [$\bar{1}$21]. The stacking of the layers (Figure 2b) is kept only by van der Waals contacts, of the types C···O, C···F, and C···N, which results in an interlayer separation of approximately 3.20 Å to one another (van der Waals radii[38] for C = 1.70 Å, N = 1.55 Å, O = 1.52 Å and F = 1.47 Å).

Cocrystal of 5-FC with Adipic Acid. The asymmetric unit of form A (Figure 1) also exhibits one molecule of 5-FC and half adipic acid since, as mentioned previously, it is sitting on an inversion center. The crystal packing preserve similar intermolecular interaction patterns such as the ones found for form S (Figure 3a): two $R_2^2(8)$ motifs, constituted via complementary N41−H41···N3 and N1−H1···O21 hydrogen bonds between 5-FC molecules and a bifurcated (N41−H41A···O3 and O3−H3···O21) interaction between 5-FC molecule and both carboxyl groups of the acid, also resulting in the formation of the nonclassical C6−H6···O4 (bond length of 2.109 Å) intermolecular interaction plus a C8−H8···F51 (bond length of 2.444 Å) one. In this way, the forms S and A exhibit a similar arrangement of the molecules in the crystal lattice. However, as a result of the increase in the length of the carbon chain in the adipic acid, the cavity formed (Figure 3a) possess a graph set of $R_6^4(48)$, and the layers are not as flat as the ones observed in form S once the adipic acid adopts a zigzag conformation in its carbon chain. The layers are offset stacked along [120], and beyond the van der Waals contacts holding these layers together, there is a nonclassical C9−H9A···F51 (bond length of 2.419 Å) hydrogen bond (Figure 3b).

Cocrystal of 5-FC with Terephtalic Acid. The asymmetric unit of form T (Figure 1) exhibits one 5-FC and half terephtalic acid molecule, for the acid is placed on an inversion center as in forms S and A. As observed in forms S and A, the two 5-FC ring motifs (Figure 4a) and the two 5-FC−acid hydrogen bonds (Figure 4a) plus the nonclassical C6−H6···O4 (bond length of 2.201 Å) are preserved in form T. As a consequence of the close packing, a nonclassical C10−H10···F51 (bond length of 2.491 Å) intermolecular interaction overcome. Form

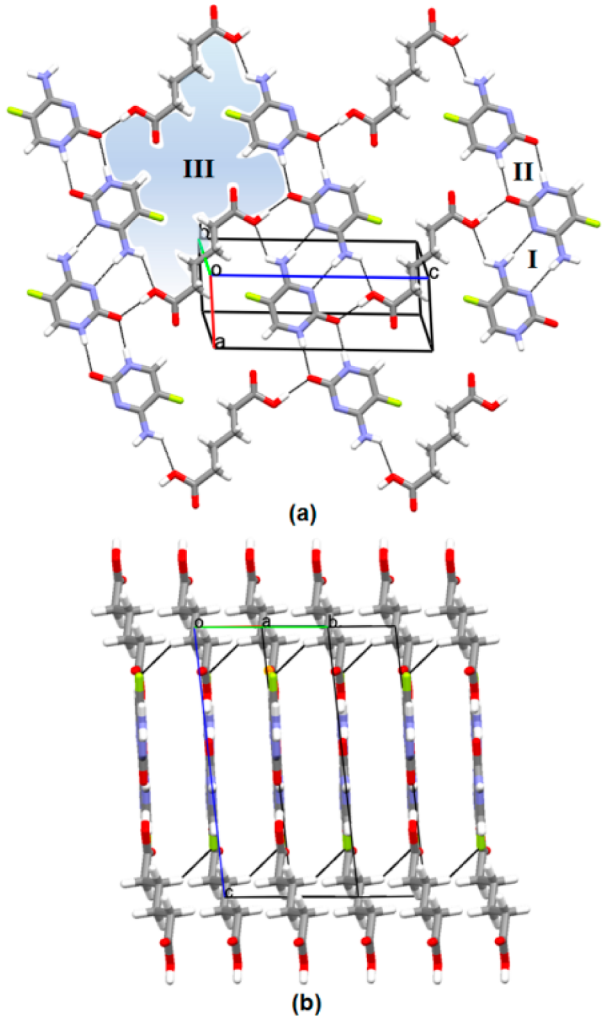

Figure 3. (a) Crystal packing diagram of form A. Black dashed lines indicate hydrogen bonds, (I) refers to the $R_2^2(8)$ motif[37a,b] involving the N−H···N 5-FC homodimers, (II) to the $R_2^2(8)$ motif[37a,b] involving the N−H···O 5-FC homodimers, and (III) to the $R_6^4(48)$ motif,[37a,b] (b) three-dimensional hydrogen-bonded network of form A.

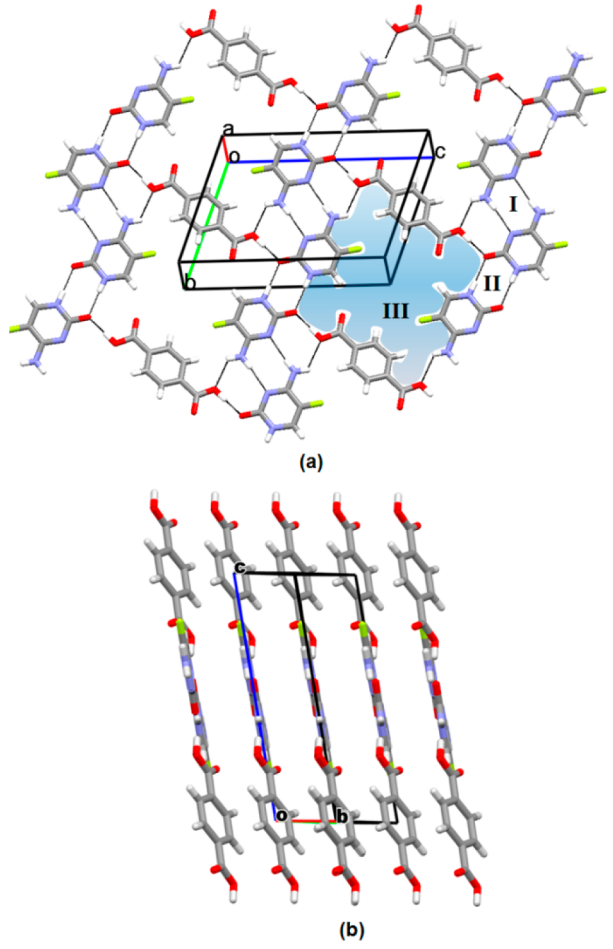

Figure 4. (a) Crystal packing diagram of form T. Black dashed lines indicate hydrogen bonds, (I) refers to the $R_2^2(8)$ motif[37a,b] involving the N−H···N 5-FC homodimers, (II) to the $R_2^2(8)$ motif[37a,b] involving the N−H···O 5-FC homodimers, and (III) to the $R_6^4(44)$ motif,[37a,b] (b) three-dimensional hydrogen-bonded network of form T.

dx.doi.org/10.1021/cg500502j | *Cryst. Growth Des.* 2014, 14, 4383−4393

T also exhibits a similar layered pattern stacked along [110]. The cavities (Figure 4a) formed in this crystalline arrangement adopts a ring graph-set with the $R_6^4(44)$ notation, smaller than the one found in form A. Although both 5-FC and terephtalic acid molecules adopt a planar conformation, they are not aligned in the same plane (Figure 4b). The angle between the plane passing through the non-hydrogen atoms of the 5-FC molecules and the one passing through the terephtalic acid is 26.66(2)°. The terephtalic molecules are stacked as the 5-FC ones, in a fashion that $\pi\cdots\pi$ interactions take place (centroid−centroid distance equal to 3.6265(3)Å for both molecules), being mainly responsible for the maintenance of form T crystalline packing.

Cocrystal of 5-FC with Benzoic Acid. The asymmetric unit of form B (Figure 1) exhibits one molecule of 5-FC and one of benzoic acid. The arrangement of the 5-FC molecules follows the same pattern observed for form T, with the two 5-FC ring motifs[37a,b] (Figure 5a) and the two 5-FC−acid hydrogen bonds preserved as is the nonclassical C6−H6···O4 (bond length of 2.071 Å). The 1-D tapes of the 5-FC molecules are surrounded by benzoic acid molecules forming stacked layers sustained only by van der Waals contacts with an interlayer separation of approximately 5.432 Å (Figure 5b). The neighboring layers are twisted 74.25° with respect to each other, forming a herringbone pattern. This supramolecular pattern arises from unconventional hydrogen bonds (Table S1 in the Supporting Information) involving fluorine atoms of the 5-FC and carbon atoms (C11 and C13) of the benzoic acid molecules (Figure 5a). As is observed in form T, the benzoic acid molecules are not exactly placed on the same plane of the 1-D tape. However, the angle between the mean plane defined by the non-hydrogen atoms of the 5-FC and the non-hydrogen atoms of the benzoic acid molecule is smaller in form B than in form T, assuming a value of 20.43°.

Cocrystal of 5-FC with Malic Acid. The asymmetric unit of form M (Figure 1) exhibits one 5-FC and one molecule of malic acid. In contrast to the other forms, form M preserves only the $R_2^2(8)$ motif accessed via complementary N1−H1···O21 hydrogen bonds among the 5-FC molecules, like that observed in the other cocrystals (Figure 6a). However, a second $R_2^2(8)$ motif is inherent of form M and arises from the interactions of 5-FC molecules with surrounding malic acid molecules (O3−H3···N3 and N41−H41B···O4), constituting a heterodimer (Figure 6a). Additional hydrogen bonds (N41−H41A···O5 and O7−H7···O21) lead to the formation of flat layers stacked along the *c* axis and of a cavity represented by the $R_6^4(36)$ graph-set notation[37a,b] (Figure 6a). The layers are held together via O5−H5···O6 hydrogen bonds involving the malic acid molecules and also via $\pi\cdots\pi$ interactions (centroid−centroid distance equal to 3.495(9)Å) between the rings of the 5-FC molecules (Figure 6b).

4. DISCUSSION

We have conducted cocrystallization experiments with 5-FC and five dicarboxylic acids presenting the following pK_a values: 4.43 (adipic acid), 4.21 (benzoic acid), 4.16 (succinic acid), 3.52 (terephtalic acid) and 3.40 (malic acid). These acids were chosen in an attempt to evaluate the extent of proton transfer to the 5-FC molecules, based on the pK_a rule,[26,27,39] contributing to the study of the salt/cocrystal continuum and providing information related to the capability of predicting and controlling the synthesis of compounds containing the fluoropyrimidine group.

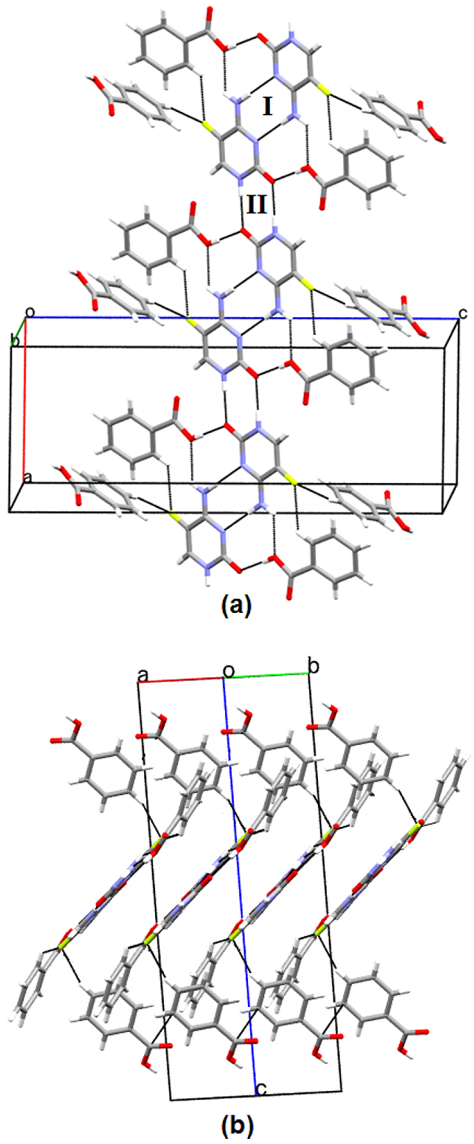

Figure 5. (a) Crystal packing diagram of form B. Black dashed lines indicate hydrogen bonds, (I) refers to the $R_2^2(8)$ motif[37a,b] involving the N−H···N 5-FC homodimers and (II) $R_2^2(8)$ motif[37a,b] involving the N−H···O 5-FC homodimers, (b) three-dimensional hydrogen-bonded network of form B.

As the pK_a value for the 5-FC is 3.26, then the respective values of ΔpK_a ($pK_{aacid} - pK_{abase}$) for adipic, benzoic, succinic, terephtalic, and malic acids are −1.16, −0.95, −0.9, −0.26, and −0.14 ranging from close to zero to more negative values. According to Bhogala et al.,[27] for negative values of ΔpK_a a cocrystal formation is expected. One method of verifying successful cocrystal formation is to calculate the C−O bond length differences of the carboxyl groups in the acid molecule, ΔD_{C-O}. If this variation is small (<0.03 Å), then a salt is formed. If, however, this difference is higher than 0.08 Å, then a cocrystal is formed. For all the structures depicted here, the ΔD_{C-O} values are above 0.08 Å (form S = 0.117(1) Å, form A = 0.119(3) Å, form T = 0.114(2) Å, form B = 0.121(2) Å, and form M = 0.109(5) Å), which means that the C−O distances are not symmetrical, as in the carboxylate anions, evidencing cocrystal formation.

4.1. Supramolecular Analysis. In our previous manuscript,[22] we synthesized three 5-FC salts also using as coformers

dx.doi.org/10.1021/cg500502j | *Cryst. Growth Des.* 2014, 14, 4383−4393

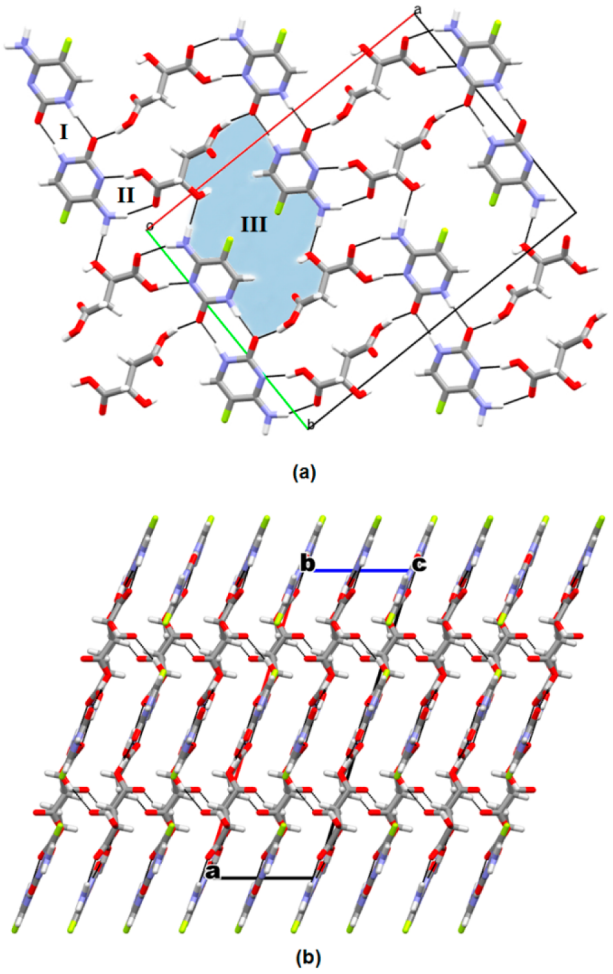

Figure 6. (a) Crystal packing diagram of form M. Black dashed lines indicate hydrogen bonds, (I) refers to the $R_2^2(8)$ motif[37a,b] involving the N−H···O 5-FC homodimers, (II) to the $R_2^2(8)$ motif[37a,b] involving the N−H···O and O−H···N 5-FC heterodimer, and (III) to the $R_6^4(36)$ motif,[37a,b] (b) three-dimensional hydrogen-bonded network of form M.

dicarboxylic acids: fumaric, maleic, and oxalic. The structures were obtained from the continuum to the salt part of the spectrum, according to the pK_a rule, where the ΔpK_a value ranged between 0 and positive values. Due the complementarity among the carboxylic group and the functional groups present in the 5-FC molecules, all the salts exhibited the same $R_2^2(8)$ motif, constituting heterodimers, via N41−H41A···O4 and $N3^+$−H3···$O3^-$ hydrogen bonds. The same supramolecular synthon was observed for the salicylate of 5-FC, reported by Portalone and Colapietro in 2007.[20] On the other hand, when we go to the other side of the spectrum, i.e., when weaker dicarboxylic acids are used as coformers, changes occur in the ionicity of the 5-FC molecule and new supramolecular synthons overcome. According to Mukherjee and Desiraju,[40] cocrystal formation is usually expected to occur when heterosynthons are formed over homosynthons. However, for the cocrystals of 5-FC with succinic, adipic, benzoic, and terephtalic acids, instead of heterodimers we observe homodimers occurring among the 5-FC molecules accessed through complementary N41−H41···N3 and N1−H1···O21 hydrogen bonds. Nevertheless, for a ΔpK_a very close to 0 ("cutoff" among cocrystals and salts for this fluoropyrimidine), as in form M (ΔpK_a = −0.1), a supramolecular transition synthon is observed. In this cocrystal, the crystal packing still preserves the heterodimer observed in the salts, except for the fact that no proton transfer is observed, but also exhibits the N1−H1···O21 homodimer among the 5-FC molecules. For this homodimer, which is common in all cocrystals, the 5-FC carbonyl bond lengths go from 1.265 to 1.249 Å. These values are significantly higher than the ones found for the 5-FC salts (1.232 to 1.219 Å). It is clear that this feature is the result of the protonation where the charge redistribution implies on a reduction of the carbonyl bond lengths, which, in turn, does not favor the geometric requirements for the formation of the synthon needed for the establishment of the homodimers present in the cocrystals. However, the geometric features of the form M show intermediate values for the carbonyl bond lengths, suggesting a partial charge redistribution that may lead to a hybrid salt/cocrystal specie. Indeed, this form shows the salts heterodimer synthon, even without protonation, possibly due the intermediate strength of malic acid (pK_a = 3.40). This transition state becomes clearer when a correlation plot between the variations of the C−O bond lengths in the carboxylic fragments (ΔD_{C-O}) of the coformers and the variations of the C−N bond lengths (ΔD_{C-N}) of the imidic fragments of the 5FC ring is carried out (Figure 7). It is worth

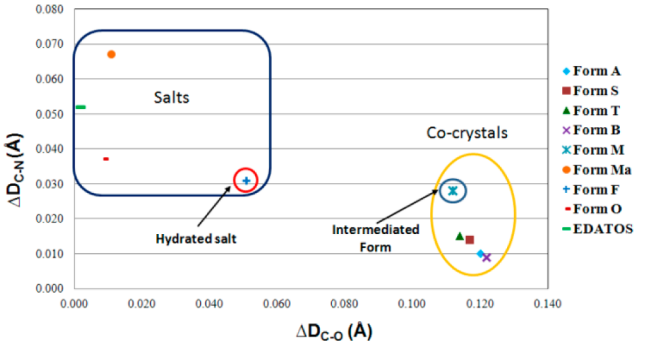

Figure 7. Correlation between the C−N bond length differences, ΔD_{C-N}, of the imidic group of 5-FC ring vs the C−O bond length differences of the carboxylic fragments, ΔD_{C-O}, evidencing the intermediary interface between salts/cocrystals of form M. The forms Ma, F, O, and EDATOS refer to the salts of 5-FC with maleic, fumaric, oxalic, and salycilic acids.[19,22]

mentioning that the fumarate salt of 5-FC[22] (form F) is hydrated, and the presence of water molecules in its crystal packing result in changes in the intermolecular interaction patterns leading to a different behavior of the 5-FC intramolecular bond lengths approximating its ΔD_{C-N} values to the ones found for form M.

In an attempt to understand which changes occur in the 5-FC molecule and consequently the specific supramolecular patterns formed, the UNI Force Field Calculations, a tool of the Mercury crystallography package,[41,42] was used to establish and compare the intermolecular potentials of the main interactions. It is important to highlight that the purpose of this application is to display those interactions between molecules which are most significant in energetic terms without performing the computationally expensive lattice energy calculations. This study allowed us to determine that in most of the cases the potentials of the complementary N1H1···O21 hydrogen bonds are the strongest ranging between −9.1 to −7.6 kcal/mol, with the exception of form T and form M. Since this homodimer was recurrent in all the cocrystals of 5-FC, this synthon can be

dx.doi.org/10.1021/cg500502j | Cryst. Growth Des. 2014, 14, 4383−4393

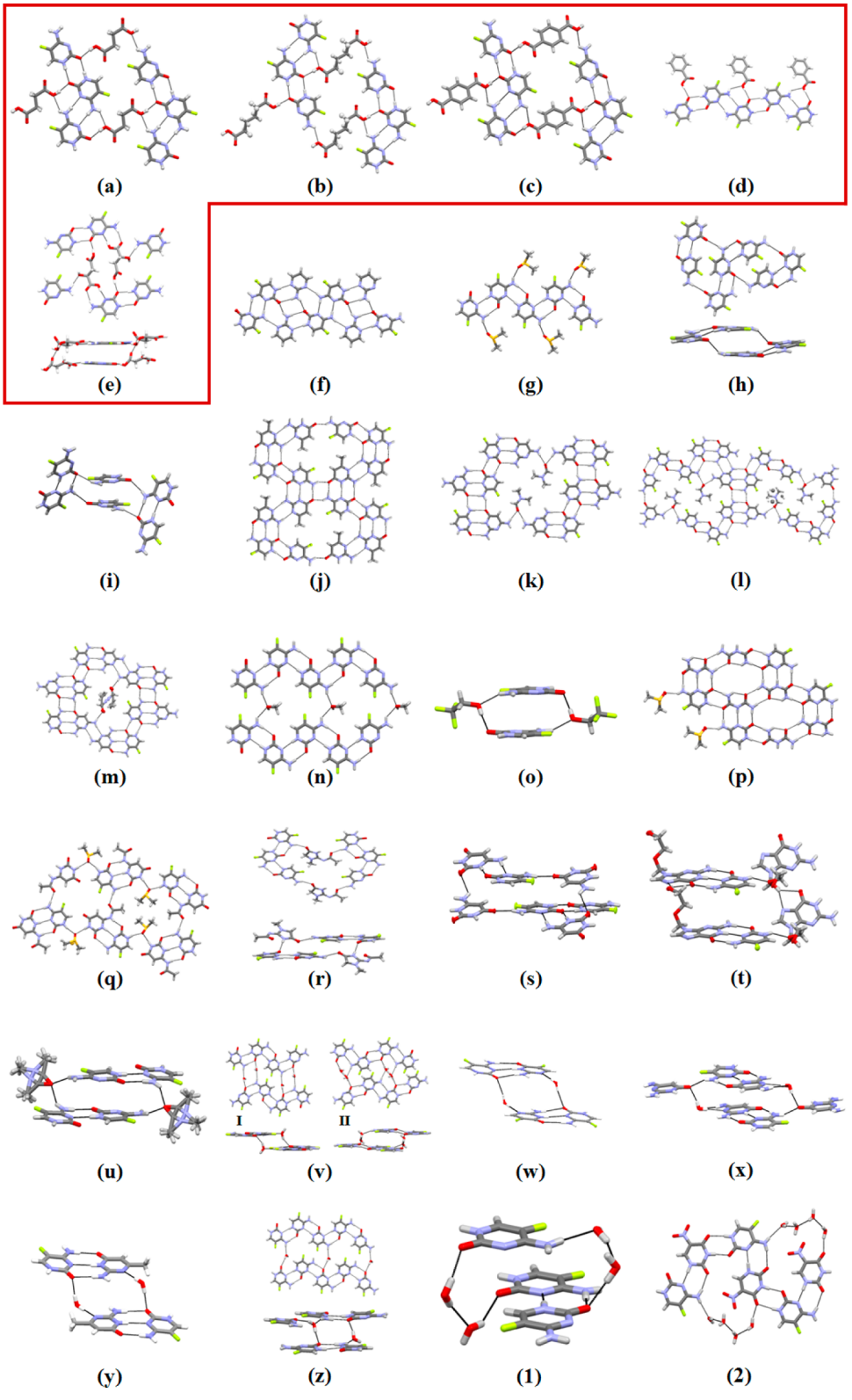

Figure 8. Comparison of the supramolecular structure of different 5-FC solid forms containing just neutral 5-FC molecules: (a) form S, (b) form A, (c) form T, (d) form B, (e) form M, (f) cocrystal under refcode MECTUL,[24] (g) solvate under refcode DUKWAI,[17] (h) polymorph under refcode MEBQEQ,[15] (i) polymorph under refcode MEBQEQ01,[15] (j) cocrystal under refcode MECXID,[25] (k) cocrystal under refcode MECVUN,[24] (l) cocrystal under refcode MECWAU[24] and (m) cocrystal under refcode MECWEY,[24] (n) solvate under refcode MEBQOA,[15] (o) solvate under refcode MEBQIU,[15] (p) cocrystal under refcode MECWUO,[25] (q) cocrystal under refcode MECXEZ,[25] (r) cocrystal under refcode MECVEX,[24] (s) cocrystal under refcode MECVIB,[24] (t) cocrystal under refcode MECWOI,[24] (u) solvate under refcode DUKWEM,[17] (v) hydrates of 5-FC (I) under refcodes BIRMEU,[14] BIRMEU01,[16] BIRMEU02,[15] and (II) under refcode BIRMEU03,[15] (w) hydrate under refcode PANLAS,[18] (x) hydrated cocrystal under refcode MECVOH,[24] (y) hydrated cocrystal under refcode MECXOJ,[25] (z) hydrate under refcode DUKWIQ,[17] (1) hydrate under refcode MEBQUG[15] and (2) hydrated cocrystal under refcode GATMUL.[23]

dx.doi.org/10.1021/cg500502j | *Cryst. Growth Des.* 2014, 14, 4383−4393

Table 2. Distribution of the Main Supramolecular Synthons Observed for the Different 5-FC Solid Forms Containing Just Neutral 5-FC

	N−H···O, N−H···N		N−H···O		N−H···N		C≡G-like base pairing				
structure[a]	homo	hetero	homo	hetero	homo	hetero	homo	hetero	planar cavity	tubular cavity	5-FC ribbons
a			√		√				√		√
b			√		√				√		√
c			√		√				√		√
d			√		√					√	√
e			√	√					√	√	
f		√			√						
g	√										
h	√									√	
i	√									√	
j			√					√	√		
k			√					√	√		
l	√		√					√	√		
m			√					√	√		
n	√								√		√
o	√									√	√
p				√				√	√		
q								√	√		
r	√								√	√	√
s		√	√							√	
t								√		√	
u	√							√		√	√
v(I)	√									√	√
v(II)			√		√					√	√
w							√			√	√
x								√		√	
y								√		√	
z	√								√	√	√
1	√									√	√
2		√		√					√		

[a]Comparison of the supramolecular structure of different 5-FC solid forms containing just neutral 5-FC molecules: (a) form S, (b) form A, (c) form T, (d) form B, (e) form M, (f) cocrystal under refcode MECTUL,[24] (g) solvate under refcode DUKWAI,[17] (h) polymorph under refcode MEBQEQ,[15] (i) polymorph under refcode MEBQEQ01,[15] (j) cocrystal under refcode MECXID,[25] (k) cocrystal under refcode MECVUN,[24] (l) cocrystal under refcode MECWAU[24] and (m) cocrystal under refcode MECWEY,[24] (n) solvate under refcode MEBQOA,[15] (o) solvate under refcode MEBQIU,[15] (p) cocrystal under refcode MECWUO,[25] (q) cocrystal under refcode MECXEZ,[25] (r) cocrystal under refcode MECVEX,[24] (s) cocrystal under refcode MECVIB,[24] (t) cocrystal under refcode MECWOI,[24] (u) solvate under refcode DUKWEM,[17] (v) hydrates of 5-FC (I) under refcodes BIRMEU,[14] BIRMEU01,[16] BIRMEU02,[15] and (II) under refcode BIRMEU03,[15] (w) hydrate under refcode PANLAS,[18] (x) hydrated cocrystal under refcode MECVOH,[24] (y) hydrated cocrystal under refcode MECXOJ,[25] (z) hydrate under refcode DUKWIQ,[17] (1) hydrate under refcode MEBQUG[15] and (2) hydrated cocrystal under refcode GATMUL.[23]

considered a key piece in the assembly of the cocrystal packing. On the other hand, the complementary N41−H41···N3 hydrogen bonds (present in the forms A, S, T, and B) show smaller potential values ranging between −5.5 to −4.9 kcal/mol. As previously discussed, form M represents an intermediate state in the border of the salt−cocrystal continuum. Instead of the N41−H41···N3 hydrogen bonds present in the homodimers, we observed interactions occurring among the 5-FC molecule and the malic acid one (N41−H41B···O4 and O3−H3···N3), this heterosynthon being typical of the organic acid salts.[19,22] The potential value of this synthon for form M is −9.7 kcal/mol, and this one is the highest potential observed for all interactions present in this crystalline form, showing that stronger acids have the ability of competing for these interactions, thus replacing the weaker N−H···N ones.

In addition, the study of the intermolecular potentials also allows us to evaluate the strength of the $\pi\cdots\pi$ interactions between the layers formed by the 5-FC-acids units. These interactions have potentials ranging from −9.6 to −4.9 kcal/mol, agreeing in all the cases with the proximity of the layers in the 3D supramolecular arrangements. A correlation is observed between the energy of these interactions and the distance of the layers. form M, which displays the closest distance between the layers, also exhibits a high potential (−8.2 kcal/mol) for the $\pi\cdots\pi$ interactions, whereas the highest potential observed to the $\pi\cdots\pi$ interactions was between terephthalic acid units of form T (−9.6 kcal/mol). All the potentials calculated are summarized in Tables A7, B7...E77 (see the Supporting Information, Sections A−E).

Extending our supramolecular study for the neutral 5-FC molecules, a comparative analysis was performed on the basis of all the crystalline structures already reported containing 5FC molecules. Polymorphs, solvates, and cocrystals, plus mixtures of them, such as solvated cocrystals, were also considered. 5-FC is a rigid molecule and presents three potential patterns of hydrogen bonding sites, two acceptor−donor involving the atoms O21−N1 and N3−N41 (ON and NN, respectively), and one acceptor−acceptor−donor involving the atoms O21−N3−

N41 (ONN). Tutughamiarso and co-workers[17] showed that the 5-FC molecule, when neutral, tends to interact to one another by self-complementary homodimers, constituting planar or tubular 5-FC ribbons. These homodimers, as observed in the cocrystals depicted here, are essentially composed by one N−H···O and one N−H···N (ON/NN), or by two N−H···O (ON/ON), or even by two N−H···N (NN/NN) intermolecular interactions. Complementing this claim, Figure 8 exhibits a schematic drawing of the classical intermolecular interactions of each reported structure considering the whole supramolecular architecture adopted by the 5-FC molecules under the different crystalline arrangements. It shows that not only ribbons are observed, but also planar and/or tubular cavities, mainly due to the intrinsic geometry of the ON, NN, ONN hydrogen bonding sites. Furthermore, Table 2 exhibits a statistical analysis of the distribution of the main supramolecular synthons observed for the 5-FC molecule, including homo- and heterodimers involving the three main hydrogen bonding sites (ON/ON, ON/NN and NN/NN) plus the formation of homo- and heterotrimers with hydrogen bonding patterns similar to the C≡G Watson and Crick base pairing.

According to Table 2, the 5-FC molecule tends to form ON/NN, ON/ON, and NN/NN homodimers. Tutughamiarso and co-workers[17] observed the particular NN/NN homodimer formation only in the hydrate under refcode BIRMEU03,[15] reporting later a cocrystal of 5-FC under refcode MECTUL[24] also exhibiting this pattern of NN/NN homodimer formation. The forms S, T, A, and B, however, exhibit the same ribbon formation that occurs for the hydrate under refcode BIRMEU03,[15] i.e., ON/ON and NN/NN $R_2^2(8)$ motifs[37a,b] per 5-FC molecule, while in the 5-FC cocrystal under refcode MECTUL[24] the free ON site of the 5-FC molecule is intercepted by the formation of a ON/NN heterodimer with the coformer molecule. In addition, two ON/NN (refcodes MECVIB[24] and e GATMUL[23]) and two ON/ON heterodimers (refcodes MECWUO[25] and GATMUL[23]) are observed. However, no NN/NN heterodimer was reported until the present.

On the other hand, for the ONN C≡G-like base pairing, the tendency is the formation of heterosynthons with a total of nine structures. Only in one hydrate (refcode PANLAS[18]) the C≡G-like base pairing is observed between the 5-FC molecules. By analyzing the crystalline packing of the 5-FC cocrystal under refcode MECTUL[24] (see Figure 8f), the occurrence of one ON/NN heterodimer disrupts the 5-FC ribbon formation. Although homoribbons (i.e., ribbons constituted only by 5-FC molecules) are prevalent in most of the crystalline structures, 12 of them exhibit heteroribbons and all refer to cocrystals (2 cocrystals and 10 solvated cocrystals).

By considering the cavity formation, two exceptions arise, one referring to the cocrystal under refcode MECTUL[24] (Figure 8f), where flat layers are stacked by van der Waals contacts and one referring to the solvate under refcode DUKWAI[17] (Figure 8g), for which small cavities are observed only when the nonclassical C−H···O and C−H···F intermolecular interactions between the dimethyl sulfoxide and 5-FC molecules are considered. Both reported polymorphs of 5-FC exhibit tubular patterns (Figure 8h, (i), constituting $R_4^4(24)$ and $R_6^4(26)$ motifs, involving four and six 5-FC molecules, respectively. Forms S, A, and T (Figure 8a−c) exhibit similar cavities, differing only in their size ($R_6^4(40)$, $R_6^4(48)$, $R_6^4(44)$, for forms S, A, and T, respectively), proportional to the size and the geometry of each acid molecule. Figure 8h exhibits the last planar cavity, $R_7^6(44)$, involving only solid coformers, concerning the cocrystal under refcode MECXID.[25] When solvents are involved in the interactions, they lead to planar and tubular cavities, for which it is not possible to establish a specific pattern for these ternary systems. In particular, the cocrystal under refcode MECVEX[24] (Figure 8r) and the hydrate under refcode DUKWIQ[17] (Figure 8z) display cavities of both tubular and planar types. It is worth mentioning that the planar cavities of the methanol solvate under refcode MEBQOA[15] (Figure 8 (l)), of the cocrystal under refcode MECVEX[24] (Figure 8r) and of the hydrate under refcode DUKWIQ[17] (Figure 8z), are similar to the one formed in forms S, A, and T. This shows that the recurrent supramolecular synthon observed for the cocrystals depicted herein is not restricted to the use of carboxylic acids as coformers. In this way, it could be expected that new structures containing 5-FC molecule can be designed and developed as new tailor-made drugs.

4.2. Cocrystal of 5-FC and 5-FU. 5-Fluorouracil, 5-fluoro-2,4-(1H,3H)-pyrimidinedione, is an antineoplastic API rationally designed by Heidelberger and co-workers in 1957.[43] It is used for the treatment of superficial skin carcinomas as a cream formulation and as injections in the treatment of various cancers, including, among others, gastrointestinal, head and neck, breast, colorectal, and ovarian. 5-FU is a synthetic pyrimidine analogue and is probably the most widely used, being of great interest in the clinical and experimental chemotherapy among the developed analogues of purine and pyrimidine, as it is structurally similar to natural bases. Nevertheless, only a fraction of the administered amount of this API becomes available in the systemic circulation after oral administration due to its poor water solubility.[44−46] Indeed, oral delivery of antineoplastic APIs is considered a challenge due their physical and chemical properties and physiological barriers.[47]

As an illustration of a controlled rational supramolecular synthesis of new solid forms of a given API using 5-FC as coformer, we designed a cocrystal of 5-FC and 5-FU (form 5F, pK_a = 8.0).[44] It is clear that the 5-FU was our first molecule of choice for this example due to its structural similarities with 5-FC. The cocrystallization experiment was developed according to the pK_a rule and a cocrystal was expected (ΔpK_a = −4.74). The aim of this particular experiment was to design a new solid form of 5-FU with enhanced physical and chemical properties that could enable this API to be orally administered together with 5-FC, which in turn exhibits high solubility and bioavailability profiles.[10] However, the solubility properties of form 5-FU are still under investigation.

The asymmetric unit of form 5F (see Figure 1) exhibits one molecule of 5-FC and one of 5-FU. The main intermolecular interactions responsible for maintaining the crystalline arrangement of this cocrystal are of the types N−H···O and N−H···F (see Table S1 in the Supporting Information section), including the formation of homodimers of 5-FC (I, in Figure 9a), homodimers of 5-FU (II, in Figure 9a) and intermolecular interactions among the 5-FC and 5-FU molecules (Figure 9a). Nonclassical intermolecular interactions are also present, as a result of the close packing: C6−H6···F51 (bond distance of 2.467 Å), C6′−H6′···F51′ (bond distance of 2.354 Å), C6′−H6′···N3 (bond distance of 2.639 Å), and C6−H6···O21′ (bond distance of 2.553 Å). The crystal packing of form 5F is composed of flat tapes in which the dimers are interspersed. These tapes are stacked constituting columns with a parallel

dx.doi.org/10.1021/cg500502j | Cryst. Growth Des. 2014, 14, 4383−4393

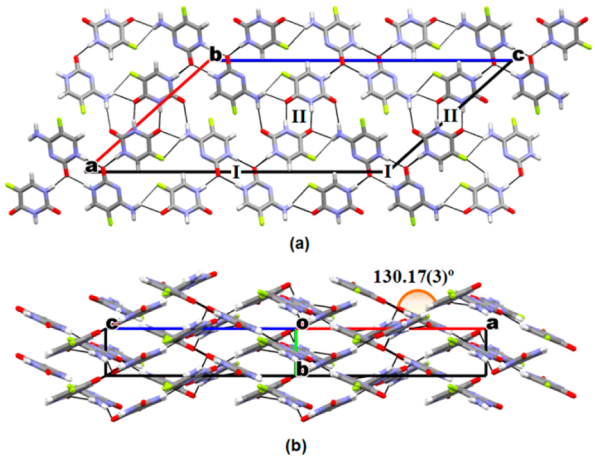

Figure 9. (a) Crystal packing diagram of form 5f. Black dashed lines indicate hydrogen bonds, (I) refers to the $R_2^2(8)$ motifs[37a,b] involving the N−H···O homodimers occurring among 5-FC molecules and (II) correspond to $R_2^2(8)$ motifs[37a,b] involving the N−H···O homodimers occurring among 5-FU molecules, (b) three-dimensional hydrogen-bonded network of form 5f.

displaced arrangement (displacement angle of 23.2°), maintained by $\pi\cdots\pi$ interactions (5-FC$_{\pi\cdots\pi}$ = 3.5604(9) Å and 5-FU$_{\pi\cdots\pi}$ = 3.5603(9)Å). Adjacent tapes (and consequently adjacent columns) exhibit two directions of growth and are connected to one another by intermolecular interactions between the molecules of 5-FC and 5-FU, forming a dihedral angle of 130.17(3)° (Figure 9b).

5. CONCLUSION

The 5-FC cocrystals with succinic, adipic, benzoic, and tereftalic acids were obtained following the tendency of the pK_a rule and have revealed a similar hydrogen-bonding pattern, leading to 5-FC ribbons, stabilized by two $R_2^2(8)$ motifs, characterized by complementary homodimeric N−H···N (NN/NN) and N−H···O (ON/ON) interactions, which was found to be a feature of cocrystals containing this fluoropyrimidine molecules. Analyzing the supramolecular characteristics of the four 5-FC cocrystals (together with some similar structures reported in the literature), it was observed that the 5-FC molecule tends to form ON/NN, ON/ON, and NN/NN homodimers, ONN C≡G-like base pairing heterotrimers, and both tubular and planar cavities. Nevertheless, when the cocrystallization experiment was conducted with malic acid, where the $\Delta pK_a = -0.1$, a supramolecular transition synthon was observed, in which the N−H···O homodimeric synthon present in the cocrystals remains, but a new heterodimeric synthon, characterized by complementary N−H···O hydrogen bonds between the 5-FC molecule and the malic acid, emerged. This last synthon was found in the 5-FC organic salts, obtained even from very small positive ΔpK_a values (such as for the fumarate of 5-FC where $\Delta pK_a = 0.23$). The discovery of this transition synthon indicates that the 5-FC molecule is a suitable candidate for the design and development of cocrystallization experiments based on crystal engineering techniques, once its behavior could be, until the present, well predicted by the pK_a rule. To check our hypothesis, we conducted a cocrystallization experiment of 5-FC with the antineoplastic drug 5-FU, aiming to obtain a cocrystal once the system exhibits a $\Delta pK_a = -3.0$. The success of this experiment points to a new path to apply 5-FC as a coformer in new controlled crystallization experiments for the development of new tailor-made drugs.

■ ASSOCIATED CONTENT

Supporting Information

Crystallographic data of the 5-FC, calculated potentials. This material is available free of charge via the Internet at: http://pubs.acs.org/.

■ AUTHOR INFORMATION

Corresponding Author

*E-mail: javiere@ifsc.usp.br. Phone: +55 16 3373 8096. Fax: +55 16 3373 9881.

Notes

The authors declare no competing financial interest.

■ ACKNOWLEDGMENTS

We thank CAPES (C.C.P.S.), FAPESP (J.C.T Project No. 2013/07581-9) and CNPq (J.E., R.O.P., C.C.M. Project No. 150076/2013-4) for the financial support. We also thank for the use of the APEX II Bruker difractometer to "Facility for advanced studies of materials/FAMa" (FAPESP Project No. 2009/540354).

■ REFERENCES

(1) Almarsson, Ö.; Zaworotko, M. J. *Chem. Commun. (Cambridge)* **2004**, *17*, 1889−1896.
(2) Blagden, N.; de Matas, M.; Gavan, P. T.; York, P. *Adv. Drug Delivery Rev.* **2007**, *59* (7), 617−630.
(3) Bond, A. D. In *Pharmaceutical Salts and Co-Crystals*; Wouters, J.; Quéré, L., Eds.; The Royal Society of Chemistry: Cambridge, UK, 2012; Chapter 2, pp 9−28.
(4) Vishweshwar, P.; McMahon, J. A.; Peterson, M. L.; Hickey, M. B.; Shattock, T. R.; Zaworotko, M. J. *Chem. Commu.* **2005**, *36*, 4601−4603.
(5) Aakeroy, C. B.; Fasulo, M. E.; Desper, J. *Mol. Pharmaceutics* **2007**, *4* (3), 317−322.
(6) Trask, A. V. *Mol. Pharmaceutics* **2007**, *4* (3), 301−309.
(7) GRAS S. Food and Drug Administration, Database of Select Committee on GRAS Substances (SCOGS) Reviews. https://www.accessdata.fda.gov/scripts/fcn/fcnNavigation.cfm?rpt=scogsListing.
(8) Shan, N.; Zaworotko, M. J. *Drug Discovery Today* **2008**, *13* (9−10), 440−446.
(9) Hoffman, M.; Lindeman, J. A. In *Pharmaceutical Salts and Co-crystals*; Wouters, J.; Quéré, L., Eds.; The Royal Society of Chemistry: Cambridge, UK, 2012; Chapter 14, pp 318 − 329.
(10) Vermes, A.; Guchelaar, H.-J.; Dankert, J. *J. Antimicrob. Chemother.* **2000**, *46* (2), 171−179.
(11) Larsen, R. A. In *Essentials of Clinical Mycology*, 2nd ed.; Kauffman, C. A., Pappas, P. G., Sobel, J. D., Dismukes, W. E., Eds.; Oxford University Press, UK, 2003; part 2, pp 57−60.
(12) Mullen, C. A.; Coale, M. M.; Lowe, R.; Blaese, R. M. *Cancer Res.* **1994**, *54* (6), 1503−1506.
(13) Allen, F. H. *Acta Crystallogr. Sect. B* **2002**, *58* (3), 380−388.
(14) Louis, T.; Low, J. N.; Tollin, P. *Cryst. Struct. Commun.* **1982**, *11*, 1059−1064.
(15) Hulme, A. T.; Tocher, D. A. *Cryst.Growth Des.* **2006**, *6* (2), 481−487.
(16) Portalone, G.; Colapietro, M. *Acta Crystallogr., Sect. E* **2006**, *62* (3), o1049−o1051.
(17) Tutughamiarso, M.; Bolte, M.; Egert, E. *Acta Crystallogr., Sect. C* **2009**, *65* (11), o574−o578.
(18) Hulme, A. T.; Tocher, D. A. *Acta Crystallogr., Sect. E* **2005**, *61* (7), 02112−o2113.
(19) Prabakaran, P.; Murugesan, S.; Muthiah, P. T.; Bocelli, G.; Righi, L. *Acta Crystallogr., Sect. E* **2001**, *57* (10), o933−o936.

(20) Portalone, G.; Colapietro, M. *J. Chem. Crystallogr.* **2007**, *37* (2), 141−145.
(21) (a) Perumalla, S. R.; Pedireddi, V. R.; Sun, C. C. *Cryst. Growth Des.* **2013**, *13* (2), 429−432. (b) Perumalla, S. R.; Pedireddi, V. R.; Sun, C. C. *Mol. Pharmaceutics* **2013**, *10* (6), 2462−2466.
(22) Da Silva, C. C. P.; Pepino, R. O.; Tenorio, J. C.; Honorato, S.; Ayala, A. P.; Ellena, J. *Cryst. Growth Des.* **2013**, *13* (10), 4315−4322.
(23) Portalone, G. *Chem. Cent. J.* **2011**, *5* (51), 1−8.
(24) Tutughamiarso, M.; Wagner, G.; Egert, E. *Acta Crystallogr., Sect. B* **2012**, *B68* (4), 431−443.
(25) Tutughamiarso, M.; Egert, E. *Acta Crystallogr., Sect. B* **2012**, *B68* (4), 444−452.
(26) Childs, S. L.; Stahly, G. P.; Park, A. *Mol. Pharmaceutics* **2007**, *4* (3), 323−338.
(27) Bhogala, B. R.; Basavoju, S.; Nangia, A. *CrystEngComm* **2005**, *7*, 551−562.
(28) *Bruker (APEX2)*; Bruker AXS Inc.: Madison, Wisconsin, USA, 2010.
(29) *SAINT*; Bruker AXS Inc.:Madison, Wisconsin, USA., 2007.
(30) *SADABS*; Bruker AXS Inc.: Madison, Wisconsin, USA, 2002.
(31) (a) Sheldrick, G. M. *Acta Crystallogr.* **2008**, *A64*, 112−122. (b) Sheldrick, G. M. *SHELXL-2013*; University of Gottingen: Germany, 2013.
(32) Farrugia, L. J. *J. Appl. Crystallogr.* **2012**, *45* (4), 849−854.
(33) *COLLECT, Data Collection Software*; Nonius: Delft, The Netherlands, 1998.
(34) Otwinowski, Z.; Minor, W. In *Methods in Enzymology: Macromolecular Crystallography*; Carter, C. W., Jr., Sweet, R. M., Eds.; Academic Press: New York, 1997, Part a, Vol. *276*, pp 307−326.
(35) Macrae, C. F.; Bruno, I. J.; Chisholh, J. A.; Edgington, P. R.; McCabe, P.; Pidcock, E.; Rodriguez-Monge, L.; Taylor, R.; van de Streek, J.; Wood, P. A. *J. Appl. Crystallogr.* **2008**, *41* (2), 466−470.
(36) Farrugia, L. J. *J. Appl. Crystallogr.* **1997**, *30* (5), 565.
(37) (a) Etter, M. C. *Acc. Chem. Res.* **1990**, *23* (4), 120−126. (b) Etter, M. C.; MacDonald, J. C.; Bernstein, J. *Acta Crystallogr., Sect. B* **1990**, *46* (2), 256−262.
(38) Bond, A. *J. Phys. Chem.* **1964**, *68* (3), 441−451.
(39) Cruz-Cabeza, A. J. *CrystEngComm* **2012**, *14*, 6362−6365.
(40) Mukherjee, A.; Desiraju, G. *Cryst. Growth Des.* **2014**, *14* (3), 1375−1385.
(41) Gavezzotti, A. *Acc. Chem. Res.* **1994**, *27* (10), 309−314.
(42) Gavezzotti, A.; Filippini, G. *J. Phys. Chem.* **1994**, *98* (18), 4831−4837.
(43) Heidelberger, C.; Chaudhuri, N. K.; Danneberg, P.; Mooren, D.; Griescach, L. *Nature* **1957**, *179*, 663−666.
(44) Malet-Martino, M.; Martino, R. *Oncologist* **2002**, *7* (4), 288−323.
(45) Delori, A.; Eddleston, m.D.; Jones, W. *CrystEngComm* **2013**, *15*, 73−77.
(46) Baker, S. D.; Khor, S. P.; Adjei, A. A.; Doucette, M.; Spector, T.; Donehower, R. C.; grochow, L. B.; Sartorius, S. E.; Noe, D. A.; hohneker, J. A.; Rowinsky, E. K. *J. Clin. Oncol.* **1996**, *14* (12), 3085−3096.
(47) Thanki, K.; Gangwal, R. P.; Sangamwar, A. T.; Jain, T. *J. Controlled Release* **2013**, *170* (1), 15−40.

4 CONCLUSION AND FUTURE PERSPECTIVES

The statistical analysis of structural information via the Cambridge Structural Database, coupled with advances in Crystal Engineering and supramolecular chemistry, opened the doors to an era of rational design and synthesis of new materials. The exploration of the supramolecular synthons approach simplified the analysis/design of the wanted crystal packing and facilitated the search for suitable cocrystallizing molecules. Making use of these tools, this thesis focused on the design of new solid forms of 5-fluorocytosine, a prodrug widely used in the gene–directed enzyme prodrug therapy for cancer treatment. The state of art of this prodrug revealed that this API exhibited some problematic physicochemical issues such as hygrocospicity, hindering its tablet formulation. By applying the ΔpKa rule it was possible to achieve a controlled supramolecular synthesis of crystal-engineered assemblies for this prodrug with the following carboxylic acids: oxalic, maleic, fumaric, malic, bezoic, terephtalic, succinic, and adipic. Particularly, the structure with malic acid was featured as a transition structure among salts and co-crystals, as it exhibited supramolecular synthons resembling both co-crystals and salts. Based on this information concerning the chemical behavior of 5-fluorocytosine, a multi-API cocrystal of 5-fluorouracil and 5-fluorocytosine was rationally designed and supramolecularly synthesized. The main goal was to introduce a potential new candidate for oral drug formulation able to act in two ways: (1) improve the antineoplastic effect of 5-fluorouracil in patients undergoing gene–directed enzyme prodrug therapy and/or (2) treat cancer and fungal infections caused by the chemotherapy. From these results, it is possible to conclude that 5-fluorocytosine has the potential to be a key compound as a co-former in new controlled synthesis experiments for the design of new tailor-made drugs.

In this context, as future perspectives, cocrystallization experiments among 5-fluorocytosine and others antineoplastic drugs will be performed. Moreover, during the development of this research project, new inorganic acids with 5-fluorocytosine were obtained, in a fashion that hereafter their complete evaluation must be performed and reported. Also, by considering the recurrence of dicarboxylic acids as suitable coformers, crystallization experiments among these acids and others antineoplastic drugs will also be performed. Finally,

new collaborations will be established to evaluate the biological activity, solubility, and bioavailability of the new drug-drug cocrystal obtained here.

REFERENCES

1 WORLD HEALTH ORGANIZATION. WHO. **World health statistics 2014.** Available at: < http://www.who.int/gho/publications/world_health_statistics/whs2014_indicatorcompendium.pdf?ua=1>. Access in: 05 Jan. 2015.

2 WORLD HEALTH ORGANIZATION. WHO. Internacional Agency for Research on Cancer. **World cancer report 2008**. Available at: <http://www.iarc.fr/en/publications/pdfs-online/wcr/2008/wcr_2008.pdf>. Access in: 30 Jan. 2015.

3 WORLD HEALTH ORGANIZATION. WHO. Internacional Agency for Research on Cancer. **World cancer report 2014**. Available at: <http://whocp3.codemantra.com/Marketing.aspx?ID=WCR2014&ISBN=9789283204299&sts=b>. Access in: 30 Jan. 2015.

4 BRASIL. Ministério da Saúde. Instituto Nacional do Câncer. **Estimativas 2014**: incidência de câncer no Brasil. 2014. Available at: <http://www.inca.gov.br/estimativa/2014/estimativa-24042014.pdf>. Access in: 30 Jan. 2015.

5 AITIPAMULA, S. et al. Polymorphs, salts, and cocrystals: what's in a name? **Crystal Growth & Design**, *v.* 12, n. 5, p. 2147-2152, 2012.

6 DESIRAJU, G. Crystal engineering: a holistic view. **Angewandte Chemie_International Edition**, v. 46, n. 44, p. 8342–8356, 2007.

7 THANKI, K.; GANGWAL, R. P.; SANGAMWAR, A. T.; JAIN, S. Oral delivery of anticancer drugs: challenges and opportunities. **Journal of Controlled Release**, v. 170, n. 1, p. 15-40, 2013.

8 DESIRAJU, G. Crystal engineering: from molecule to crystal. **Journal of the American Chemical Society**, 2013. doi: 10.1021/ja403264c. Available at: <http://pubs.acs.org/doi/pdf/10.1021/ja403264c>. Access in: 18 June 2013.

9 ALLEN, F. H. The Cambridge structural database: a quarter of a million crystal structures and rising. **Acta Crystallographica B**: structural science, crystal engineering and materials, v. 58, n. 3 pt. 1, p. 380-388, 2002.

10 FOOD AND DRUG ADMINISTRATION. FDA. **Lista dos compostos geralmente referidos como seguros**. GRAS. Available at: <http://www.fda.gov/Food/IngredientsPackagingLabeling/GRAS/SCOGS/ucm084104.htm>. Access in: 25 June 2013.

11 GUILLORY, J. K. Generation of polymorphs, hydrates, solvates, and amorphous solids. In: BRITTAIN, H. G. (Ed.). **Polymorphism in pharmaceutical solids**. New York: Marcel Decker, Inc., 1999. cap. 5. p. 184-226.

12 ZAITSEVA, N. et al. Application of solution techniques for rapid growth of organic crystals. **Journal of Crystal Growth**, v. 314, n. 1, p. 163-170, 2011.

13 WEYNA, D. R.; SHATTOCK, T.; VISHWESHWAR, P.; ZAWOROTKO, M. J. Synthesis and structural characterization of cocrystals and pharmaceutical cocrystals: mechanochemistry *vs* slow evaporation from solution. **Crystal Growth & Design**, v. 9, n. 2, p. 1106-1123, 2009.

14 HADJU, S. I. A note from history: landmarks in history of cancer, part 1. **Cancer**, v. 117, n. 5, p. 1097-1102, 2011.

15 SHELFER, L. The alchemy of jargon: etymologies of urologic neologisms. number 5: oncology and its vocabulary. **Prostate**, v. 69, n. 13, p. 1369-1371, 2009.

16 FAGUET, G. B. A brief history of cancer: age-old milestones underlying our current knowledge database. **International Journal for Cancer**, v. 136, n. 9, p. 2022-2036, 2014.

17 HANAHAN, D.; WEINBERG, R.A. The hallmarks of cancer. **Cell**, v. 100, n. 1, p. 57-70, 2000.

18 WORLD HEALTH ORGANIZATION. WHO. **International statistical classification of diseases and related health problems**. 10th revision (ICD-10)-2014-WHO version for 2014. Available at: <http://apps.who.int/classifications/icd10/browse/2014/en#/II>. Access in: 28 Jan. 2015.

19 PARIMIGIANI, R. B.; CAMARGO, A. A. O genoma humano e o câncer. In: FERREIRA, C. G.; ROCHA, J. C. C. (Ed.). **Oncologia molecular.** 2. ed. São Paulo: Editora Atheneu, 2010. cap. 1, p. 3-14.

20 WEINBERG, R. **The biology of cancer**. 2nd ed. New York: Garland Science, 2013. 960 p.

21 CALLERY, P. S.; GANNETT, P. M. Cancer and cancer chemotherapy. In: WILLIAMS, D. A.; LEMKE, T. L. (Ed) **Foye's principles of medicinal chemistry**. 5th ed. Baltimore: Williams & Wilkins, 2002. cap. 38, p. 924-951.

22 BASKAR, R.; LEE, K. A.; YEO, R.; YEOH, K-W. Cancer and radiation therapy: current advances and future directions. **International Journal of Medical Sciences**, v. 9, n. 3, p. 193-199, 2012.

23 VOGLER, J. B.; MURPHY, W. A. Bone marrow imaging. **Radiology**, v. 168, n. 3, p. 679-693, 1988.

24 EREMIN, O.; SEWELL, H. **Essential immunology for surgeons**. Oxford: Oxford University Press, 2011. 546 p.

25 MAELLMAN, I.; COUKOS, G.; DRANOFF, G. Cancer immunotherapy comes of age. **Nature**, v. 480, n. 7378, p. 480-489, 2011.

26 JONES, A.; BARRETT-LEE, P. J.; MASON, M. D. Hormonal therapy in cancer. **Medicine**, v. 32, n. 3, p. 30-32, 2004. doi: 10.1383/medc.32.3.30.28618.

27 CHABNER, B. A.; ROBERTS JR, T. G. Chemotherapy and the war on cancer. **Nature Reviews Cancer**, v. 5, n.1, p. 65-72, 2005.

28 EINHORN, J. Nitrogen mustard: the origin of chemotherapy for cancer. **International Journal of Radiation Oncology**, v. 11, n. 7, p. 1375-1378, 1985.

29 GALLAGNER, S. M.; SELMAN, S. H. From the battlefield to the bladder: the development of thioTEPA. **World Journal of Clinical Urology**, v. 3, n. 3, p. 195-200, 2014.

30 WORLD HEALTH ORGANIZATION. WHO. **World health statistics 2008.** Available at: <http://www.iarc.fr/en/publications/pdfs-online/wcr/2008/wcr_2008.pdf>. Access in: 10 Feb. 2015.

31 LANORE, D.; DELPRAT, C. **Quimioterapia anticancerígena**. São Paulo: Roca, 2004. 191p.

32 MULLANEY, I. An introduction to anticancer drugs. In: DOGGRELL, S. (Ed) **Pharmacology in one semester**. 2012. cap. 24. p. 221-230. Available at: <http://eprints.qut.edu.au/54563/1/CreativeCommonsPharmacologyinOneSemester2012.pdf>. Acess in: 10 Feb. 2015.

33 BRASIL. Ministério da Saúde. Instituto Nacional do Câncer. **Tratamento do câncer**. Available at: <http://www.inca.gov.br.> Access in: 15 Feb. 2015.

34 AMERICAN CANCER SOCIETY. ACS. **Different types of chemotherapy drugs**. Available at: <http://www.cancer.org/treatment/treatmentsandsideeffects/treatmenttypes/chemotherapy/chemotherapyprinciplesanindepthdiscussionofthetechniquesanditsroleintreatment/chemotherapy-principles-types-of-chemo-drugs> Access in: 15 Feb. 2015.

35 THANKI, K.; GANGWAL, R. P.; SANGAMWAR, A. T.; JAIN, S. Oral delivery of anticancer drugs: challenges and opportunities. **Journal of Controlled Release**, v. 170, n. 1, p. 15-40, 2013.

36 MALET-MARTINO, M; MARTINO, R. Clinical studies of three oral prodrugs of 5-fluorouracil (Capecitabine, UFT, S-1): a review. **The Oncologist**, v. 7, n. 4, p. 288-323, 2002.

37 PERUMALLA, S. R.; PEDIREDDI, V. R.; SUN, C. C. Design, synthesis, and characterization of new 5-fluorocytosine Salts. **Molecular Pharmaceutics**, v.10, n.6, p. 2462-2466, 2013.

38 HEIDELBERGER, C.; CHAUDHURI, N. K.; DANNEBERG, P.; MOOREN, D.; GRIESCACH, L. Fluorinated pyrimidines, a new class of tumour-inhibitory compounds. **Nature**, v. 179, n. 4561, p. 663-666, 1957.

39 MAZZAFERRO, S.; BOUCHEMAL, K.; PONCHEL, G. Oral delivery of anticancer drugs II: the prodrug strategy. **Drug Discovery Today**, v. 18, n. 1-2, p. 93-98, 2013.

40 FALLON III, L. The crystal and molecular structure of 5-fluorouracil. **Acta Crystallographica, Section B:** structural science, crystal engineering and materials, v. 29,n. 11, p. 2549-2556, 1973.

41 KIM, S. H.; RICH, A. Crystal structure of the 1: 1 complex of 5-fluorouracil and 9-ethylhypoxanthine. **Science**, v.158, n. 3804, p. 1046-1048, 1967.

42 VOET, D.; RICH, A. Structure of an intermolecular complex between cytosine and 5-fluorouracil. **Journal of the American Chemical Society**, v. 91, n. 11, p. 3069-3075, 1969.

43 KIM, H.; RICH, A. A non-complementary hydrogen-bonded complex containing 5-fluorouracil and 1-methylcytosine. **Journal of Molecular Biology**, v. 42, n. 1, p. 87, 1969.

44 ZAITU, S.; MIWA, Y.; TAGA, T. A 2:1 molecular complex of theophylline and 5-fluorouracil as the monohydrate. **Acta Crystallographica C:** crystal structure communications, v. 51, n. 9, p. 1857-1859, 1995.

45 HULME, A. T.; TOCHER, D. A. 5-Fluorouracil-1,4-dioxane (4/1). **Acta Crystallographica E:** crystallographic communications, v. 60, n. 10, p.o1781-o1782, 2004.

46 HULME, A. T.; TOCHER, D. A. 5-Fluorouracil-dimethylformamide (2/1). **Acta Crystallographica E:** crystallographic communications, v. 60, n.10 ,p. o1783-o1785, 2004.

47 HULME, A. T.; TOCHER, D. A. 5-Fluorouracil-dimethyl sulfoxide (1/1). **Acta Crystallographica E:** crystallographic communications, v. 60, n.10 ,p. o1786-o1787, 2004.

48 HULME, A. T.; TOCHER, D. A. 5-Fluorouracil-2,2,2-trifluoroethanol (1/1). **Acta Crystallographica E:** crystallographic communications, v. 61, n. 11, p. o3661-o3663, 2005.

49 HULME, A. T.; TOCHER, D. A.; PRICE, S. L. a new polymorph of 5-fluorouracil found following computational crystal structure predictions. **Journal of the American Chemical Society**, v. 127, n. 4, p. 1116-1117, 2005.

50 BARNETT, S. A.; HULME, A. T.; TOCHER, D. A. 5-fluorouracil and thymine form a crystalline solid solution. **Acta Crystallographica C:** crystal structure communications, v. 62, n. 7, p. o412-o415, 2006.

51 WU, H.; SHEN, Y. Copper(II) complex of 1,10-phenanthroline containig two 5-fluorouracil arranging in a new way: synthesis and crystal structure. **Synthesis and Reactivity in Inorganic Metal-organic and Nano-metal Chemistry**, v.36, n. 4, p.313-315, 2006.

52 PORTALONE, G.; COLAPIETRO, M. The 1:1 complex of cytosine and 5-fluorouracil monohydrate revisited. **Acta Crystallographica C:** crystal structure communications, v. 63, n. 7, p. o423-o425, 2007.

53 BARNETT, S. A. et al. The observed and energetically feasible crystal structures of 5-substituted uracils. **New Journal of Chemistry**, v. 32, n. 10, p. 1761-1775, 2008.

54 JARZEMBSKA, K. N.; KUBSIK, M.; KAMINSKI, R.; WOZNIAK, K.; DOMINIAK, P. M. From a single molecule to molecular crystal architectures: structural and energetic studies of selected uracil derivatives. **Crystal Growth & Design**, v. 12, n. 5, p. 2508-2524, 2012.

55 DELORI, A.; EDDLESTON, M. D.; JONES, W. Cocrystals of 5-fluorouracil. **CrystEngComm**, v. 15,n. 1 , p. 73-77, 2013.

56 SONG, L.; JIA-MEI, C.; TONG-BU, L. Synthon polymorphs of 1 : 1 co-crystal of 5-fluorouracil and 4-hydroxybenzoic acid: their relative stability and solvent polarity dependence of grinding outcomes. **CrystEngComm**, v.16, n. 28, p.6450-6458, 2014.

57 VERMES, A.; GUCHELAAR, H.-J.; DANKERT, J. Flucytosine: a review of its pharmacology, clinical indications, pharmacokinetics, toxicity and drug interactions. **Journal of Antimicrobial Chemotherapy**, v. 46, n. 2, p. 171–179, 2000.

58 LARSEN, R. A. Flucytosine. In: KAUFFMAN, C. A.; PAPPAS, P. G.; SOBEL, J. D.; DISMUKES, W. E. (Ed.) **Essentials of clinical mycology**. 2nd ed. New York: Springer Science+Business Media, LLC. 2011. p. 57-60.

59 MULLEN, C. A.; COALE, M. M.; LOWE, R.; BLAESE, R. M. Tumors expressing the cytosine deaminase suicide gene can be eliminatedin vivo with 5-fluorocytosine and induce protective immunity to wild type tumor. **Cancer Research**, v.54, n. 6, p.1503-1506, 1994.

60 LONGLEY, D. B.; HARKIN, D. P.; JOHNSTON, P. G. 5-Fluorouracil: mechanisms of action and clinical strategies. **Nature Publishing Group**, v. 3, n. 5, p. 330-338, 2003.

61 NISHIYAMA, T.; KAWAMURA, Y.; KAWAMOTO, K.; MATSUMURA, H.; YAMAMOTO, N.; ITO, T.; OHYAMA, A.; KATSURAGI, T.; SAKAI, T.V. Z. Antineoplastic effects in rats of 5-fluorocytosine in combination with cytosine deaminase capsules. **Cancer Research**, v. 45, n. 4, p. 1753-1761, 1985.

62 XU, G.; MCLEOD, H. L. Strategies for enzyme/prodrug cancer therapy. **Clinical Cancer Research**, v. 7, n. 11, p. 3314-3324, 2001.

63 ZHANG, J.; KALE, V.; CHEN, M. Gene-directed enzyme prodrug therapy. **The AAPS Journal**, v. 17, n. 1, p. 102-110, 2015.

64 LOUIS, T.; LOW, J. N.; TOLLIN, P. 5-fluorocytosine, C4H4FN3O.H2O. **Crystal Structure Communication**., n.11, p. 1059–1064, 1982.

65 PRABAKARAN, P.; MURUGESAN, S.; MUTHIAH, P.T.; BOCELLI, G.; RIGHI, L. Intermolecular N-H···O hydrogen-bonding interactions in 5-fluorocytosinium salicylate. **Acta Crystallographica E**: crystallographic communications**,** v. 57, n. 10, p. o933–o936, 2001.

66 HULME, A. T.; TOCHER, D. A. 4-Amino-5-fluoropyrimidin-2(1H)-one-2-amino-5-fluoropyrimidin-4(3H)-one-water (1/1/1). **Acta Crystallographica E**: crystallographic communications, v. 61, n. 7, p. o2112–o2113, 2005.

67 PORTALONE, G.; COLAPIETRO, M. Redetermination of 5-fluorocytosine monohydrate. **Acta Crystallographica E**: crystallographic communications**,** v. 62, n. 3, p. o1049–o1051, 2006.

68 HULME, A. T.; TOCHER, D. A**.** The discovery of new crystal forms of 5-fluorocytosine**. Crystal Growth & Design**., v. 6, n. 2, p. 481–487, 2006.

69 PORTALONE, G.; COLAPIETRO, M**.** Asymmetric base pairing in the complex 5-fluorocytosinium chloride/5-fluorocytosine monohydrate. **Journal of Chemical Crystallography**, v. 37, n. 2, p.141–145, 2007.

70 TUTUGHAMIARSO, M.; BOLTE, M.; EGERT, E. New pseudopolymorphs of 5-fluorocytosine. **Acta Crystallographica C**: crystal structure communications**,** v. 65, n. 11, p. o574–o578, 2009.

71 PORTALONE, G. Solid-phase molecular recognition of cytosine based on proton-transfer reaction. Part II. supramolecular architecture in the cocrystals of cytosine and its 5-Fluoroderivative with 5-Nitrouracil. **Chemistry Central Journal**, v. 5, n. 51, p.1–8, 2011.

72 TUTUGHAMIARSO, M.; WAGNER, G.; EGERT, E. Cocrystals of 5-fluorocytosine. **Acta Crystallographica, Section B**: structural science, crystal engineering and materials, v.68, n.4, p.431–443, 2012.

73 TUTUGHAMIARSO, M.; EGERT, E. Cocrystals of 5-fluorocytosine. **Acta Crystallographica, Section B**: structural science, crystal engineering and materials, v. 68, n. 4, p. 444–452, 2012.

74 PERUMALLA, S. R.; PEDIREDDI, V. R.; SUN, C. C. protonation of cytosine: cytosinium vs hemicytosinium duplexes. **Crystal Growth & Design**, v. 13, n. 2, p. 429-432, 2013.

75 LEHN, J-M. Supramolecular chemistry – scope and perspectives: molecules – supermolecules – molecular devices. **Journal of Inclusion Phenomena**, v. 6, n. 4, p. 351-396, 1988.

76 DESIRAJU, G. R. **Crystal engineering**: the design of organic solids. Amsterdam: Elsevier, 1989. 312 p.

77 ETTER, M. C.; MACDONALD, J. C.; BERNSTEIN, J. Graph-set analysis of hydrogen-bond patterns in organic crystals. **Acta Crystallographica, Section B**: structural science, crystal engineering and materials, v. 46, n. 2, p. 256-262, 1990.

78 ETTER, M. C. Encoding and decoding hydrogen-bond patterns of organic compounds. **Accounts of Chemical Research**, v. 23, n. 4, p. 120-126, 1990.

79 GRELL, J.; BERNSTEIN, J.; TINHOFER, G. Graph-set analysis of hydrogen-bond patterns: some mathematical concepts. **Acta Crystallographica, Section B**: structural science, crystal engineering and materials, v. 55, n. 6, p. 1030-1043, 1999.

80 BERNSTEIN, J.; DAVIS, R. E.; SHIMONI, L.; CHANG, L-L. Patterns in hydrogen bonding: functionality and graph set analysis in crystals. **Angewandte Chemie International Edition in English**, v. 34, n. 15, p. 1555-1573, 1995.

81 DESIRAJU, D. R. Supramolecular synthons in crystal engeneering – a new organic synthesis. **Angewandte Chemie International Edition**, v. 34, n. 21, p. 2311-2327, 1995.

82 COREY, E. J. General methods for the construction of complex molecules. **Pure and Applied Chemistry**, v. 14, n. 1, p. 19-97, 1967.

83 MOULTON, B.; ZAWOROTKO, M. J. From molecules to crystal engineering: supramolecular isomerism and polymorphism in network solids. **Chemical Reviews**, v. 101, n. 6, p. 1629-1658, 2001.

84 MACRAE, C. F. et al. Mercury CSD 2.0 - new features for the visualization and investigation of crystal structures. **Journal of Applied Crystallography**, v.41, n. 2, p. 466-470, 2008.

85 FLEISCHMAN, S. G.; KUDUVA, S. S.; MCMAHON, J. A.; MOULTON, B.; WALSH, R. D. B.; RODRÍGUEZ-HORNEDO, N.; ZAWOROTKO, M. J. Crystal engineering of the composition of pharmaceutical phases: multiple-component crystalline solids involving Carbamazepine. **Crystal Growth & Design**, v. 3, n. 6, p. 909-919, 2003.

86 WLASH, R. D. B.; BRADNER, M. W.; FLEISCHMAN, S.; MORALES, L. A.; MOULTON, B.; RODRÍGUEZ-HORNEDO, N.; ZAWOROTKO, M. J. Crystal engineering of the composition of pharmaceutical phases. **Chemical Communications**, v. 2, p. 186-187, 2003.

87 ALMARSSON, Ö.; ZAWOROTKO, M. J. Crystal engineering in the composition of pharmaceutical phases. Do pharmaceutical co-crystals represent a new path to improved medicines?. **Chemical Communications**, v. 17, p. 1889-1896, 2004. DOI: 10.1039/B402150A

88 CHENEY, M. L.; WEYNA, D. R.; SHAN, N.; HANNA, M.; WOJTAS, L.; ZAWOROTKO, M. J. Coformer selection in pharmaceutical cocrystal development: a case study of a meloxicam aspirin cocrystal that exhibits enhanced solubility and pharmacokinetics. **Journal of Pharmacutical Sciences**, v. 100, n. 6, p. 2172-2181, 2011.

89 GALEK, P. T. A.; PIDCOCK, E.; WOOD, P. A.; BRUNO, I. J.; GROOM, C. R. One in a half a million: a solid form informatics study of a pharmaceutical crystal structure. **CrystEngComm**, v. 14, n. 7, p. 2391-2403, 2012. doi: 10.1039/C2CE06362J.

90 WOOD, P. A.; FEEDER, N.; FURLOW, M.; GALEK, P. T. A.; GROOM, C. R. Knowledge-based approaches to co-crystal design. **CrystEngComm**, v. 16, p. 5839-5848, 2014.

91 WOUTERS, J.; QUÉRÉ, L. (Ed.) **Pharmaceutical salts and co-crystals**. London: Royal Society of Chemistry, 2012. 391 p. doi: 10.1039/9781849733502.

92 COQUEREL, G. Crystallization of molecular systems from solution: phase diagrams, supersaturation and other basic concepts. **Chemical Society Reviews**, v. 43, n. 7, p. 2286-2300, 2014.

93 TRASK, A. V. An overview of pharmaceutical cocrystals as intellectual property. **Molecular Pharmaceuticals**, v. 4, n. 3, p. 301-309, 2007.

94 AITIPAMULA, S. et al. Polymoprhs, salts, and cocrystals: what's in a name? **Crystal Growth & Design,** v. 12, n. 5, p. 2147-2152, 2012.

95 HAYNES, W. M. **CRC Handbook of chemistry and physics**. 95th ed. Boca Raton: CRC Press, 2014. Available at: <http://www.hbcpnetbase.com/>. Access in: 28 Feb. 2015.

APPENDIX A – Supporting information of the paper: the continuum in 5-fluorocytosine. towards salt formation

A. FUMARATE MONOHYDRATE OF 5-FLUOROCYTOSINE

Table A1 - Crystal data and structure refinement for the fumarate monohydrate of 5-FC.

Empirical formula	$C_6 H_8 F N_3 O_4$
Formula weight	205.15
Temperature	100.0(2) K
Wavelength	0.71073Å
Crystal system, space group	Monoclinic, $P2_1/c$
Unit cell dimensions	a = 3.550(5) Å
	b = 9.093(5) Å β = 91.737(5)º
	c = 24.527(5) Å
Volume	791.4(12) A^3
Z, Calculated density	4, 1.722 Mg/m^3
Absorption coefficient	0.159 mm^{-1}
F(000)	424
Crystal size	0.41 x 0.21 x 0.14 mm
Theta range for data collection	3.32 to 26.29º
Limiting indices	$-4\leq h\leq 4$, $-11\leq k\leq 11$, $-30\leq l\leq 30$
Reflections collected / unique	3085 / 1600 [$R_{(int)}$ = 0.0178]
Completeness to θ= 26.29º	99.0 %
Max. and min. transmission	0.9781 and 0.9377
Refinement method	Full-matrix least-squares on F^2
Data / restraints / parameters	1600 / 0 / 130
Goodness-of-fit on F^2	1.055
Final R indices [I>2σ(I)]	R_1 = 0.0348, wR_2 = 0.0970
R indices (all data)	R_1 = 0.0383, wR_2 = 0.1004
Largest diff. peak and hole	0.326 and -0.398 $e.A^{-3}$

Source: By the author.

Table A2 - Atomic coordinates (x 10^4) and equivalent isotropic displacement parameters (A^2 x 10^3) for the fumarate monohydrate of 5-FC. U(eq) is defined as one third of the trace of the orthogonalized Uij tensor.

	x	y	z	U(eq)
C(2)	3792(3)	5953(1)	1861(1)	15(1)
C(4)	5582(3)	4572(1)	1082(1)	14(1)
C(5)	4505(4)	3265(1)	1355(1)	15(1)
C(6)	3152(3)	3319(1)	1860(1)	15(1)
F(51)	4945(2)	1978(1)	1088(1)	20(1)
O(21)	3441(3)	7139(1)	2097(1)	19(1)
N(1)	2827(3)	4654(1)	2108(1)	16(1)
N(3)	5154(3)	5866(1)	1342(1)	14(1)
N(41)	6986(3)	4554(1)	590(1)	16(1)
C(7)	8571(3)	8380(1)	457(1)	15(1)
C(8)	9533(3)	9875(1)	254(1)	16(1)
O(4)	9223(3)	7268(1)	181(1)	19(1)
O(3)	7023(3)	8366(1)	927(1)	17(1)
O(1W)	9716(3)	4843(1)	3121(1)	21(1)

Source: By the author.

Table A3 - Bond lengths [Å] and angles [º] for the fumarate monohydrate of 5-FC.

C(2)-O(21)	1.2318(17)	C(5)-C(6)	1.3422(19)
C(2)-N(3)	1.3757(17)	C(5)-F(51)	1.3536(15)
C(2)-N(1)	1.3758(17)	C(6)-N(1)	1.3643(18)
C(4)-N(41)	1.3193(17)	C(7)-O(4)	1.2414(16)
C(4)-N(3)	1.3503(17)	C(7)-O(3)	1.2922(16)
C(4)-C(5)	1.4221(19)	C(7)-C(8)	1.4906(19)
O(21)-C(2)-N(3)	121.83(11)	F(51)-C(5)-C(4)	117.21(11)
O(21)-C(2)-N(1)	120.94(12)	C(5)-C(6)-N(1)	118.78(12)
N(3)-C(2)-N(1)	117.24(11)	C(6)-N(1)-C(2)	122.77(11)
N(41)-C(4)-N(3)	119.63(11)	C(4)-N(3)-C(2)	122.33(11)
N(41)-C(4)-C(5)	122.37(12)	O(4)-C(7)-O(3)	124.66(12)
N(3)-C(4)-C(5)	118.00(12)	O(4)-C(7)-C(8)	120.89(12)
C(6)-C(5)-F(51)	121.92(11)	O(3)-C(7)-C(8)	114.45(11)
C(6)-C(5)-C(4)	120.86(12)	C(8)#1-C(8)-C(7)	122.56(15)

Symmetry transformations used to generate equivalent atoms: #1 -x+2,-y+2,-z

Source: By the author.

Table A4 - Anisotropic displacement parameters ($Å^2 x\ 10^3$). The anisotropic displacement factor exponent takes the form: $-2\pi^2[\ h^2 a^{*2} U_{11} + ... + 2\ h\ k\ a^*\ b^*\ U_{12}\ ]$

	U11	U22	U33	U23	U13	U12
C(2)	13(1)	17(1)	16(1)	1(1)	-1(1)	0(1)
C(4)	11(1)	17(1)	14(1)	0(1)	-1(1)	0(1)
C(5)	16(1)	12(1)	16(1)	-2(1)	-1(1)	1(1)
C(6)	14(1)	15(1)	17(1)	2(1)	-1(1)	-1(1)
F(51)	28(1)	13(1)	20(1)	-3(1)	4(1)	-1(1)
O(21)	25(1)	16(1)	17(1)	-3(1)	2(1)	1(1)
N(1)	17(1)	17(1)	13(1)	1(1)	2(1)	0(1)
N(3)	15(1)	13(1)	14(1)	0(1)	1(1)	-1(1)
N(41)	19(1)	15(1)	14(1)	-1(1)	3(1)	-1(1)
C(7)	13(1)	16(1)	15(1)	0(1)	-1(1)	0(1)
C(8)	16(1)	14(1)	18(1)	-1(1)	2(1)	0(1)
O(4)	26(1)	14(1)	17(1)	-1(1)	6(1)	-2(1)
O(3)	22(1)	16(1)	14(1)	0(1)	4(1)	-1(1)
O(1W)	26(1)	19(1)	16(1)	1(1)	2(1)	0(1)

Source: By the author.

Table A5 - Hydrogen coordinates ($x\ 10^4$) and isotropic displacement parameters ($Å^2\ x\ 10^3$).

	x	y	z	U(eq)
H(6)	2449	2463	2037	18
H(1)	1951	4705	2444	33(5)
H(3)	6019	6789	1194	21
H(41A)	7815	5430	440	25(4)
H(41B)	7357	3693	417	32(5)
H(8)	9445	10696	525	20
H(11W)	11175	4715	3405	31
H(12W)	8381	3963	3110	31

Source: By the author.

Table A6 - Torsion angles [º] for the fumarate monohydrate of 5-FC.

N(41)-C(4)-C(5)-C(6)	178.74(11)
N(3)-C(4)-C(5)-C(6)	-0.89(18)
N(41)-C(4)-C(5)-F(51)	-0.53(18)
N(3)-C(4)-C(5)-F(51)	179.84(10)
F(51)-C(5)-C(6)-N(1)	179.18(10)
C(4)-C(5)-C(6)-N(1)	-0.05(19)
C(5)-C(6)-N(1)-C(2)	0.70(18)
O(21)-C(2)-N(1)-C(6)	179.60(11)
N(3)-C(2)-N(1)-C(6)	-0.38(18)
N(41)-C(4)-N(3)-C(2)	-178.40(11)
C(5)-C(4)-N(3)-C(2)	1.24(18)
O(21)-C(2)-N(3)-C(4)	179.39(11)
N(1)-C(2)-N(3)-C(4)	-0.63(18)
O(4)-C(7)-C(8)-C(8)#1	12.4(2)
O(3)-C(7)-C(8)-C(8)#1	-167.06(15)

Symmetry transformations used to generate equivalent atoms: #1 -x+2,-y+2,-z

Source: By the author.

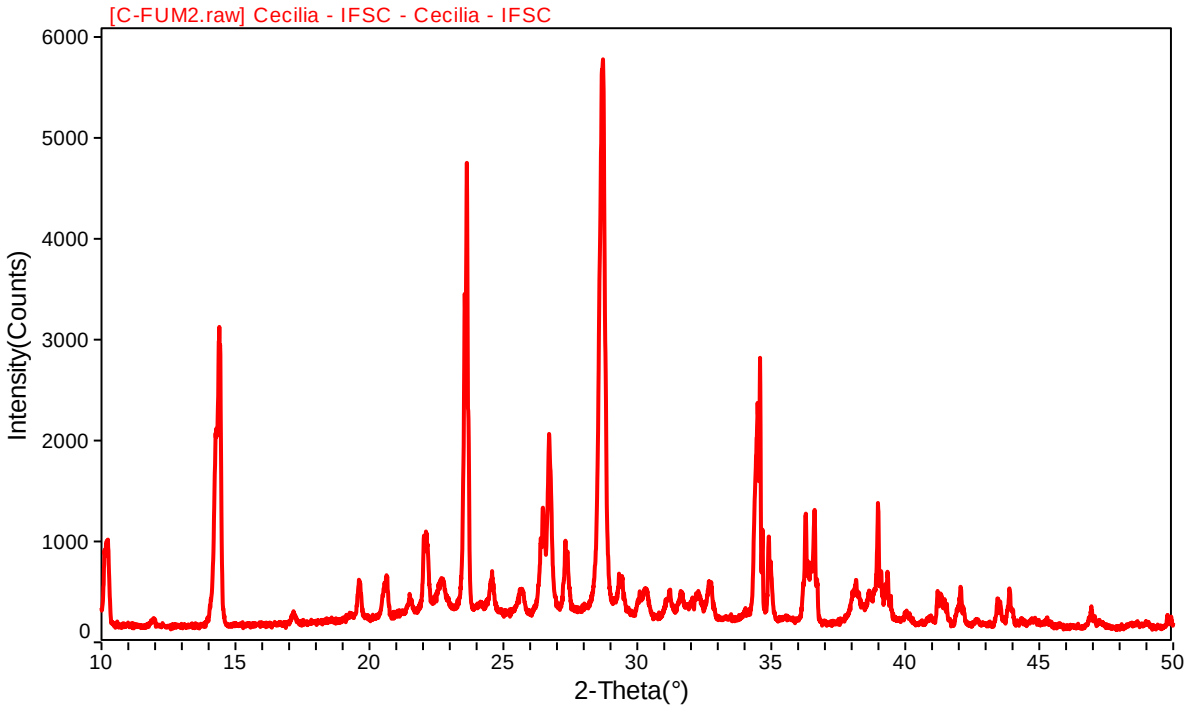

Figure A1 - Experimental powder X-ray diffractogram of the fumarate monohydrate of 5-FC.

Source: By the author.

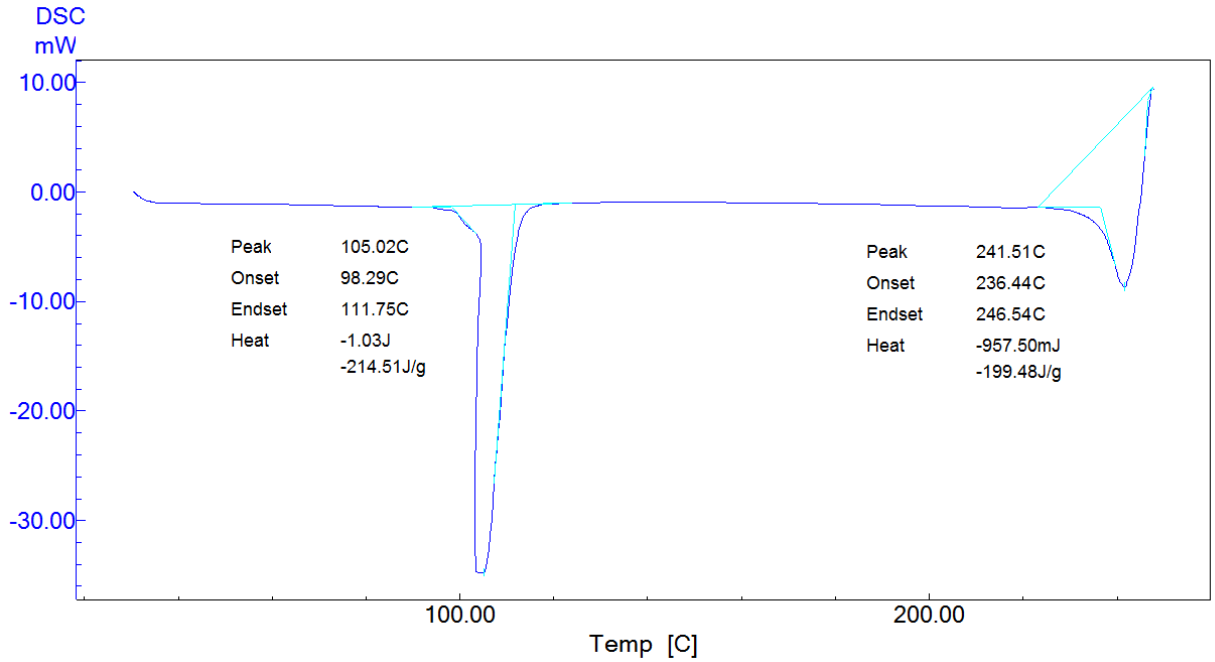

Figure A2 - DSC curve of the fumarate monohydrate of 5-FC.
Source: By the author.

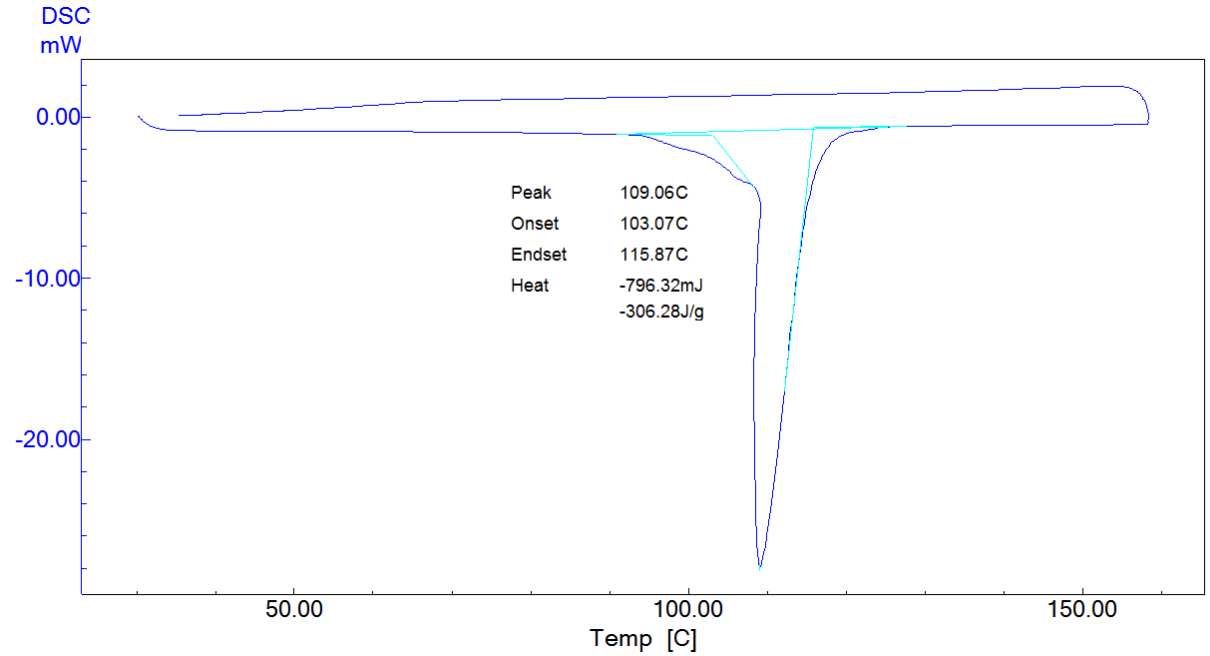

Figure A3 - DSC curve of the fumarate monohydrate of 5-FC recorded from 30ºC to 170ºC and from 170ºC to 30ºC.
Source: By the author.

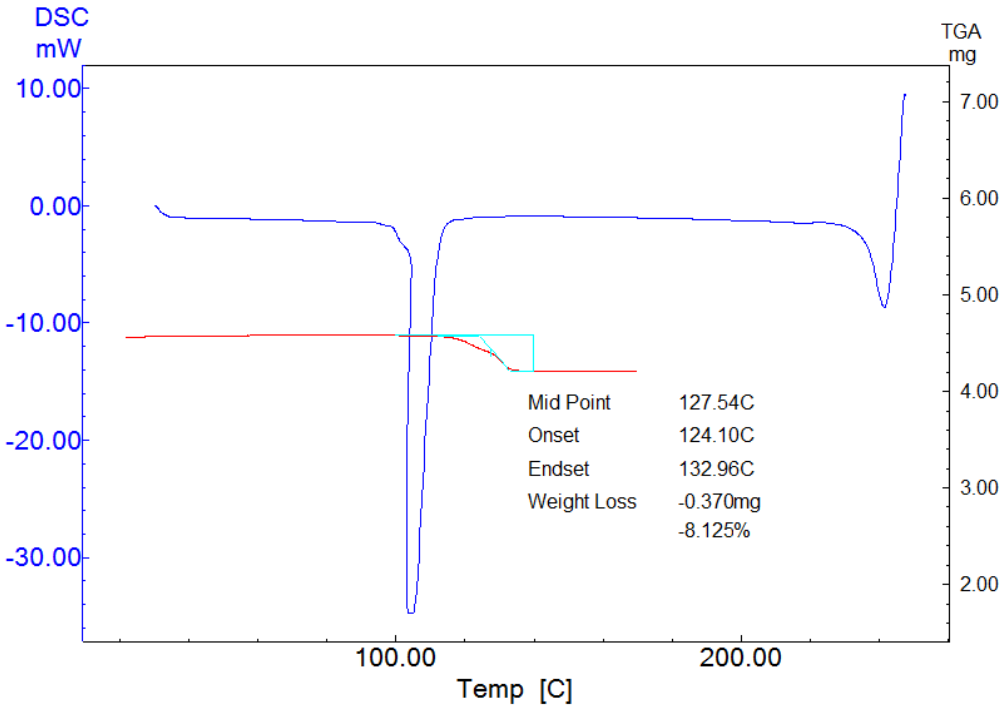

Figure A4 - DSC and TGA curves of the fumarate monohydrate of 5-FC.
Source: By the author.

B. OXALATE OF 5-FLUOROCYTOSINE

Table B1 - Crystal data and structure refinement for the oxalate of 5-FC.

Empirical formula	$C_5 H_5 F N_3 O_3$
Formula weight	174.12
Temperature	100.0(2) K
Wavelength	0.71073Å
Crystal system, space group	Monoclinic, $P2_1/c$
Unit cell dimensions	a = 5.2610(2) Å
	b = 15.1970(6) Å β = 92.206(3)°
	c = 7.8840(3) Å
Volume	629.87(4) A^3
Z, Calculated density	4, 1.836 Mg/m^3
Absorption coefficient	0.170 mm^{-1}
F(000)	356
Crystal size	0.27 x 0.08 x 0.06 mm
Theta range for data collection	3.73 to 26.42°
Limiting indices	$-6\leq h\leq 6$, $-18\leq k\leq 18$, $-9\leq l\leq 9$
Reflections collected / unique	2467 / 1287 [$R_{(int)}$ = 0.0298]
Completeness to θ = 26.42°	99.2 %
Refinement method	Full-matrix least-squares on F^2
Data / restraints / parameters	1287 / 0 / 109
Goodness-of-fit on F^2	1.046
Final R indices [I>2σ(I)]	R_1 = 0.0466, wR_2 = 0.1214
R indices (all data)	R_1 = 0.0648, wR_2 = 0.1360
Largest diff. peak and hole	0.351 and -0.288 $e.A^{-3}$

Source: By the author.

Table B2 - Atomic coordinates (x 10^4) and equivalent isotropic displacement parameters (A^2 x 10^3) for the oxalate of 5-FC. U(eq) is defined as one third of the trace of the orthogonalized Uij tensor.

	x	y	z	U(eq)
C(2)	471(3)	2571(1)	2499(2)	24(1)
C(4)	1772(3)	1076(1)	1846(2)	23(1)
C(5)	3835(3)	1439(1)	987(2)	23(1)
C(6)	4161(3)	2312(1)	872(2)	24(1)
F(51)	5485(2)	865(1)	319(1)	31(1)
N(1)	2483(3)	2864(1)	1599(2)	24(1)
N(3)	213(3)	1659(1)	2573(2)	23(1)
N(41)	1358(3)	227(1)	1980(2)	26(1)
O(21)	-1003(2)	3054(1)	3210(2)	29(1)
C(7)	6078(3)	185(1)	4453(2)	23(1)
O(4)	7366(2)	-368(1)	3661(2)	30(1)
O(3)	6363(2)	1002(1)	4423(2)	26(1)

Source: By the author.

Table B3 - Bond lengths [Å] and angles [º] for the oxalate of 5-FC.

C(2)-O(21)	1.220(2)	C(5)-C(6)	1.341(3)
C(2)-N(1)	1.371(2)	C(5)-F(51)	1.353(2)
C(2)-N(3)	1.393(3)	C(6)-N(1)	1.360(2)
C(4)-N(41)	1.313(3)	C(7)-O(3)	1.251(2)
C(4)-N(3)	1.350(2)	C(7)-O(4)	1.260(2)
C(4)-C(5)	1.413(2)	C(7)-C(7)#1	1.556(3)
O(21)-C(2)-N(1)	124.05(17)	F(51)-C(5)-C(4)	116.80(16)
O(21)-C(2)-N(3)	120.92(16)	C(5)-C(6)-N(1)	119.61(16)
N(1)-C(2)-N(3)	115.03(15)	C(6)-N(1)-C(2)	123.01(16)
N(41)-C(4)-N(3)	120.36(16)	C(4)-N(3)-C(2)	124.95(15)
N(41)-C(4)-C(5)	123.71(17)	O(3)-C(7)-O(4)	125.79(16)
N(3)-C(4)-C(5)	115.93(17)	O(3)-C(7)-C(7)#1	117.36(19)
C(6)-C(5)-F(51)	121.75(15)	O(4)-C(7)-C(7)#1	116.84(19)
C(6)-C(5)-C(4)	121.44(16)		

Symmetry transformations used to generate equivalent atoms: #1 -x+1,-y,-z+1

Source: By the author.

Table B4 - Anisotropic displacement parameters ($Å^2$ x 10^3). The anisotropic displacement factor exponent takes the form: $-2\pi^2[h^2 a^{*2} U_{11} + ... + 2 h k a^* b^* U_{12}]$

	U11	U22	U33	U23	U13	U12
C(2)	23(1)	24(1)	25(1)	0(1)	0(1)	0(1)
C(4)	22(1)	25(1)	22(1)	1(1)	1(1)	0(1)
C(5)	21(1)	24(1)	25(1)	-2(1)	6(1)	2(1)
C(6)	23(1)	24(1)	24(1)	1(1)	5(1)	-1(1)
F(51)	31(1)	24(1)	40(1)	-2(1)	16(1)	1(1)
N(1)	24(1)	21(1)	28(1)	1(1)	4(1)	-1(1)
N(3)	21(1)	22(1)	26(1)	1(1)	5(1)	-1(1)
N(41)	26(1)	21(1)	30(1)	-1(1)	8(1)	-1(1)
O(21)	28(1)	25(1)	35(1)	-2(1)	6(1)	3(1)
C(7)	22(1)	22(1)	26(1)	2(1)	2(1)	0(1)
O(4)	31(1)	21(1)	39(1)	-1(1)	14(1)	0(1)
O(3)	26(1)	20(1)	32(1)	1(1)	7(1)	-1(1)

Source: By the author.

Table B5 - Hydrogen coordinates (x 10^4) and isotropic displacement parameters (Å^2 x 10^3).

	x	y	z	U(eq)
H(6)	5527	2539	298	28
H(1)	2663	3492	1508	37
H(3)	-1209	1453	3179	34
H(41B)	2559	-147	1438	38
H(41A)	-263	-4	2639	38

Source: By the author.

Table B6 - Torsion angles [º] for the oxalate of 5-FC.

N(41)-C(4)-C(5)-C(6)	179.32(17)
N(3)-C(4)-C(5)-C(6)	-1.8(3)
N(41)-C(4)-C(5)-F(51)	-1.9(3)
N(3)-C(4)-C(5)-F(51)	176.98(14)
F(51)-C(5)-C(6)-N(1)	-178.45(15)
C(4)-C(5)-C(6)-N(1)	0.2(3)
C(5)-C(6)-N(1)-C(2)	1.8(2)
O(21)-C(2)-N(1)-C(6)	177.35(17)
N(3)-C(2)-N(1)-C(6)	-2.0(2)
N(41)-C(4)-N(3)-C(2)	-179.54(16)
C(5)-C(4)-N(3)-C(2)	1.5(2)
O(21)-C(2)-N(3)-C(4)	-179.07(17)
N(1)-C(2)-N(3)-C(4)	0.3(2)

Symmetry transformations used to generate equivalent atoms: #1 -x+1,-y,-z+1

Source: By the author.

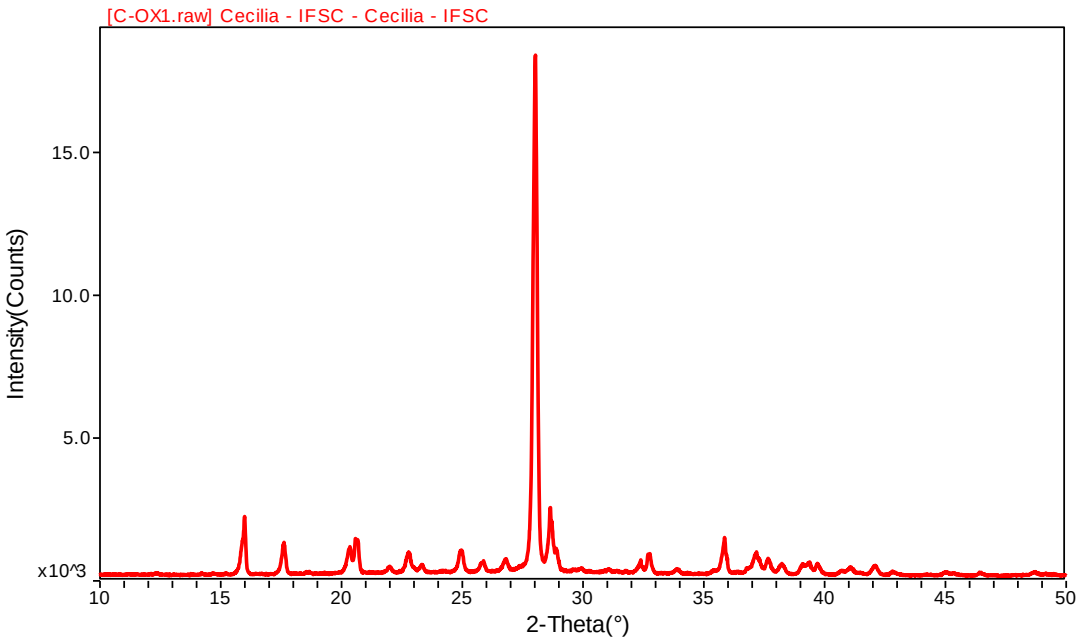

Figure B1 - Experimental powder X-ray diffractogram of the oxalate of 5-FC.

Source: By the author.

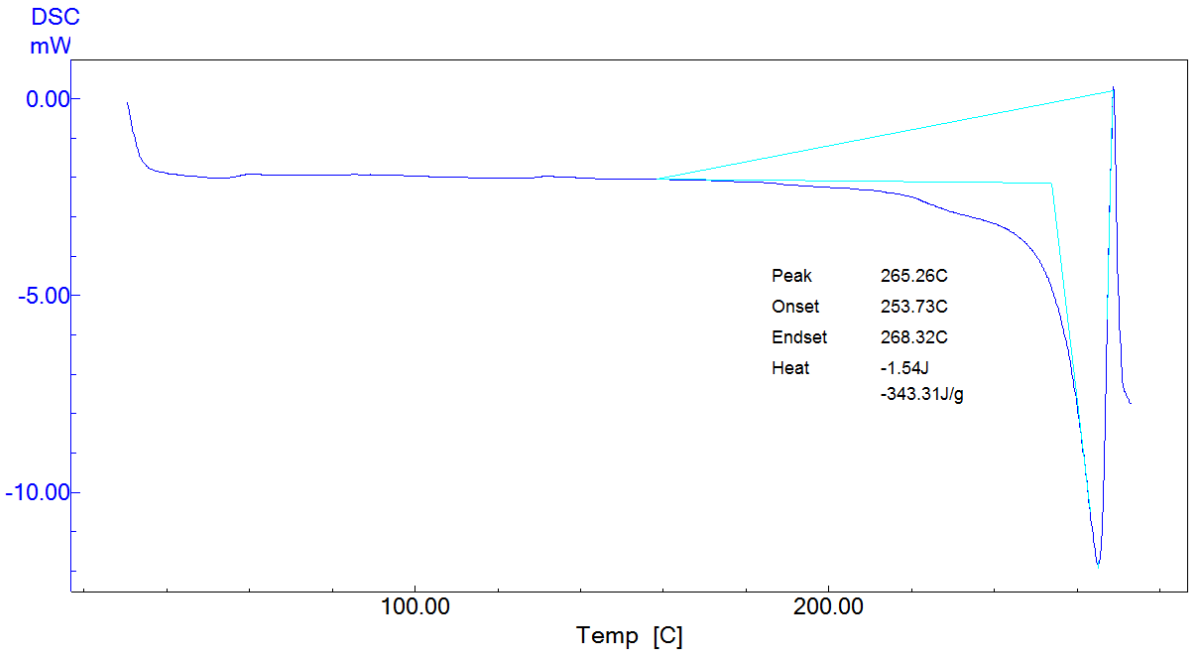

Figure B2 - DSC curve of the oxalate of 5-FC.
Source: By the author.

C. MALEATE OF 5-FLUOROCYTOSINE

Table C1 - Crystal data and structure refinement for the maleate of 5-FC.

Empirical formula	$C_8 H_8 F N_3 O_5$
Formula weight	245.17
Temperature	100.0(2) K
Wavelength	0.71073Å
Crystal system, space group	Monoclinic, $P2_1/c$
Unit cell dimensions	*a* = 9.3450(5)Å
	b = 11.8620(6)Å β = 113.573(3) º
	c = 18.9540(8)Å
Volume	1925.73(16) A^3
Z, Calculated density	8, 1.691 Mg/m^3
Absorption coefficient	0.154 mm^{-1}
F(000)	1008
Crystal size	0.19 x 0.11 x 0.04 mm
Theta range for data collection	2.93 to 26.37 º
Limiting indices	-11≤h≤11, -14≤k≤14, -23≤l≤23
Reflections collected / unique	7612 / 3907 [$R_{(int)}$ = 0.0570]
Completeness to θ = 26.37º	99.2 %
Max. and min. transmission	0.9939 and 0.9714
Refinement method	Full-matrix least-squares on $F^{\wedge 2}$
Data / restraints / parameters	3907 / 0 / 307
Goodness-of-fit on $F^{\wedge 2}$	1.035
Final R indices [I>2σa(I)]	R_1 = 0.0545, wR_2 = 0.1171
R indices (all data)	R_1 = 0.1258, wR_2 = 0.1464
Largest diff. peak and hole	0.412 and -0.294 $e.A^{-3}$

Source: By the author.

Table C2 - Atomic coordinates (x 10^4) and equivalent isotropic displacement parameters (A^2 x 10^3) for the maleate of 5-FC. U(eq) is defined as one third of the trace of the orthogonalized Uij tensor.

	x	y	z	U(eq)
F(51)	5873(2)	-566(1)	1015(1)	31(1)
N(1)	9602(2)	472(2)	2312(1)	24(1)
N(3)	7973(2)	1986(2)	1724(1)	24(1)
N(4)	5411(2)	1718(2)	871(1)	26(1)
O(21)	10452(2)	2285(1)	2603(1)	30(1)
C(2)	9418(3)	1627(2)	2241(2)	23(1)
C(4)	6762(3)	1304(2)	1315(2)	23(1)
C(5)	7058(3)	132(2)	1422(2)	24(1)
C(6)	8441(3)	-260(2)	1904(2)	25(1)
F(51')	805(2)	1775(1)	1087(1)	29(1)
N(1')	4578(2)	2794(2)	2362(1)	25(1)
N(3')	2940(2)	4314(2)	1810(1)	23(1)
N(41')	377(2)	4069(2)	943(1)	26(1)
O(21')	5434(2)	4595(2)	2672(1)	29(1)
C(3')	4393(3)	3942(2)	2307(2)	24(1)
C(4')	1710(3)	3641(2)	1390(2)	22(1)
C(5')	2013(3)	2462(2)	1486(2)	24(1)
C(6')	3397(3)	2061(2)	1954(2)	24(1)
O(6)	7561(2)	2029(1)	5073(1)	26(1)
O(5)	7089(2)	220(1)	4809(1)	27(1)
O(4)	4747(2)	-917(1)	4062(1)	26(1)
O(3)	2266(2)	-659(1)	3292(1)	28(1)
C(10)	6636(3)	1282(2)	4723(2)	24(1)
C(9)	5010(3)	1591(2)	4209(2)	25(1)
C(8)	3764(3)	975(2)	3791(2)	26(1)
C(7)	3589(3)	-280(2)	3711(2)	23(1)
O(6')	-2537(2)	9373(2)	-107(1)	31(1)
O(5')	-2086(2)	7561(2)	153(1)	30(1)
O(4')	202(2)	6412(2)	917(1)	29(1)
O(3')	2666(2)	6660(1)	1740(1)	27(1)
C(10')	-1619(3)	8619(2)	224(2)	26(1)
C(9')	27(3)	8917(2)	713(2)	26(1)
C(8')	1261(3)	8291(2)	1142(2)	27(1)
C(7')	1362(3)	7041(2)	1265(2)	23(1)

Source: By the author.

Table C3 - Bond lengths [Å] and angles [º] for the maleate of 5-FC.

F(51)-C(5)	1.351(3)	N(41')-C(4')	1.296(3)
N(1)-C(6)	1.363(3)	O(21')-C(3')	1.220(3)
N(1)-C(2)	1.380(3)	C(4')-C(5')	1.424(4)
N(3)-C(4)	1.354(3)	C(5')-C(6')	1.330(4)
N(3)-C(2)	1.381(3)	O(6)-C(10)	1.232(3)
N(4)-C(4)	1.301(3)	O(5)-C(10)	1.318(3)
O(21)-C(2)	1.218(3)	O(4)-C(7)	1.268(3)
C(4)-C(5)	1.416(4)	O(3)-C(7)	1.255(3)
C(5)-C(6)	1.333(4)	C(10)-C(9)	1.486(4)
F(51')-C(5')	1.352(3)	C(9)-C(8)	1.334(3)
N(1')-C(3')	1.370(3)	C(8)-C(7)	1.499(3)
N(1')-C(6')	1.375(3)	O(6')-C(10')	1.224(3)
N(3')-C(4')	1.364(3)	O(5')-C(10')	1.319(3)
N(3')-C(3')	1.379(3)		

continues

continuation

O(4')-C(7')	1.263(3)	C(10')-C(9')	1.487(4)
O(3')-C(7')	1.274(3)	C(9')-C(8')	1.339(3)
		C(8')-C(7')	1.498(3)
C(6)-N(1)-C(2)	122.4(2)	C(6')-C(5')-F(51')	122.0(2)
C(4)-N(3)-C(2)	125.3(2)	C(6')-C(5')-C(4')	121.8(2)
O(21)-C(2)-N(1)	122.8(2)	F(51')-C(5')-C(4')	116.2(2)
O(21)-C(2)-N(3)	122.1(2)	C(5')-C(6')-N(1')	119.8(2)
N(1)-C(2)-N(3)	115.1(2)	O(6)-C(10)-O(5)	120.0(2)
N(4)-C(4)-N(3)	121.2(2)	O(6)-C(10)-C(9)	119.3(2)
N(4)-C(4)-C(5)	123.1(2)	O(5)-C(10)-C(9)	120.7(2)
N(3)-C(4)-C(5)	115.7(2)	C(8)-C(9)-C(10)	132.5(2)
C(6)-C(5)-F(51)	121.8(2)	C(9)-C(8)-C(7)	129.6(2)
C(6)-C(5)-C(4)	121.4(2)	O(3)-C(7)-O(4)	122.5(2)
F(51)-C(5)-C(4)	116.9(2)	O(3)-C(7)-C(8)	117.4(2)
C(5)-C(6)-N(1)	120.0(2)	O(4)-C(7)-C(8)	120.2(2)
C(3')-N(1')-C(6')	122.5(2)	O(6')-C(10')-O(5')	120.5(2)
C(4')-N(3')-C(3')	125.6(2)	O(6')-C(10')-C(9')	119.0(2)
O(21')-C(3')-N(1')	122.7(2)	O(5')-C(10')-C(9')	120.5(2)
O(21')-C(3')-N(3')	121.9(2)	C(8')-C(9')-C(10')	132.2(3)
N(1')-C(3')-N(3')	115.4(2)	C(9')-C(8')-C(7')	129.0(3)
N(41')-C(4')-N(3')	121.2(2)	O(4')-C(7')-O(3')	122.6(2)
N(41')-C(4')-C(5')	123.9(2)	O(4')-C(7')-C(8')	121.0(2)
N(3')-C(4')-C(5')	114.9(2)	O(3')-C(7')-C(8')	116.4(2)

Source: By the author.

Table C4 - Anisotropic displacement parameters ($Å^2 \times 10^3$). The anisotropic displacement factor exponent takes the form: $-2\pi^2 [h^2 a^{*2} U_{11} + ... + 2 h k a^* b^* U_{12}]$

	U11	U22	U33	U23	U13	U12
F(51)	27(1)	24(1)	38(1)	-3(1)	7(1)	-4(1)
N(1)	19(1)	22(1)	28(1)	-2(1)	5(1)	-1(1)
N(3)	23(1)	18(1)	26(1)	0(1)	7(1)	-2(1)
N(4)	23(1)	20(1)	32(1)	-2(1)	8(1)	-1(1)
O(21)	25(1)	24(1)	35(1)	-2(1)	7(1)	-1(1)
C(2)	22(2)	23(2)	24(2)	-1(1)	9(1)	-1(1)
C(4)	18(2)	25(2)	25(2)	-1(1)	7(1)	-2(1)
C(5)	22(2)	21(2)	30(2)	-4(1)	10(1)	-6(1)
C(6)	28(2)	20(2)	29(2)	0(1)	12(1)	-1(1)
F(51')	25(1)	22(1)	34(1)	-2(1)	6(1)	-3(1)
N(1')	19(1)	23(1)	28(1)	1(1)	4(1)	1(1)
N(3')	23(1)	19(1)	24(1)	2(1)	7(1)	0(1)
N(41')	22(1)	21(1)	32(1)	-2(1)	5(1)	-3(1)
O(21')	27(1)	24(1)	31(1)	-1(1)	6(1)	-4(1)
C(3')	24(2)	22(2)	25(2)	1(1)	10(1)	1(1)
C(4')	20(2)	24(1)	21(1)	-1(1)	8(1)	-1(1)
C(5')	25(2)	20(2)	25(2)	-5(1)	10(1)	-5(1)
C(6')	26(2)	20(1)	27(2)	0(1)	10(1)	-1(1)
O(6)	26(1)	20(1)	30(1)	-1(1)	9(1)	-2(1)
O(5)	23(1)	21(1)	33(1)	-1(1)	8(1)	-1(1)
O(4)	24(1)	22(1)	31(1)	2(1)	8(1)	2(1)
O(3)	24(1)	25(1)	30(1)	-1(1)	5(1)	-2(1)
C(10)	24(2)	21(2)	27(2)	2(1)	10(1)	1(1)
C(9)	26(2)	19(2)	27(2)	0(1)	9(1)	2(1)
C(8)	22(2)	24(1)	28(2)	3(1)	8(1)	5(1)

continues

continuation

C(7)	21(2)	24(2)	21(2)	-1(1)	7(1)	-2(1)
O(6')	29(1)	24(1)	37(1)	4(1)	9(1)	4(1)
O(5')	23(1)	26(1)	36(1)	2(1)	5(1)	-1(1)
O(4')	22(1)	26(1)	33(1)	-2(1)	4(1)	-2(1)
O(3')	21(1)	25(1)	30(1)	0(1)	4(1)	1(1)
C(10')	30(2)	22(2)	26(2)	-2(1)	11(1)	-2(1)
C(9')	26(2)	23(2)	28(2)	0(1)	9(1)	1(1)
C(8')	25(2)	24(2)	28(2)	-3(1)	7(1)	-2(1)
C(7')	23(2)	22(1)	26(2)	-1(1)	12(1)	1(1)

Source: By the author.

Table C5 - Hydrogen coordinates (x 10^4) and isotropic displacement parameters (Å^2 x 10^3).

	x	y	z	U(eq)
H(1)	10567	179	2682	37
H(3)	7941	2785	1717	35
H(41A)	5290	2505	867	39
H(41B)	4555	1231	599	39
H(6)	8614	-1033	1962	30
H(1')	5538	2532	2645	37
H(3')	2789	5065	1771	35
H(41C)	282	4831	918	40
H(41D)	-441	3598	683	40
H(6')	3566	1287	2006	29
H(5)	6190	-286	4495	32
H(9)	4824	2363	4173	30
H(8)	2872	1386	3505	31
H(5')	-1099	7019	457	36
H(9')	241	9684	723	31
H(8')	2183	8687	1400	32

Source: By the author.

Table C6 - Torsion angles [°] for the maleate of 5-FC.

C(6)-N(1)-C(2)-O(21)	-179.8(3)
C(6)-N(1)-C(2)-N(3)	-0.2(4)
C(4)-N(3)-C(2)-O(21)	-178.6(3)
C(4)-N(3)-C(2)-N(1)	1.7(4)
C(2)-N(3)-C(4)-N(4)	176.2(2)
C(2)-N(3)-C(4)-C(5)	-2.0(4)
N(4)-C(4)-C(5)-C(6)	-177.4(3)
N(3)-C(4)-C(5)-C(6)	0.7(4)
N(4)-C(4)-C(5)-F(51)	2.4(4)
N(3)-C(4)-C(5)-F(51)	-179.5(2)
F(51)-C(5)-C(6)-N(1)	-179.2(2)
C(4)-C(5)-C(6)-N(1)	0.6(4)
C(2)-N(1)-C(6)-C(5)	-0.9(4)
C(6')-N(1')-C(3')-O(21')	179.5(3)
C(6')-N(1')-C(3')-N(3')	-0.4(4)
C(4')-N(3')-C(3')-O(21')	-179.1(3)
C(4')-N(3')-C(3')-N(1')	0.8(4)
C(3')-N(3')-C(4')-N(41')	179.1(3)
C(3')-N(3')-C(4')-C(5')	-0.7(4)

continues

continuation

N(41')-C(4')-C(5')-C(6')	-179.6(3)
N(3')-C(4')-C(5')-C(6')	0.2(4)
N(41')-C(4')-C(5')-F(51')	-1.0(4)
N(3')-C(4')-C(5')-F(51')	178.8(2)
F(51')-C(5')-C(6')-N(1')	-178.4(2)
C(4')-C(5')-C(6')-N(1')	0.1(4)
C(3')-N(1')-C(6')-C(5')	0.0(4)
O(6)-C(10)-C(9)-C(8)	-177.0(3)
O(5)-C(10)-C(9)-C(8)	2.6(5)
C(10)-C(9)-C(8)-C(7)	1.3(5)
C(9)-C(8)-C(7)-O(3)	178.0(3)
C(9)-C(8)-C(7)-O(4)	-1.6(5)
O(6')-C(10')-C(9')-C(8')	179.0(3)
O(5')-C(10')-C(9')-C(8')	-0.4(5)
C(10')-C(9')-C(8')-C(7')	0.1(5)
C(9')-C(8')-C(7')-O(4')	3.3(5)
C(9')-C(8')-C(7')-O(3')	-176.1(3)

Source: By the author.

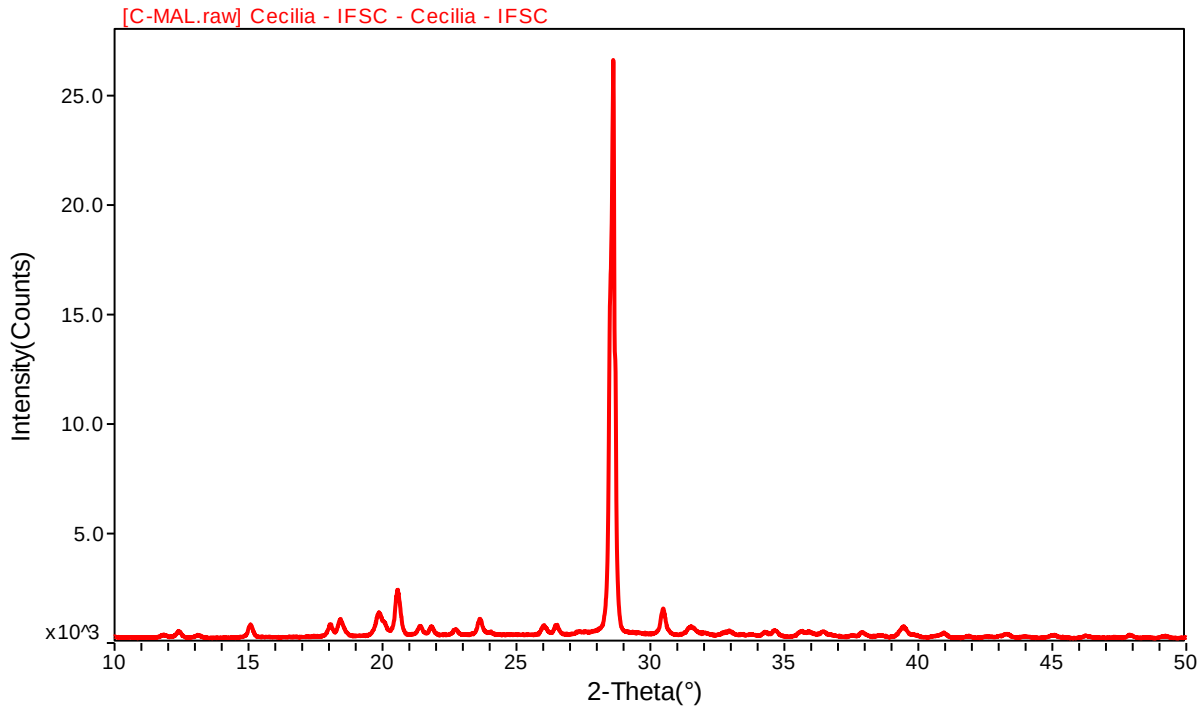

Figure C1 - Experimental powder X-ray diffractogram of the maleate of 5-FC.
Source: By the author.

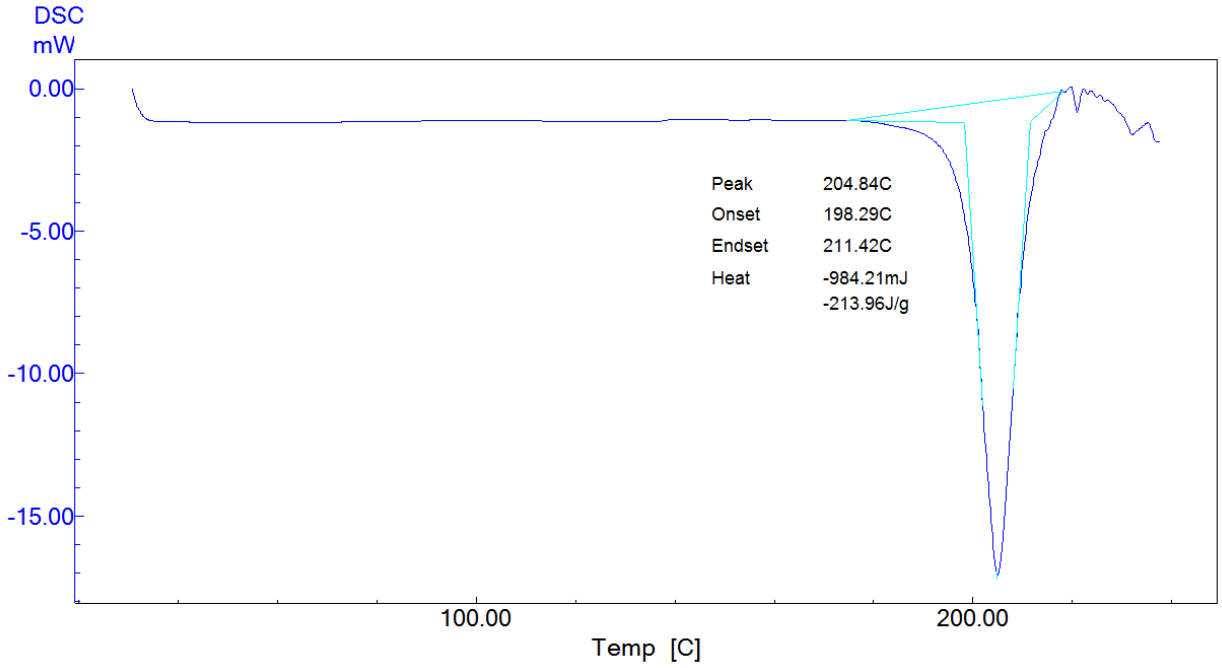

Figure C2 - DSC curve of the maleate of 5-FC.
Source: By the author.

D. RAW 5-FLUOROCYTOSINE

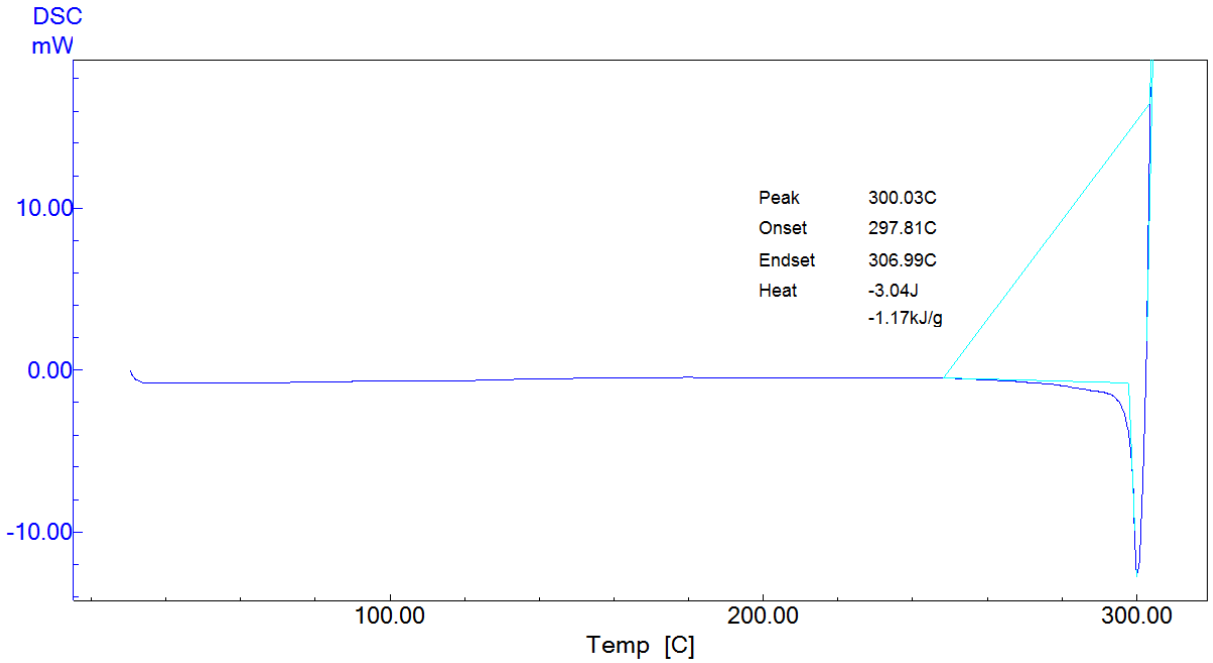

Figure D1 - DSC curve of the raw 5-FC.
Source: By the author.

COMPLEMENTAR FIGURES AND TABLE

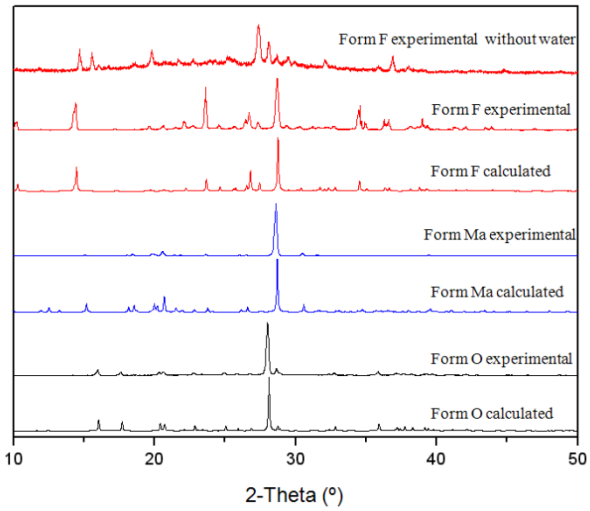

Figure 7 - Calculated and experimental X-ray powder diffraction patterns for Forms O, Ma and F, including the diffraction pattern of the Form F after the water loss.
Source: By the author.

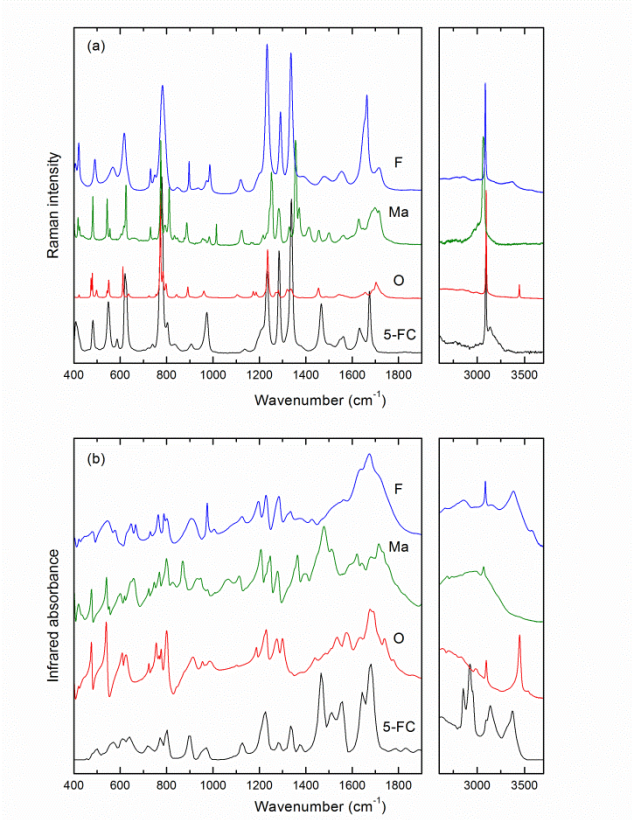

Figure 8 - A) IR, and b) Raman spectra of Forms O, Ma and F.
Source: By the author.

Table 2 - Hydrogen-bonds geometry (Å,º) in Forms O, F and Ma.

Structure	Interaction	D...A(Å)	H...A(Å)	D-H...A(º)	Symmetry code
Form O	N3-H3···O3	2.731(2)	1.704	174.07	x-1,+y,+z
	N41-H41A···O4	2.683(2)	1.654	178.38	x-1,+y,+z
	N1-H1···O4	2.697(2)	1.671	173.58	-x+1,+y+1/2,-z+1/2
	N41-H41B···F51	2.754(2)	2.355	101.65	intramolecular
	N41-H41B···F51	3.005(2)	2.003	163.41	-x+1,-y,-z
	C6-H6•••O21	3.405(2)	2.553	135.17	x+1,-y+1/2,+z-1/2
	C6-H6•••O3	3.052(2)	2.275	127.21	x,-y+1/2,+z-1/2
Form F	N3-H3···O3	2.586(2)	1.560	173.86	x,y,z
	N41-H41A···O4	2.788(2)	1.761	174.82	x,y,z
	N41-H41B···O4	2.879(2)	2.023	138.77	-x+2,-y+1,-z
	N41-H41B···F51	2.749(2)	2.421	97.31	Intramolecular
	N1-H1···O1W	2.754(2)	1.727	174.81	x-1,+y,+z
	O1W-H12W···O21	2.748(2)	1.838	162.77	-x+1,+y-1/2,-z+1/2
	O1W-H11W···O3	2.905(2)	2.067	147.96	-x+2,+y-1/2,-z+1/2
	C6-H6•••O21	2.996(2)	2.512	106.06	-x+1,+y-1/2,-z+1/2
	C6-H6•••O1W	3.322(2)	2.411	141.18	-x+1,+y-1/2,-z+1/2
Form Ma	N3-H3···O3	2.802(3)	1.774	175.47	-x+1,+y+1/2,-z+1/2
	N3'-H3'···O3'	2.793(3)	1.766	174.44	x,y,z
	N41-H41A···O4	2.815(3)	1.788	173.95	-x+1,+y+1/2,-z+1/2
	N41'-H41C···O4'	2.784(3)	1.756	176.32	x,y,z
	N1-H1···O3	2.784(2)	1.769	167.82	x+1,+y,+z
	N1'-H1'···O3'	2.798(2)	1.789	165.67	-x+1,+y-1/2,-z+1/2
	N41'-H41D···O6	2.805(2)	1.800	164.37	x-1,-y+1/2,+z-1/2
	N41-H41B···O6'	2.806(3)	1.806	162.55	-x,-y+1,-z
	N41-H41B···F51	2.740(2)	2.420	96.78	Intramolecular
	N41'-H41D···F51'	2.747(2)	2.412	97.74	Intramolecular
	O5-H5···O4	2.476(2)	1.543	172.74	Intramolecular
	O5'-H5'···O4'	2.459(2)	1.524	173.95	Intramolecular
	C6-H6•••O21	3.108(3)	2.059	162.98	-x+2,+y-1/2,-z+1/2
	C6'-H6'•••O21'	3.104(3)	2.050	164.22	-x+1,+y-1/2,-z+1/2

Source: By the author.

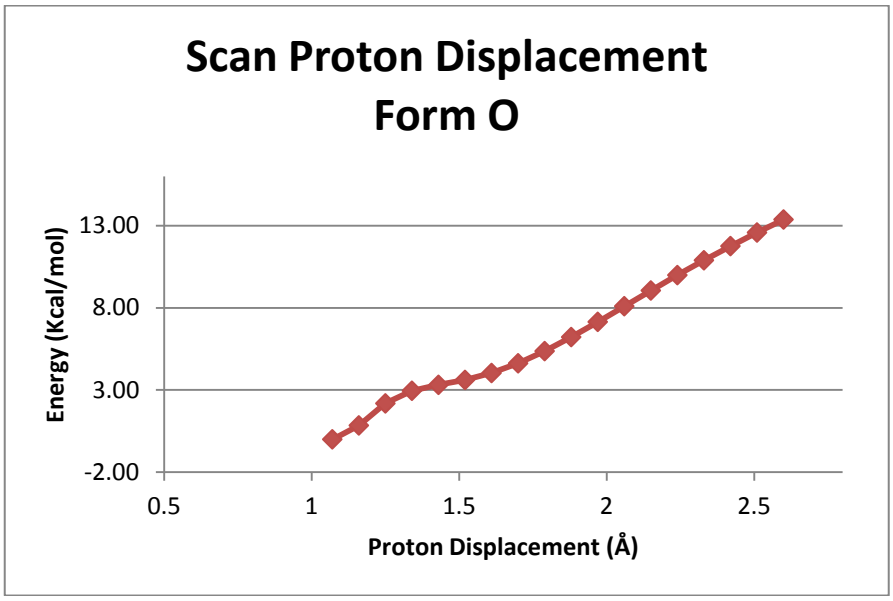

Source: By the author.

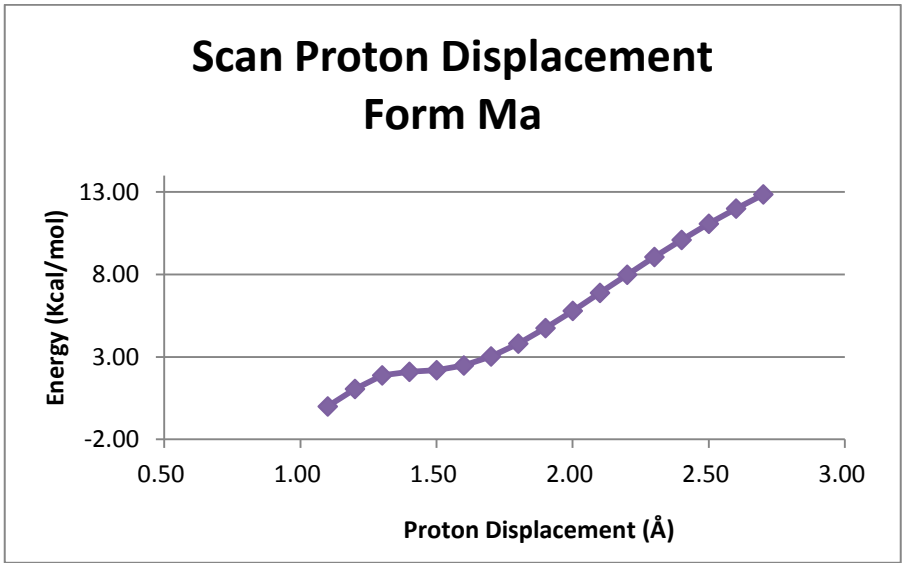

Source: By the author.

APPENDIX B– Supporting information of the paper: controlled synthesis of new 5-fluorocytosine co-crystals based on the pKa rule

REFINEMENT DETAILS

Co-crystals of 5-FC with adipic, succinic and terephtalic acids and with 5-FU – All data collections were performed at 100.0(2) K. Data collection, indexing, and initial cell refinements were all carried out with APEX 2[28] software. Final unit cell parameters based on all reflections were obtained by least-squares refinement. The data were integrated via SAINT[29]. Lorentz and polarization effect and multiscan absorption corrections were applied with SADABS[30]. The structure was solved by direct methods and the obtained model was refined by full–matrix least squares on F^2 (SHELXL–97[31a] for the co-crystals with adipic, succinic and terephtalic acids and SHELXL–2013[31b] for the co-crystal of 5-FC and 5-FU), using the APEX 2[28] and the WinGX v1.70.01[32] program packages. All the hydrogen atoms were stereochemically positioned, refined with fixed individual displacement parameters [$U_{iso}(H) = 1.2U_{eq}$] according to the riding model. N-H and O-H hydrogen atoms were located on the difference Fourier maps, fixed and refined with fixed isotropic thermal parameters (Uiso(H) = 1.2Ueq(N) or 1.5Ueq(O)).

Co-crystals of 5-FC with malic and benzoic acids – Intensity data were collected at room temperature. Both the software COLLECT[33] and the package of softwares Denzo–Scalepack [34] were applied for acquisition, indexing, integration, and scaling of Bragg reflections. The final cell parameters were obtained using all reflections. No absorption correction was applied. The structures were solved by direct methods and the model obtained were refined by full–matrix least squares on F^2 (SHELXL–2013[31b]) within WinGX v1.70.01[32] program packages. Hydrogen atoms were stereochemically positioned and refined with fixed individual displacement parameters [$U_{iso}(H) = 1.2U_{eq}$] according to the riding model, except for the N-H and O-H ones, which were located on the difference Fourier maps and refined on their positions.

COMPLEMENTAR FIGURES AND TABLES

A. CO-CRYSTAL OF 5-FC WITH SUCCINIC ACID

Table A1 - Crystal data and structure refinement for the co-crystal of 5-FC with succinic acid.

Empirical formula	$C_6 H_7 F N_3 O_3$	
Formula weight	188.15	
Temperature	100.0(2) K	
Wavelength	0.71073 Å	
Crystal system, space group	Triclinic, $P\bar{1}$	
Unit cell dimensions	a = 4.9209(3) Å	α= 72.466(3) º
	b = 8.6115(5) Å	β= 75.129(3) º
	c = 9.4689(6) Å	γ= 89.747(3) º
Volume	368.64(4) A^3	
Z, Calculated density	2, 1.695 Mg/m^3	
Absorption coefficient	0.153 mm^{-1}	
F(000)	194	

continues

continuation

Crystal size	0.38 x 0.20 x 0.08 mm
θ range for data collection	2.34 to 33.45 º
Limiting indices	$-7\leq h\leq 7$, $-13\leq k\leq 12$, $-14\leq l\leq 14$
Reflections collected / unique	7458 / 2572 [$R_{(int)}$ = 0.0219]
Completeness to θ= 25.00	99.2 %
Max. and min. transmission	0.9879 and 0.9443
Refinement method	Full-matrix least-squares on F^2
Data / restraints / parameters	2572 / 0 / 118
Goodness-of-fit on F^2	1.103
Final R indices [I>2σ(I)]	R_1 = 0.0381, wR_2 = 0.1153
R indices (all data)	R_1 = 0.0436, wR_2 = 0.1273
Largest diff. peak and hole	0.584 and -0.405 e.A^{-3}

Source: By the author.

Table A2 - Atomic coordinates (x 10^4) and equivalent isotropic displacement parameters (A^2 x 10^3) for the co-crystal of 5-FC with succinic acid. U(eq) is defined as one third of the trace of the orthogonalized Uij tensor.

	x	y	z	U(eq)
C(2)	6710(2)	1855(1)	7898(1)	11(1)
C(4)	6792(2)	3140(1)	5334(1)	11(1)
C(5)	4609(2)	1977(1)	5468(1)	13(1)
C(6)	3550(2)	793(1)	6807(1)	13(1)
N(1)	4624(2)	729(1)	8014(1)	12(1)
N(3)	7781(2)	3056(1)	6551(1)	11(1)
N(41)	7813(2)	4318(1)	4010(1)	14(1)
O(21)	7570(2)	1734(1)	9074(1)	14(1)
F(51)	3608(1)	2126(1)	4233(1)	19(1)
C(7)	1952(2)	3290(1)	544(1)	12(1)
C(8)	4257(2)	4311(1)	723(1)	11(1)
O(3)	1611(1)	3673(1)	-867(1)	14(1)
O(4)	503(2)	2209(1)	1616(1)	26(1)

Source: By the author.

Table A3 - Bond lengths [Å] and angles [º] for the co-crystal of 5-FC with succinic acid.

C(2)-O(21)	1.2652(11)	N(3)-C(2)-N(1)	120.00(8)
C(2)-N(3)	1.3561(11)	N(41)-C(4)-N(3)	120.24(8)
C(2)-N(1)	1.3761(11)	N(41)-C(4)-C(5)	119.78(8)
C(4)-N(41)	1.3295(12)	N(3)-C(4)-C(5)	119.97(8)
C(4)-N(3)	1.3445(11)	C(6)-C(5)-F(51)	121.53(8)
C(4)-C(5)	1.4268(13)	C(6)-C(5)-C(4)	120.06(9)
C(5)-C(6)	1.3442(13)	F(51)-C(5)-C(4)	18.40(8)
C(5)-F(51)	1.3529(10)	C(5)-C(6)-N(1)	118.52(8)
C(6)-N(1)	1.3636(12)	C(6)-N(1)-C(2)	121.75(8)
C(7)-O(4)	1.2129(11)	C(4)-N(3)-C(2)	119.69(7)
C(7)-O(3)	1.3305(11)	O(4)-C(7)-O(3)	122.55(8)
C(7)-C(8)	1.5124(12)	O(4)-C(7)-C(8)	122.16(9)
C(8)-C(8)#1	1.5270(18)	O(3)-C(7)-C(8)	115.29(8)
O(21)-C(2)-N(3)	121.82(8)	C(7)-C(8)-C(8)#1	115.11(9)
O(21)-C(2)-N(1)	118.18(8)		

Symmetry transformations used to generate equivalent atoms: #1 -x+1,-y+1,-z

Source: By the author.

Table A4 - Anisotropic displacement parameters ($Å^2$ x 10^3). The anisotropic displacement factor exponent takes the form: $-2\pi^2[h^2 a^{*2} U_{11} + ... + 2 h k a^* b^* U_{12}]$

	U11	U22	U33	U23	U13	U12
C(2)	11(1)	11(1)	10(1)	-2(1)	-3(1)	-1(1)
C(4)	11(1)	11(1)	10(1)	-2(1)	-2(1)	-1(1)
C(5)	15(1)	14(1)	10(1)	-2(1)	-6(1)	-2(1)
C(6)	14(1)	12(1)	12(1)	-2(1)	-5(1)	-3(1)
N(1)	14(1)	11(1)	9(1)	0(1)	-4(1)	-4(1)
N(3)	13(1)	12(1)	9(1)	-1(1)	-3(1)	-3(1)
N(41)	17(1)	15(1)	8(1)	1(1)	-3(1)	-5(1)
O(21)	16(1)	15(1)	10(1)	-1(1)	-6(1)	-4(1)
F(51)	24(1)	22(1)	12(1)	-1(1)	-11(1)	-7(1)
C(7)	12(1)	12(1)	12(1)	-2(1)	-4(1)	-2(1)
C(8)	12(1)	13(1)	10(1)	-2(1)	-3(1)	-3(1)
O(3)	15(1)	16(1)	10(1)	-2(1)	-5(1)	-5(1)
O(4)	31(1)	26(1)	14(1)	4(1)	-8(1)	-19(1)

Source: By the author.

Table A5 - Hydrogen coordinates (x 10^4) and isotropic displacement parameters ($Å^2$ x 10^3).

	x	y	z	U(eq)
H(6)	2117	34	6909	15
H(1)	4027	11	8887	18
H(41A)	7256	4349	3218	21
H(41B)	9062	5054	3897	21
H(8A)	5656	3597	1053	14
H(8B)	3446	4783	1532	14
H(3)	290	3107	-977	21

Source: By the author.

Table A6 - Torsion angles [º] for the co-crystal of 5-FC with succinic acid.

N(41)-C(4)-C(5)-C(6)	-179.38(9)	O(21)-C(2)-N(1)-C(6)	178.85(8)
N(3)-C(4)-C(5)-C(6)	0.37(15)	N(3)-C(2)-N(1)-C(6)	-0.99(14)
N(41)-C(4)-C(5)-F(51)	0.88(14)	N(41)-C(4)-N(3)-C(2)	179.56(8)
N(3)-C(4)-C(5)-F(51)	178.14(8)	C(5)-C(4)-N(3)-C(2)	0.55(14)
F(51)-C(5)-C(6)-N(1)	178.93(8)	O(21)-C(2)-N(3)-C(4)	-179.72(8)
C(4)-C(5)-C(6)-N(1)	0.47(15)	N(1)-C(2)-N(3)-C(4)	0.11(13)
C(5)-C(6)-N(1)-C(2)	1.15(14)	O(4)-C(7)-C(8)-C(8)#1	176.23(11)
		O(3)-C(7)-C(8)-C(8)#1	3.10(14)

Symmetry transformations used to generate equivalent atoms: #1 -x+1,-y+1,-z
Source: By the author.

Table A7 - Calculated potentials for form S.

Cocrystal	Synthon/Interaction	Intermolecular Potential (kcal/mol)
	homodimer NO/ON 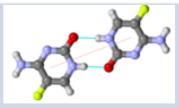	-7,6
	OH•••O2 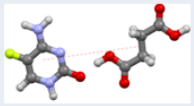	-5,5
Form S 5FC-Succinic Acid	Homodimer NN/NN 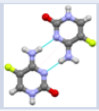	-4,9
	π•••π 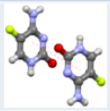	-4,9
	N4H•••O 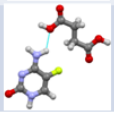	-4,4

Source: By the author.

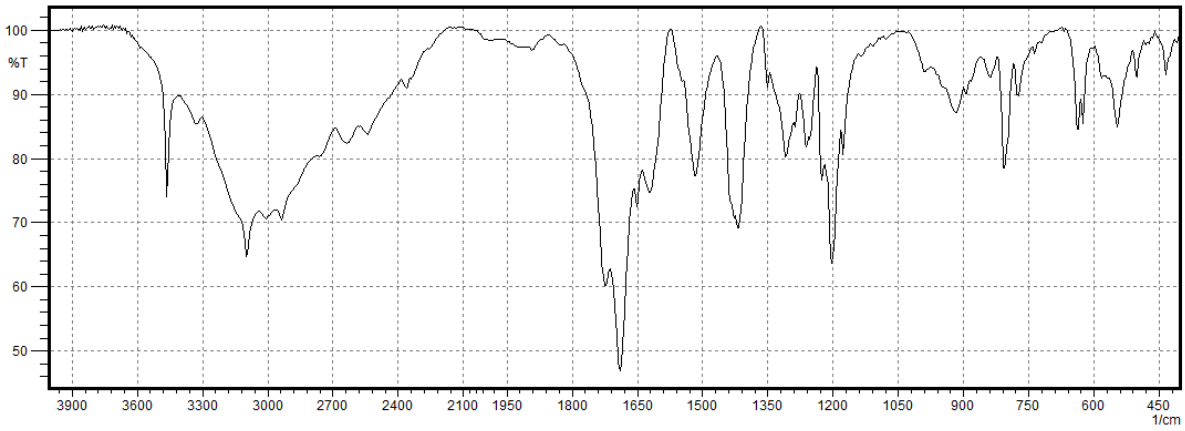

Figure A1 - IR spectrum of Form S.
Source: By the author.

B. CO-CRYSTAL OF 5-FC WITH ADIPIC ACID

Table B1 - Crystal data and structure refinement for the co-crystal of 5-FC with adipic acid.

Empirical formula	$C_7 H_9 F N_3 O_3$	
Formula weight	202.17	
Temperature	100.0 (2) K	
Wavelength	0.71073 Å	
Crystal system, space group	Triclinic, $P\bar{1}$	
Unit cell dimensions	a = 5.2742(5)Å	α= 86.411(6)º
	b = 6.6650(7)Å	β = 80.757(6)º
	c = 12.8441(13)Å	γ= 71.970(6)º
Volume	423.72(7) A^3	
Z, Calculated density	2, 1.585 Mg/m^3	
Absorption coefficient	0.139 mm^{-1}	
F(000)	210	
Crystal size	0.28 x 0.17 x 0.13 mm	
θ range for data collection	3.21 to 25.80 deg.	
Limiting indices	$-6\leq h\leq 6$, $-8\leq k\leq 8$, $-15\leq l\leq 15$	
Reflections collected / unique	6153 / 1624 [$R_{(int)}$ = 0.0280]	
Completeness to θ= 25.80	99.4 %	
Max. and min. transmission	0.9822 and 0.9622	
Refinement method	Full-matrix least-squares on F^2	
Data / restraints / parameters	1624 / 0 / 127	
Goodness-of-fit on F^2	1.112	
Final R indices [I>2σ(I)]	R_1 = 0.0506, wR_2 = 0.1380	
R indices (all data)	R_1 = 0.0590, wR_2 = 0.1436	
Largest diff. peak and hole	0.546 and -0.478 $e.A^{-3}$	

Source: By the author.

Table B2 - Atomic coordinates (x 10^4) and equivalent isotropic displacement parameters (A^2 x 10^3) for the co-crystal of 5-FC with adipic acid. U(eq) is defined as one third of the trace of the orthogonalized Uij tensor.

	x	y	z	U(eq)
C(2)	6131(4)	1930(3)	4831(2)	14(1)
C(4)	3088(4)	3680(3)	3705(2)	15(1)
C(5)	5037(4)	2768(3)	2823(2)	16(1)
C(6)	7453(4)	1465(3)	2969(2)	18(1)
N(1)	7981(4)	1051(3)	3972(1)	16(1)
N(3)	3669(3)	3232(3)	4686(1)	15(1)
N(41)	688(4)	4965(3)	3557(2)	18(1)
O(21)	6800(3)	1485(2)	5736(1)	17(1)
F(51)	4358(3)	3254(2)	1844(1)	23(1)
C(7)	5115(5)	7853(4)	1611(2)	22(1)
C(8)	7046(7)	7343(5)	601(2)	49(1)
C(9)	9060(5)	5247(4)	505(2)	30(1)
O(3)	6305(3)	7247(3)	2460(1)	20(1)
O(4)	2736(3)	8749(3)	1653(1)	36(1)

Source: By the author.

Table B3 - Bond lengths [Å] and angles [º] for the co-crystal of 5-FC with adipic acid.

C(2)-O(21)	1.259(3)	C(5)-F(51)	1.355(2)
C(2)-N(3)	1.354(3)	C(6)-N(1)	1.355(3)
C(2)-N(1)	1.377(3)	C(7)-O(4)	1.205(3)
C(4)-N(41)	1.326(3)	C(7)-O(3)	1.324(3)
C(4)-N(3)	1.337(3)	C(7)-C(8)	1.501(3)
C(4)-C(5)	1.427(3)	C(8)-C(9)	1.468(4)
C(5)-C(6)	1.336(3)	C(9)-C(9)#1	1.488(5)
O(21)-C(2)-N(3)	122.06(19)	C(5)-C(6)-N(1)	118.0(2)
O(21)-C(2)-N(1)	118.22(18)	C(6)-N(1)-C(2)	122.32(18)
N(3)-C(2)-N(1)	119.71(19)	C(4)-N(3)-C(2)	119.44(18)
N(41)-C(4)-N(3)	119.75(19)	O(4)-C(7)-O(3)	123.1(2)
N(41)-C(4)-C(5)	120.1(2)	O(4)-C(7)-C(8)	123.9(2)
N(3)-C(4)-C(5)	120.11(19)	O(3)-C(7)-C(8)	113.0(2)
C(6)-C(5)-F(51)	121.48(19)	C(9)-C(8)-C(7)	118.1(2)
C(6)-C(5)-C(4)	120.4(2)	C(8)-C(9)-C(9)#1	117.6(3)
F(51)-C(5)-C(4)	118.17(18)		

Symmetry transformations used to generate equivalent atoms: #1 -x+2,-y+1,-z

Source: By the author.

Table B4 - Anisotropic displacement parameters ($Å^2 \times 10^3$). The anisotropic displacement factor exponent takes the form: $-2\pi^2 [h^2 a^{*2} U_{11} + ... + 2 h k a^* b^* U_{12}]$

	U11	U22	U33	U23	U13	U12
C(2)	13(1)	14(1)	16(1)	-1(1)	-1(1)	-3(1)
C(4)	13(1)	14(1)	18(1)	-1(1)	-3(1)	-4(1)
C(5)	16(1)	21(1)	12(1)	1(1)	-3(1)	-6(1)
C(6)	15(1)	19(1)	17(1)	-3(1)	3(1)	-4(1)
N(1)	10(1)	17(1)	18(1)	0(1)	-1(1)	0(1)
N(3)	12(1)	15(1)	17(1)	-1(1)	-2(1)	-2(1)
N(41)	13(1)	23(1)	15(1)	-1(1)	-3(1)	1(1)
O(21)	14(1)	19(1)	16(1)	-1(1)	-4(1)	0(1)
F(51)	21(1)	32(1)	13(1)	0(1)	-4(1)	-2(1)
C(7)	20(1)	22(1)	17(1)	-1(1)	-4(1)	3(1)
C(8)	48(2)	48(2)	17(1)	7(1)	9(1)	26(2)
C(9)	29(1)	25(1)	21(1)	3(1)	7(1)	5(1)
O(3)	14(1)	26(1)	15(1)	-2(1)	-1(1)	2(1)
O(4)	17(1)	50(1)	27(1)	-5(1)	-6(1)	11(1)

Source: By the author.

Table B5 - Hydrogen coordinates ($\times 10^4$) and isotropic displacement parameters ($Å^2 \times 10^3$).

	x	y	z	U(eq)
H(6)	8735	860	2399	21
H(1)	9527	208	4075	19
H(41A)	-489	5507	4090	22
H(41B)	307	5257	2928	22
H(8A)	5993	7517	29	59
H(8B)	8003	8387	491	59
H(9A)	8107	4201	622	35
H(9B)	10131	5077	1070	35
H(3)	5155	7646	3066	30

Source: By the author.

Table B6 - Torsion angles [º] for the co-crystal of 5-FC with adipic acid.

N(41)-C(4)-C(5)-C(6)	-179.7(2)
N(3)-C(4)-C(5)-C(6)	-0.2(3)
N(41)-C(4)-C(5)-F(51)	0.0(3)
N(3)-C(4)-C(5)-F(51)	179.56(18)
F(51)-C(5)-C(6)-N(1)	-179.84(18)
C(4)-C(5)-C(6)-N(1)	-0.1(3)
C(5)-C(6)-N(1)-C(2)	-0.4(3)
O(21)-C(2)-N(1)-C(6)	-179.00(19)
N(3)-C(2)-N(1)-C(6)	1.1(3)
N(41)-C(4)-N(3)-C(2)	-179.53(18)
C(5)-C(4)-N(3)-C(2)	0.9(3)
O(21)-C(2)-N(3)-C(4)	178.75(18)
N(1)-C(2)-N(3)-C(4)	-1.4(3)
O(4)-C(7)-C(8)-C(9)	-136.8(3)
O(3)-C(7)-C(8)-C(9)	44.2(4)
C(7)-C(8)-C(9)-C(9)#1	179.3(3)

Symmetry transformations used to generate equivalent atoms: #1 -x+2,-y+1,-z

Source: By the author.

Table B7 - Calculated potentials for form A.

Cocrystal	Synthon/Interaction	Intermolecular Potential (kcal/mol)
	homodimer NO/ON 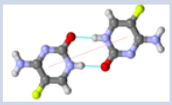	-8,1
	OH•••O2 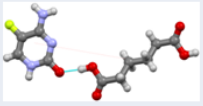	-6,0
Form A 5FC-Adipic Acid	π•••π 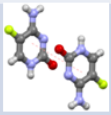	-5,6
	Homodimer NN/NN 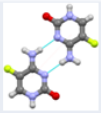	-5,1
	N4H•••O 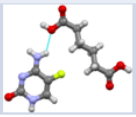	-4,2

Source: By the author.

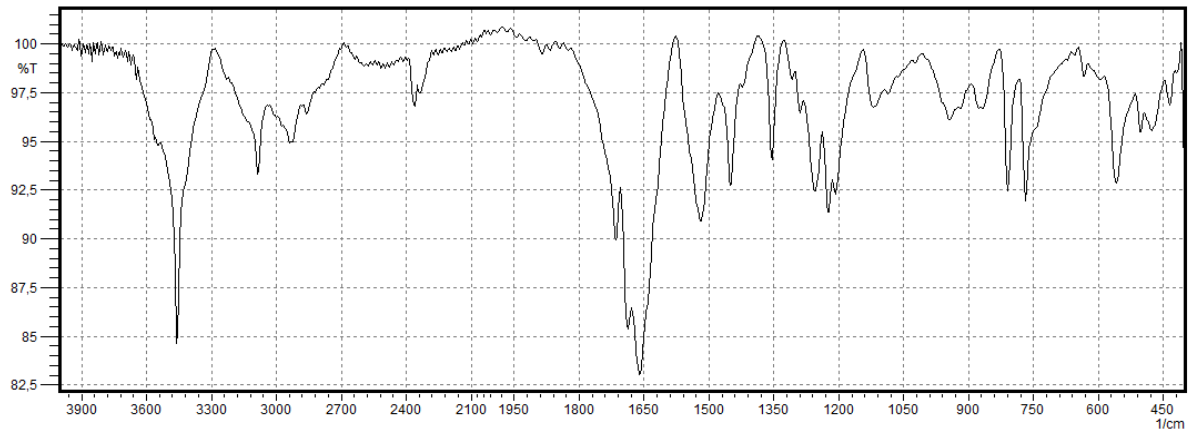

Figure B1 - IR spectrum of Form A.
Source: By the author.

C. CO-CRYSTAL OF 5-FC WITH TEREPHTALIC ACID

Table C1 - Crystal data and structure refinement for the co-crystal of 5-FC with terephtalic acid.

Empirical formula	$C_8 H_7 F N_3 O_3$
Formula weight	212.17
Temperature	100.0(2) K
Wavelength	0.71073 Å
Crystal system, space group	Triclinic, $P\bar{1}$
Unit cell dimensions	a = 3.6265(3) Å α = 107.812(5)º b = 9.5274(8) Å β = 92.036(4)º c = 13.7902(12) Å γ = 96.844(4)º
Volume	449.09(7) A^3
Z, Calculated density	2, 1.569 Mg/m^3
Absorption coefficient	0.135 mm^{-1}
F(000)	218
Crystal size	0.27 x 0.10 x 0.04 mm
θ range for data collection	1.56 to 30.24 deg.
Limiting indices	$-4\leq h\leq 4$, $-13\leq k\leq 13$, $-19\leq l\leq 19$
Reflections collected / unique	7867 / 2602 [$R_{(int)}$ = 0.0302]
Completeness to θ = 27.50	99.2 %
Refinement method	Full-matrix least-squares on F^2
Data / restraints / parameters	2602 / 0 / 136
Goodness-of-fit on F^2	1.074
Final R indices [I>2σ (I)]	R_1 = 0.0449, wR_2 = 0.1131
R indices (all data)	R_1 = 0.0607, wR_2 = 0.1216
Largest diff. peak and hole	0.427 and -0.293 $e.A^{-3}$

Source: By the author.

Table C2 - Atomic coordinates (x 10^4) and equivalent isotropic displacement parameters (A^2 x 10^3) for the co-crystal of 5-FC with terephtalic acid. U(eq) is defined as one third of the trace of the orthogonalized Uij tensor.

	x	y	z	U(eq)
C(2)	8252(4)	1909(2)	4807(1)	13(1)
C(4)	7015(4)	3337(2)	3764(1)	12(1)
C(5)	8023(4)	2210(2)	2907(1)	14(1)
C(6)	9047(4)	959(2)	3020(1)	13(1)
F(51)	7850(3)	2428(1)	1983(1)	22(1)
N(1)	9159(4)	819(1)	3974(1)	13(1)
N(3)	7135(3)	3157(1)	4690(1)	13(1)
N(41)	5929(4)	4555(1)	3643(1)	15(1)
O(21)	8498(3)	1705(1)	5665(1)	18(1)
C(7)	3271(4)	6992(2)	1917(1)	13(1)
C(8)	4159(4)	5943(2)	930(1)	12(1)
C(9)	5511(4)	6531(2)	183(1)	14(1)
C(10)	3644(4)	4406(2)	745(1)	14(1)
O(3)	2416(3)	6340(1)	2618(1)	19(1)
O(4)	3347(3)	8316(1)	2060(1)	19(1)

Source: By the author.

Table C3 - Bond lengths [Å] and angles [º] for the co-crystal of 5-FC with terephtalic acid.

C(2)-O(21)	1.2590(18)	C(6)-N(1)	1.3622(18)
C(2)-N(3)	1.3533(19)	C(7)-O(4)	1.2126(18)
C(2)-N(1)	1.3721(18)	C(7)-O(3)	1.3263(18)
C(4)-N(41)	1.3239(19)	C(7)-C(8)	1.4944(19)
C(4)-N(3)	1.3396(19)	C(8)-C(9)	1.392(2)
C(4)-C(5)	1.4250(19)	C(8)-C(10)	1.395(2)
C(5)-C(6)	1.340(2)	C(9)-C(10)#1	1.3858(19)
C(5)-F(51)	1.3535(17)	C(10)-C(9)#1	1.3858(19)
O(21)-C(2)-N(3)	121.97(13)	C(6)-N(1)-C(2)	121.99(13)
O(21)-C(2)-N(1)	118.03(13)	C(4)-N(3)-C(2)	119.62(12)
N(3)-C(2)-N(1)	120.00(13)	O(4)-C(7)-O(3)	123.51(13)
N(41)-C(4)-N(3)	120.02(13)	O(4)-C(7)-C(8)	122.78(13)
N(41)-C(4)-C(5)	120.05(13)	O(3)-C(7)-C(8)	113.71(12)
N(3)-C(4)-C(5)	119.93(13)	C(9)-C(8)-C(10)	120.01(13)
C(6)-C(5)-F(51)	121.41(13)	C(9)-C(8)-C(7)	118.43(13)
C(6)-C(5)-C(4)	120.35(13)	C(10)-C(8)-C(7)	121.55(13)
F(51)-C(5)-C(4)	118.23(13)	C(10)#1-C(9)-C(8)	120.19(13)
C(5)-C(6)-N(1)	118.08(13)	C(9)#1-C(10)-C(8)	119.80(13)

Symmetry transformations used to generate equivalent atoms: #1 -x+1,-y+1,-z

Source: By the author.

Table C4 - Anisotropic displacement parameters ($Å^2$ x 10^3). The anisotropic displacement factor exponent takes the form: $-2\pi^2[h^2 a^{*2} U_{11} + ... + 2 h k a^* b^* U_{12}]$

	U11	U22	U33	U23	U13	U12
C(2)	14(1)	12(1)	13(1)	2(1)	2(1)	4(1)
C(4)	10(1)	12(1)	14(1)	4(1)	0(1)	1(1)
C(5)	18(1)	14(1)	10(1)	4(1)	2(1)	3(1)
C(6)	15(1)	13(1)	11(1)	2(1)	2(1)	3(1)
F(51)	36(1)	20(1)	11(1)	7(1)	5(1)	11(1)

continues

continuation

N(1)	18(1)	11(1)	11(1)	3(1)	2(1)	6(1)
N(3)	15(1)	11(1)	12(1)	3(1)	2(1)	5(1)
N(41)	21(1)	13(1)	13(1)	4(1)	2(1)	6(1)
O(21)	31(1)	16(1)	11(1)	4(1)	5(1)	11(1)
C(7)	13(1)	16(1)	11(1)	3(1)	1(1)	4(1)
C(8)	11(1)	14(1)	11(1)	3(1)	1(1)	4(1)
C(9)	16(1)	12(1)	13(1)	2(1)	2(1)	3(1)
C(10)	15(1)	15(1)	12(1)	5(1)	2(1)	4(1)
O(3)	33(1)	15(1)	10(1)	4(1)	6(1)	9(1)
O(4)	29(1)	13(1)	17(1)	3(1)	7(1)	6(1)

Source: By the author.

Table C5 - Hydrogen coordinates (x 10^4) and isotropic displacement parameters (Å^2 x 10^3).

	x	y	z	U(eq)
H(6)	9663	209	2463	16
H(1)	9891	58	4103	20
H(41A)	5300	5231	4159	18
H(41B)	5852	4671	3048	18
H(9)	5848	7555	307	17
H(10)	2736	4011	1242	16
H(3)	2214	7079	3240	28

Source: By the author.

Table C6 - Torsion angles [º] for the maleate of 5-FC.

N(41)-C(4)-C(5)-C(6)	-178.54(14)
N(3)-C(4)-C(5)-C(6)	0.9(2)
N(41)-C(4)-C(5)-F(51)	0.3(2)
N(3)-C(4)-C(5)-F(51)	179.70(13)
F(51)-C(5)-C(6)-N(1)	179.95(13)
C(4)-C(5)-C(6)-N(1)	-1.3(2)
C(5)-C(6)-N(1)-C(2)	0.2(2)
O(21)-C(2)-N(1)-C(6)	-178.62(13)
N(3)-C(2)-N(1)-C(6)	1.3(2)
N(41)-C(4)-N(3)-C(2)	-179.95(14)
C(5)-C(4)-N(3)-C(2)	0.6(2)
O(21)-C(2)-N(3)-C(4)	178.24(14)
N(1)-C(2)-N(3)-C(4)	-1.7(2)
O(4)-C(7)-C(8)-C(9)	7.0(2)
O(3)-C(7)-C(8)-C(9)	-172.67(13)
O(4)-C(7)-C(8)-C(10)	-172.61(15)
O(3)-C(7)-C(8)-C(10)	7.7(2)
C(10)-C(8)-C(9)-C(10)#1	-0.1(2)
C(7)-C(8)-C(9)-C(10)#1	-179.78(14)
C(9)-C(8)-C(10)-C(9)#1	0.1(2)
C(7)-C(8)-C(10)-C(9)#1	179.77(14)

Symmetry transformations used to generate equivalent atoms: #1 -x+1,-y+1,-z

Source: By the author.

Table C7 - Calculated potentials for form T.

Cocrystal	Synthon/Interaction	Intermolecular Potential (kcal/mol)
	π•••π T/T 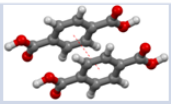	-9,6
	Homodimer NO/ON 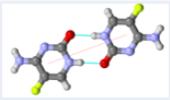	-8,2
Form T 5FC-Terephtalic Acid	π•••π 5FC/5FC 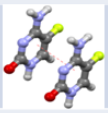	-7,6
	OH•••O2 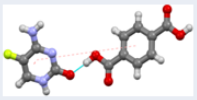	-6,5
	Homodimer NN/NN 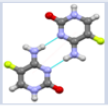	-5,0
	N4H•••O 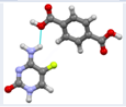	-4,3

Source: By the author.

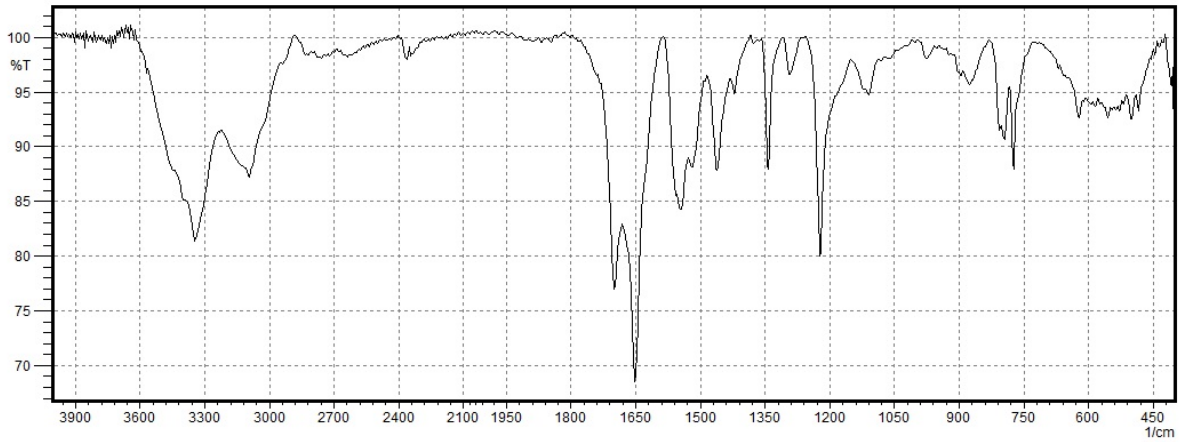

Figure C1 - IR spectrum of Form T.
Source: By the author.

D. CO-CRYSTAL OF 5-FC WITH MALIC ACID

Table D1 - Crystal data and structure refinement for the co-crystal of 5-FC with malic acid.

Empirical formula	$C_8 H_{10} F N_3 O_6$
Formula weight	263.19
Temperature	293(2) K
Wavelength	0.71073 Å
Crystal system, space group	Monoclinic, *C* 2/c
Unit cell dimensions	*a* = 20.8980(4)Å
	b = 14.8590(9)Å β = 107.178(3)º
	c = 7.2440(11)Å
Volume	2149.1(4) A^3
Z, Calculated density	8, 1.627 Mg/m^3
Absorption coefficient	0.150 mm^{-1}
F(000)	1088
Crystal size	0.270 x 0.080 x 0.050 mm
θ range for data collection	3.132 to 27.489 deg.
Limiting indices	$-27\leq h\leq 27$, $-19\leq k\leq 19$, $-9\leq l\leq 9$
Reflections collected / unique	4716 / 2451 [$R_{(int)}$ = 0.0547]
Completeness to θ = 25.242	99.7 %
Refinement method	Full-matrix least-squares on F^2
Data / restraints / parameters	2451 / 0 / 167
Goodness-of-fit on F^2	1.012
Final R indices [I>2σ(I)]	R_1 = 0.0719, wR_2 = 0.1742
R indices (all data)	R_1 = 0.1620, wR_2 = 0.2266
Largest diff. peak and hole	0.466 and -0.221 $e.A^{-3}$

Source: By the author.

Table D2 - Atomic coordinates (x 10^4) and equivalent isotropic displacement parameters (A^2 x 10^3) for the co-crystal of 5-FC with malic acid. U(eq) is defined as one third of the trace of the orthogonalized Uij tensor.

	x	y	z	U(eq)
C(2)	44(2)	3608(3)	9974(5)	48(1)
C(4)	605(2)	2272(3)	9713(5)	49(1)
C(5)	1158(2)	2784(3)	9573(6)	56(1)
C(6)	1140(2)	3675(3)	9621(6)	62(1)
F(51)	1703(1)	2339(2)	9405(4)	87(1)
N(1)	580(2)	4088(2)	9810(5)	57(1)
N(3)	66(1)	2704(2)	9929(4)	49(1)
N(41)	606(2)	1387(2)	9610(5)	60(1)
O(21)	-456(1)	4025(2)	10143(4)	61(1)
C(7)	1058(2)	1028(3)	4789(6)	59(1)
C(8)	1684(2)	677(3)	4381(8)	72(1)
C(9)	2252(2)	1230(4)	5154(10)	103(2)
C(10)	2869(2)	1038(3)	4531(9)	71(1)
O(3)	977(2)	1881(2)	4462(6)	101(1)
O(4)	679(2)	565(2)	5280(5)	79(1)
O(5)	1777(2)	-245(2)	4659(5)	72(1)
O(6)	2868(2)	650(3)	3061(6)	91(1)
O(7)	3398(2)	1337(2)	5751(5)	85(1)

Source: By the author.

Table D3 - Bond lengths [Å] and angles [º] for the co-crystal of 5-FC with benzoic acid.

C(2)-O(21)	1.251(4)	N(41)-C(4)-N(3)	119.9(3)
C(2)-N(3)	1.346(5)	N(41)-C(4)-C(5)	121.3(3)
C(2)-N(1)	1.362(4)	N(3)-C(4)-C(5)	118.8(3)
C(4)-N(41)	1.317(5)	C(6)-C(5)-F(51)	121.5(3)
C(4)-N(3)	1.346(4)	C(6)-C(5)-C(4)	120.4(3)
C(4)-C(5)	1.412(5)	F(51)-C(5)-C(4)	118.0(4)
C(5)-C(6)	1.324(6)	C(5)-C(6)-N(1)	119.0(3)
C(5)-F(51)	1.354(4)	C(2)-N(1)-C(6)	121.7(3)
C(6)-N(1)	1.363(5)	C(2)-N(3)-C(4)	121.0(3)
C(7)-O(4)	1.181(4)	O(4)-C(7)-O(3)	124.4(4)
C(7)-O(3)	1.291(5)	O(4)-C(7)-C(8)	123.5(4)
C(7)-C(8)	1.517(5)	O(3)-C(7)-C(8)	112.0(3)
C(8)-O(5)	1.390(5)	O(5)-C(8)-C(9)	116.7(4)
C(8)-C(9)	1.417(6)	O(5)-C(8)-C(7)	113.7(3)
C(9)-C(10)	1.514(6)	C(9)-C(8)-C(7)	113.2(4)
C(10)-O(6)	1.210(5)	C(8)-C(9)-C(10)	117.4(4)
C(10)-O(7)	1.274(5)	O(6)-C(10)-O(7)	123.6(4)
O(21)-C(2)-N(3)	122.2(3)	O(6)-C(10)-C(9)	124.9(5)
O(21)-C(2)-N(1)	118.8(3)	O(7)-C(10)-C(9)	111.5(5)
N(3)-C(2)-N(1)	119.1(3)		

Source: By the author.

Table D4 - Anisotropic displacement parameters ($Å^2 \times 10^3$). The anisotropic displacement factor exponent takes the form: $-2\pi^2[h^2 a^{*2} U_{11} + ... + 2 h k a^* b^* U_{12}]$.

	U11	U22	U33	U23	U13	U12
C(2)	45(2)	46(2)	56(2)	1(2)	17(2)	1(2)
C(4)	46(2)	49(2)	54(2)	-1(2)	16(2)	3(2)
C(5)	43(2)	52(2)	78(3)	-6(2)	27(2)	5(2)
C(6)	47(2)	59(3)	86(3)	-4(2)	27(2)	-6(2)
F(51)	58(2)	67(2)	151(2)	-10(2)	52(2)	5(1)
N(1)	48(2)	44(2)	82(2)	0(2)	26(2)	0(1)
N(3)	43(2)	40(2)	65(2)	1(1)	19(2)	2(1)
N(41)	53(2)	44(2)	85(2)	-3(2)	24(2)	2(2)
O(21)	47(2)	47(2)	93(2)	-3(1)	28(2)	3(1)
C(7)	54(2)	47(2)	81(3)	3(2)	30(2)	2(2)
C(8)	66(3)	45(2)	121(4)	16(2)	51(3)	8(2)
C(9)	62(3)	68(3)	194(6)	-36(4)	61(4)	-11(2)
C(10)	57(3)	44(2)	118(4)	-10(3)	37(3)	-4(2)
O(3)	82(2)	54(2)	197(4)	29(2)	86(3)	18(2)
O(4)	65(2)	53(2)	134(3)	4(2)	54(2)	-1(1)
O(5)	65(2)	51(2)	109(2)	7(2)	41(2)	3(1)
O(6)	63(2)	101(3)	113(3)	-25(2)	32(2)	-21(2)
O(7)	64(2)	92(3)	110(3)	-26(2)	44(2)	-19(2)

Source: By the author.

Table D5 - Hydrogen coordinates (x 10^4) and isotropic displacement parameters (Å^2 x 10^3).

	x	y	z	U(eq)
H(6)	1503	4013	9528	74
H(1)	511	4743	9829	99(16)
H(41A)	1012	969	9526	72
H(41B)	224	992	9638	72
H(8)	1587	751	2981	87
H(9A)	2377	1185	6551	124
H(9B)	2121	1849	4819	124
H(3)	560	2134	4540	150(20)
H(5)	2097	-312	5503	180(40)
H(7)	3818	1288	5384	130(20)

Source: By the author.

Table D6 - Torsion angles [º] for the co-crystal of 5-FC with malic acid.

N(41)-C(4)-C(5)-C(6)	177.9(4)
N(3)-C(4)-C(5)-C(6)	-1.1(6)
N(41)-C(4)-C(5)-F(51)	-2.6(6)
N(3)-C(4)-C(5)-F(51)	178.4(3)
F(51)-C(5)-C(6)-N(1)	-179.4(3)
C(4)-C(5)-C(6)-N(1)	0.1(6)
O(21)-C(2)-N(1)-C(6)	-180.0(4)
N(3)-C(2)-N(1)-C(6)	-0.7(5)
C(5)-C(6)-N(1)-C(2)	0.8(6)
O(21)-C(2)-N(3)-C(4)	178.9(3)
N(1)-C(2)-N(3)-C(4)	-0.4(5)
N(41)-C(4)-N(3)-C(2)	-177.8(3)
C(5)-C(4)-N(3)-C(2)	1.2(5)
O(4)-C(7)-C(8)-O(5)	-0.7(7)
O(3)-C(7)-C(8)-O(5)	-178.1(4)
O(4)-C(7)-C(8)-C(9)	-137.0(5)
O(3)-C(7)-C(8)-C(9)	45.6(6)
O(5)-C(8)-C(9)-C(10)	55.9(7)
C(7)-C(8)-C(9)-C(10)	-169.2(4)
C(8)-C(9)-C(10)-O(6)	22.8(8)
C(8)-C(9)-C(10)-O(7)	-157.3(5)

Source: By the author.

NOTE: *It was not possible to measure the IR spectrum of Form M due the instability of the cocrystal.*

Table D7 - Calculated potentials for form M.

Cocrystal	Synthon/Interaction	Intermolecular Potential (kcal/mol)
	Heterodimer NCN/OCO 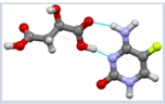	-9,7
	Homodimer NO/ON 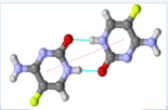	-9,1
Form M 5FC-Malic Acid	π•••π 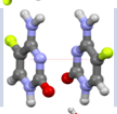	-8,2
	N4H•••O 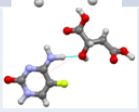	-8,1
	Dimer M 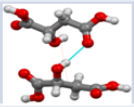	-7,1
	OH•••O2 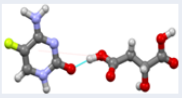	-6,6

Source: By the author.

E. CO-CRYSTAL OF 5-FC WITH BENZOIC ACID

Table E1 - Crystal data and structure refinement for the co-crystal of 5-FC with benzoic acid.

Empirical formula	$C_{11}\ H_{10}\ F\ N_3\ O_3$	
Formula weight	251.22	
Temperature	293(2) K	
Wavelength	0.71073 Å	
Crystal system	Monoclinic	
Space group	$P\ 2_1/n$	
Unit cell dimensions	a = 9.0565(2) Å	α = 90°
	b = 5.4318(2) Å	β = 92.8700(10)°
	c = 22.8887(8) Å	γ = 90°
Volume	1124.55(6) $Å^3$	
Z, Density (calculated)	4, 1.484 Mg/m^3	
Absorption coefficient	0.121 mm^{-1}	
F(000)	520	
Crystal size	0.230 x 0.190 x 0.130 mm^3	
θ range for data collection	3.409 to 26.384°.	
Index ranges	-11≤h≤11, -6≤k≤6, -28≤l≤28	
Reflections collected	4334	
Independent reflections	2306 [$R_{(int)}$ = 0.0252]	
Completeness to θ = 25.242°	99.9 %	
Refinement method	Full-matrix least-squares on F^2	
Data / restraints / parameters	2306 / 0 / 179	

continues

continuation

Goodness-of-fit on F^2	0.943
Final R indices [I>2σ(I)]	R_1 = 0.0488, wR_2 = 0.1286
R indices (all data)	R_1 = 0.0814, wR_2 = 0.1545
Largest diff. peak and hole	0.310 and -0.191 e.Å^{-3}

Source: By the author.

Table E2 - Atomic coordinates (x 10^4) and equivalent isotropic displacement parameters (A^2 x 10^3) for the co-crystal of 5-FC with benzoic acid. U(eq) is defined as one third of the trace of the orthogonalized Uij tensor.

	x	y	z	U(eq)
F(51)	5171(1)	6183(2)	1217(1)	66(1)
O(21)	1030(1)	2383(3)	-247(1)	55(1)
O(3)	6140(2)	6622(3)	4071(1)	60(1)
O(4)	3895(2)	5667(3)	3699(1)	69(1)
N(3)	3381(2)	2146(3)	155(1)	44(1)
N(41)	5710(2)	1994(4)	598(1)	56(1)
N(1)	1757(2)	5324(3)	399(1)	47(1)
C(4)	4402(2)	3091(3)	531(1)	44(1)
C(8)	5222(2)	8850(4)	3249(1)	47(1)
C(13)	6318(2)	10617(3)	3329(1)	53(1)
C(5)	4088(2)	5247(4)	851(1)	45(1)
C(6)	2777(2)	6331(4)	780(1)	47(1)
C(2)	2041(2)	3224(3)	90(1)	43(1)
C(7)	5001(2)	6893(3)	3689(1)	49(1)
C(9)	4315(2)	8896(5)	2744(1)	64(1)
C(12)	6498(3)	12384(4)	2908(1)	64(1)
C(10)	4506(3)	10687(5)	2323(1)	74(1)
C(11)	5595(3)	12433(5)	2411(1)	72(1)

Source: By the author.

Table E3 - Bond lengths [Å] and angles [º] for the co-crystal of 5-FC with benzoic acid.

F(51)-C(5)	1.356(2)	N(1)-C(2)	1.374(2)
O(21)-C(2)	1.253(2)	N(1)-H(1)	0.88(2)
O(3)-C(7)	1.326(2)	C(4)-C(5)	1.418(3)
O(3)-H(3)	0.81(3)	C(8)-C(9)	1.385(3)
O(4)-C(7)	1.205(2)	C(8)-C(13)	1.386(3)
N(3)-C(4)	1.335(2)	C(8)-C(7)	1.484(3)
N(3)-C(2)	1.349(2)	C(13)-C(12)	1.375(3)
N(41)-C(4)	1.327(2)	C(5)-C(6)	1.329(3)
N(41)-H(41A)	0.89(2)	C(9)-C(10)	1.386(3)
N(41)-H(41B)	0.94(2)	C(12)-C(11)	1.368(4)
N(1)-C(6)	1.353(2)	C(10)-C(11)	1.376(4)
C(7)-O(3)-H(3)	115.9(19)	N(41)-C(4)-C(5)	120.78(18)
C(4)-N(3)-C(2)	119.64(16)	N(3)-C(4)-C(5)	120.05(15)
C(4)-N(41)-H(41A)	117.1(15)	C(9)-C(8)-C(13)	119.17(19)
C(4)-N(41)-H(41B)	122.2(13)	C(9)-C(8)-C(7)	119.02(18)
H(41A)-N(41)-H(41B)	121(2)	C(13)-C(8)-C(7)	121.81(19)
C(6)-N(1)-C(2)	121.89(16)	C(12)-C(13)-C(8)	120.1(2)
C(6)-N(1)-H(1)	118.0(14)	C(6)-C(5)-F(51)	121.60(17)
C(2)-N(1)-H(1)	120.1(14)	C(6)-C(5)-C(4)	120.26(17)
N(41)-C(4)-N(3)	119.17(17)		

continues

continuation

F(51)-C(5)-C(4)	118.12(15)	O(4)-C(7)-C(8)	123.34(19)
C(5)-C(6)-N(1)	118.50(17)	O(3)-C(7)-C(8)	113.56(17)
O(21)-C(2)-N(3)	122.30(16)	C(8)-C(9)-C(10)	120.3(2)
O(21)-C(2)-N(1)	118.06(16)	C(11)-C(12)-C(13)	120.6(2)
N(3)-C(2)-N(1)	119.65(17)	C(11)-C(10)-C(9)	119.7(2)
O(4)-C(7)-O(3)	123.09(18)	C(12)-C(11)-C(10)	120.2(2)

Source: By the author.

Table E4 - Anisotropic displacement parameters ($Å^2 \times 10^3$). The anisotropic displacement factor exponent takes the form: $-2\pi^2 [h^2 a^{*2} U_{11} + ... + 2 h k a^* b^* U_{12}]$

	U11	U22	U33	U23	U13	U12
F(51)	59(1)	66(1)	72(1)	-22(1)	-18(1)	11(1)
O(21)	44(1)	55(1)	65(1)	-20(1)	-8(1)	9(1)
O(3)	56(1)	58(1)	66(1)	23(1)	-8(1)	-12(1)
O(4)	54(1)	69(1)	83(1)	15(1)	1(1)	-21(1)
N(3)	40(1)	42(1)	51(1)	-7(1)	-2(1)	7(1)
N(41)	45(1)	55(1)	68(1)	-16(1)	-10(1)	14(1)
N(1)	40(1)	47(1)	55(1)	-9(1)	-2(1)	12(1)
C(4)	42(1)	43(1)	46(1)	1(1)	3(1)	7(1)
C(8)	42(1)	48(1)	52(1)	8(1)	6(1)	3(1)
C(13)	51(1)	48(1)	62(1)	7(1)	5(1)	-1(1)
C(5)	45(1)	45(1)	43(1)	-7(1)	-6(1)	4(1)
C(6)	50(1)	41(1)	50(1)	-9(1)	-1(1)	7(1)
C(2)	42(1)	40(1)	46(1)	-6(1)	1(1)	6(1)
C(7)	44(1)	47(1)	57(1)	3(1)	4(1)	-4(1)
C(9)	52(1)	71(1)	68(1)	6(1)	-2(1)	-4(1)
C(12)	65(1)	51(1)	77(2)	14(1)	14(1)	-4(1)
C(10)	70(2)	90(2)	61(1)	15(1)	-4(1)	16(1)
C(11)	82(2)	65(2)	70(2)	24(1)	17(1)	15(1)

Source: By the author.

Table E5 - Hydrogen coordinates ($\times 10^4$) and isotropic displacement parameters ($Å^2 \times 10^3$).

	x	y	z	U(eq)
H(13)	6932	10608	3667	64
H(6)	2565	7751	987	56
H(9)	3576	7720	2687	76
H(12)	7240	13558	2962	76
H(10)	3900	10709	1983	88
H(11)	5718	13649	2131	86
H(1)	880(30)	6050(40)	357(10)	59(6)
H(41A)	6350(30)	2630(40)	860(11)	65(7)
H(41B)	5960(20)	610(40)	375(10)	57(6)
H(3)	6120(30)	5420(50)	4275(11)	76(8)

Source: By the author.

Table E6 - Torsion angles [º] for the co-crystal of 5-FC with benzoic acid.

C(2)-N(3)-C(4)-N(41)	178.94(17)	C(6)-N(1)-C(2)-O(21)	178.87(18)
C(2)-N(3)-C(4)-C(5)	-1.4(3)	C(6)-N(1)-C(2)-N(3)	-1.4(3)
C(9)-C(8)-C(13)-C(12)	-0.1(3)	C(9)-C(8)-C(7)-O(4)	-16.8(3)
C(7)-C(8)-C(13)-C(12)	179.25(18)	C(13)-C(8)-C(7)-O(4)	163.80(19)
N(41)-C(4)-C(5)-C(6)	179.89(19)	C(9)-C(8)-C(7)-O(3)	163.23(19)
N(3)-C(4)-C(5)-C(6)	0.2(3)	C(13)-C(8)-C(7)-O(3)	-16.2(3)
N(41)-C(4)-C(5)-F(51)	1.5(3)	C(13)-C(8)-C(9)-C(10)	0.1(3)
N(3)-C(4)-C(5)-F(51)	-178.22(17)	C(7)-C(8)-C(9)-C(10)	-179.3(2)
F(51)-C(5)-C(6)-N(1)	178.74(17)	C(8)-C(13)-C(12)-C(11)	0.5(3)
C(4)-C(5)-C(6)-N(1)	0.4(3)	C(8)-C(9)-C(10)-C(11)	-0.4(4)
C(2)-N(1)-C(6)-C(5)	0.2(3)	C(13)-C(12)-C(11)-C(10)	-0.8(4)
C(4)-N(3)-C(2)-O(21)	-178.34(17)	C(9)-C(10)-C(11)-C(12)	0.8(4)
C(4)-N(3)-C(2)-N(1)	2.0(3)		

Source: By the author.

Table E7 - Calculated potentials for form B.

Cocrystal	Synthon/Interaction	Intermolecular Potential (kcal/mol)
	Homodimer NO/ON 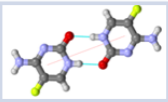	-8,5
	π•••π 5FC/5FC 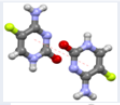	-7,3
Form B 5FC-Benzoic Acid	Homodimer NN/NN 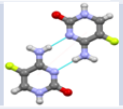	-5,5
	OH•••O2 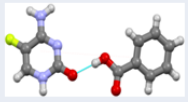	-4,6
	π•••π 5FC/B 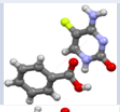	-5,0
	N4H•••O 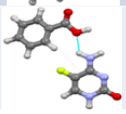	-3,9

Source: By the author.

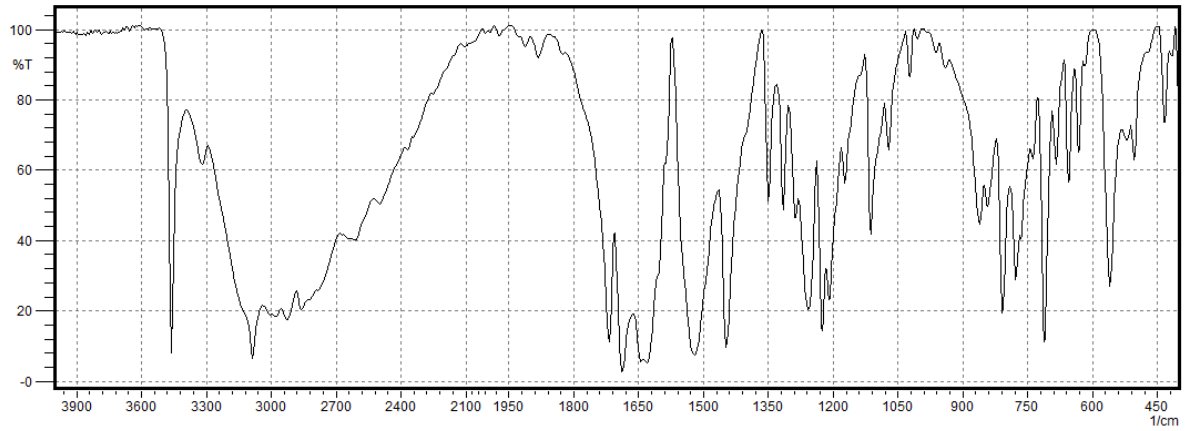

Figure E1 - IR spectrum of Form B.
Source: By the author.

F. CO-CRYSTAL OF 5-FC WITH 5-FLUOROURACIL

Table F1 - Crystal data and structure refinement for the co-crystal of 5-FC with 5-FU.

Empirical formula	$C_8 H_7 F_2 N_5 O_3$
Formula weight	259.19
Temperature	293(2) K
Wavelength	1.54178 Å
Crystal system	Monoclinic
Space group	*P* 2_1/c
Unit cell dimensions	*a* = 15.0176(3) Å
	b = 3.56040(10) Å β= 138.2820(10)°
	c = 27.3113(4) Å
Volume	971.78(4) $Å^3$
Z, Density (calculated)	4, 1.772 Mg/m^3
Absorption coefficient	1.439 mm^{-1}
F(000)	528
Crystal size	0.240 x 0.030 x 0.030 mm^3
θ range for data collection	3.332 to 66.685°.
Index ranges	-17<=h<=17, -4<=k<=3, -31<=l<=32
Reflections collected	5219
Independent reflections	1628 [$R_{(int)}$ = 0.0284]
Completeness to θ = 66.500°	95.0 %
Refinement method	Full-matrix least-squares on F^2
Data / restraints / parameters	1628 / 0 / 169
Goodness-of-fit on F^2	1.069
Final R indices [I>2σ(I)]	R_1 = 0.0312, wR_2 = 0.0841
R indices (all data)	R_1 = 0.0359, wR_2 = 0.0879
Largest diff. peak and hole	0.199 and -0.247 e.$Å^{-3}$

Source: By the author.

Table F2 - Atomic coordinates (x 10^4) and equivalent isotropic displacement parameters (A^2 x 10^3) for the co-crystal of 5-FC with 5-FU. U(eq) is defined as one third of the trace of the orthogonalized Uij tensor.

	x	y	z	U(eq)
F(51)	4724(1)	7775(3)	2789(1)	20(1)
F(51')	1137(1)	3010(3)	2897(1)	24(1)
O(41')	3718(1)	663(3)	4073(1)	20(1)
O(21')	3671(1)	4364(4)	5657(1)	23(1)
N(41)	3382(1)	4396(4)	2974(1)	20(1)
N(3)	1470(1)	3875(4)	1714(1)	17(1)
N(1)	1567(1)	5901(4)	930(1)	17(1)
O(21)	-316(1)	3349(3)	466(1)	20(1)
N(1')	1759(1)	4983(4)	4422(1)	18(1)
N(3')	3673(1)	2471(4)	4858(1)	16(1)
C(4)	2748(2)	4953(4)	2293(1)	16(1)
C(2)	882(1)	4349(5)	1034(1)	16(1)
C(6)	2859(2)	7085(5)	1507(1)	16(1)
C(5)	3445(1)	6688(5)	2183(1)	16(1)
C(2')	3066(1)	3974(5)	5023(1)	17(1)
C(4')	3101(2)	2040(4)	4167(1)	16(1)
C(5')	1737(2)	3305(5)	3583(1)	18(1)
C(6')	1099(2)	4666(5)	3715(1)	18(1)

Source: By the author.

Table F3 - Bond lengths [Å] and angles [º] for the co-crystal of 5-FC with 5-FU.

F(51)-C(5)	1.3545(17)	N(1)-C(2)	1.3718(19)
F(51')-C(5')	1.3483(17)	O(21)-C(2)	1.2664(18)
O(41')-C(4')	1.2326(19)	N(1')-C(2')	1.3659(19)
O(21')-C(2')	1.2221(18)	N(1')-C(6')	1.3664(18)
N(41)-C(4)	1.327(2)	N(3')-C(4')	1.379(2)
N(41)-H(41A)	0.86(2)	N(3')-C(2')	1.3916(19)
N(41)-H(41B)	0.85(2)	C(4)-C(5)	1.427(2)
N(3)-C(4)	1.342(2)	C(6)-C(5)	1.332(2)
N(3)-C(2)	1.3445(19)	C(4')-C(5')	1.437(2)
N(1)-C(6)	1.364(2)	C(5')-C(6')	1.340(2)
C(4)-N(41)-H(41A)	117.5(13)	C(6)-C(5)-F(51)	122.05(13)
C(4)-N(41)-H(41B)	120.9(13)	C(6)-C(5)-C(4)	120.54(14)
H(41A)-N(41)-H(41B)	120.9(18)	F(51)-C(5)-C(4)	117.37(13)
C(4)-N(3)-C(2)	118.61(12)	O(21')-C(2')-N(1')	123.70(13)
C(6)-N(1)-C(2)	121.69(13)	O(21')-C(2')-N(3')	121.87(13)
C(2')-N(1')-C(6')	123.53(12)	N(1')-C(2')-N(3')	114.43(12)
C(4')-N(3')-C(2')	126.60(13)	O(41')-C(4')-N(3')	122.09(14)
N(41)-C(4)-N(3)	120.50(14)	O(41')-C(4')-C(5')	124.35(14)
N(41)-C(4)-C(5)	119.22(14)	N(3')-C(4')-C(5')	113.56(13)
N(3)-C(4)-C(5)	120.28(13)	C(6')-C(5')-F(51')	122.15(14)
O(21)-C(2)-N(3)	121.72(13)	C(6')-C(5')-C(4')	121.88(14)
O(21)-C(2)-N(1)	117.26(13)	F(51')-C(5')-C(4')	115.97(13)
N(3)-C(2)-N(1)	121.01(13)	C(5')-C(6')-N(1')	119.94(13)
C(5)-C(6)-N(1)	117.79(13)		

Source: By the author.

Table F4 - Anisotropic displacement parameters ($Å^2 \times 10^3$). The anisotropic displacement factor exponent takes the form: $-2\pi^2[h^2 a^{*2} U_{11} + ... + 2 h k a^* b^* U_{12}]$

	U11	U22	U33	U23	U13	U12
F(51)	13(1)	26(1)	16(1)	-2(1)	10(1)	-3(1)
F(51')	19(1)	38(1)	15(1)	-1(1)	12(1)	2(1)
O(41')	19(1)	25(1)	21(1)	1(1)	17(1)	4(1)
O(21')	19(1)	32(1)	16(1)	-1(1)	14(1)	2(1)
N(41)	16(1)	28(1)	16(1)	-1(1)	11(1)	-3(1)
N(3)	15(1)	18(1)	18(1)	0(1)	12(1)	0(1)
N(1)	15(1)	21(1)	16(1)	1(1)	12(1)	-1(1)
O(21)	14(1)	27(1)	16(1)	-1(1)	11(1)	-4(1)
N(1')	16(1)	22(1)	18(1)	-1(1)	14(1)	2(1)
N(3')	12(1)	20(1)	15(1)	2(1)	10(1)	3(1)
C(4)	17(1)	13(1)	19(1)	1(1)	14(1)	2(1)
C(2)	16(1)	14(1)	20(1)	0(1)	14(1)	1(1)
C(6)	16(1)	14(1)	21(1)	1(1)	14(1)	0(1)
C(5)	12(1)	16(1)	17(1)	-2(1)	10(1)	-1(1)
C(2')	17(1)	15(1)	19(1)	0(1)	14(1)	0(1)
C(4')	19(1)	14(1)	20(1)	-1(1)	15(1)	-3(1)
C(5')	18(1)	20(1)	15(1)	-2(1)	12(1)	-2(1)
C(6')	14(1)	19(1)	17(1)	2(1)	11(1)	0(1)

Source: By the author.

Table F5 - Hydrogen coordinates ($\times 10^4$) and isotropic displacement parameters ($Å^2 \times 10^3$).

	x	y	z	U(eq)
H(1)	1172	6134	490	20
H(1')	1328	5866	4493	21
H(3')	4489	1736	5224	20
H(6)	3316	8136	1432	19
H(6')	207	5393	3325	21
H(41A)	2964(19)	3170(60)	3027(10)	27
H(41B)	4210(20)	4930(60)	3343(11)	27

Source: By the author.

Table F6 - Torsion angles [º] for the co-crystal of 5-FC with 5-FU.

C(2)-N(3)-C(4)-N(41)	-177.27(15)
C(2)-N(3)-C(4)-C(5)	2.2(2)
C(4)-N(3)-C(2)-O(21)	179.13(15)
C(4)-N(3)-C(2)-N(1)	0.0(2)
C(6)-N(1)-C(2)-O(21)	179.62(14)
C(6)-N(1)-C(2)-N(3)	-1.2(2)
C(2)-N(1)-C(6)-C(5)	0.0(2)
N(1)-C(6)-C(5)-F(51)	179.90(14)
N(1)-C(6)-C(5)-C(4)	2.2(2)
N(41)-C(4)-C(5)-C(6)	176.09(15)
N(3)-C(4)-C(5)-C(6)	-3.4(2)
N(41)-C(4)-C(5)-F(51)	-1.7(2)
N(3)-C(4)-C(5)-F(51)	178.76(13)
C(6')-N(1')-C(2')-O(21')	177.61(16)

continues

continuation	
C(6')-N(1')-C(2')-N(3')	-1.8(2)
C(4')-N(3')-C(2')-O(21')	-177.40(15)
C(4')-N(3')-C(2')-N(1')	2.1(2)
C(2')-N(3')-C(4')-O(41')	-179.79(15)
C(2')-N(3')-C(4')-C(5')	-0.4(2)
O(41')-C(4')-C(5')-C(6')	177.69(16)
N(3')-C(4')-C(5')-C(6')	-1.7(2)
O(41')-C(4')-C(5')-F(51')	-1.8(2)
N(3')-C(4')-C(5')-F(51')	178.83(13)
F(51')-C(5')-C(6')-N(1')	-178.62(14)
C(4')-C(5')-C(6')-N(1')	2.0(3)
C(2')-N(1')-C(6')-C(5')	-0.1(2)

Source: By the author.

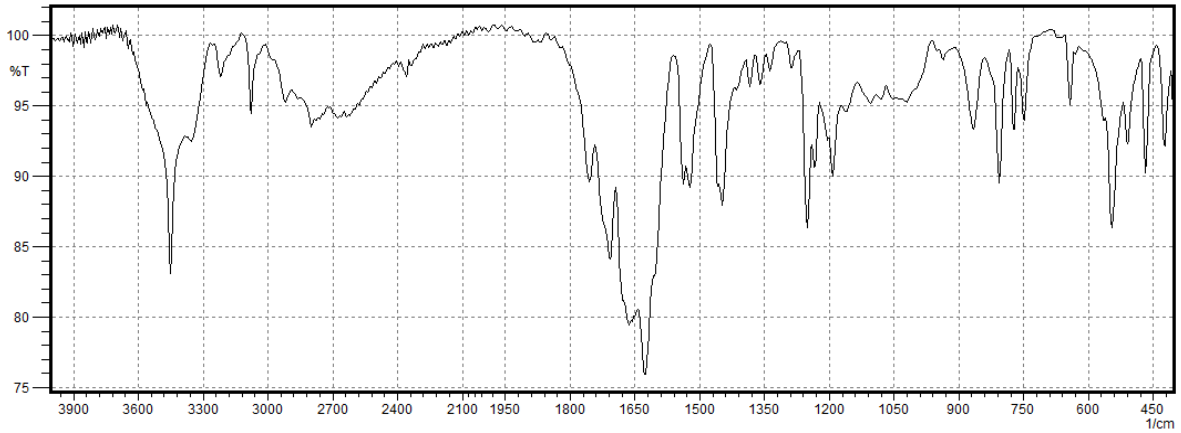

Figure F1 - IR spectrum of Form 5F.
Source: By the author.

Table S1 - Hydrogen-bonds geometry (Å,º) in crystal structures of Forms S, T, A, B, M and 5F.

Structure	Interaction	D…H(Å)	D...A(Å)	H...A(Å)	D-H...A(º)	Symmetry code
Form S	N41–H41B•••F51	1.030	2.731(1)	2.387	98.16	intramolecular
	N1–H1•••O21	1.030	2.870(1)	1.841	176.58	-x+1,-y,-z+2
	N41–H41B•••O3	1.030	2.898(1)	2.189	124.40	-x+1,-y+1,-z
	N41–H41A•••N3	1.030	2.971(1)	1.943	175.67	-x+2,-y+1,-z+1
	O3–H3•••O21	0.938	2.624(1)	1.694	170.85	x-1,+y,+z-1
Form A	N41–H41B•••F51	1.030	2.733(2)	2.375	99.01	intramolecular
	N1–H1•••O21	1.030	2.819(2)	1.793	173.8	-x+2,-y,-z+1
	N41–H41B•••O3	1.030	2.871(2)	2.171	123.49	x-1,+y,+z
	N41–H41A•••N3	1.030	2.963(2)	1.938	173.54	-x,-y+1,-z+1
	O3–H3•••O21	0.938	2.634(2)	1.699	173.89	-x+1,-y+1,-z+1
Form T	N41–H41B•••F51	1.030	2.729(1)	2.370	99.04	intramolecular
	N1–H1•••O21	1.030	2.818(2)	1.789	177.45	-x+2,-y,-z+1
	N41–H41B•••O3	1.030	2.893(2)	2.242	119.65	x, y, z
	N41–H41A•••N3	1.030	2.994(2)	1.974	169.85	-x+1,-y+1,-z+1
	O3–H3•••O21	0.938	2.586(1)	1.651	175	-x+1,-y+1,-z+1
Form M	N41–H41B•••F51	1.030	2.734(4)	2.513	91.09	intramolecular
	N1–H1•••O21	1.030	2.818(4)	1.790	174.99	-x,-y+1,-z+2
	N41–H41B•••O4	1.030	2.972(5)	1.976	162.01	-x,+y,-z+1/2+1
	N41–H41A•••O5	1.030	2.969(5)	1.943	174.09	x,-y,z+1/2
	O3-H3•••N3	0.938	2.647(5)	1.722	168.06	-x,+y,-z+1/2+1
	O5–H5•••O6	0.938	2.884(5)	1.959	168.45	x,-y,z+1/2
	O7–H7•••O21	0.938	2.618(5)	1.699	165.57	x+1/2,-y+1/2,z-1/2
Form B	N41–H41B•••F51	1.030	2.737(2)	2.346	101.01	intramolecular
	N1–H1•••O21	1.030	2.821(2)	1.791	178.50	-x,-y+1,-z
	N41–H41B•••O3	1.030	2.923(2)	2.250	121.49	-x+1/2+1,y-1/2,-z+1/2
	N41–H41A•••N3	1.030	2.974(2)	1.949	173.67	-x+1,-y,-z
	O3–H3•••O21	0.938	2.682(2)	1.745	178.69	x+1/2,-y+1/2,z+1/2
	C11-H11•••F51	1.080	3.415(3)	2.396	156.87	x,y+1,+z
	C13-H13•••F51	1.080	3.311(2)	2.553	126.55	-x+1/2+1,y-1/2,-z+1/2
Form 5F	N41–H41B•••F51	1.030	2.698(3)	2.347	98.41	intramolecular
	N41–H41A•••F51	1.030	3.256(3)	2.349	146.23	x, y, z
	N41–H41A•••O41’	1.030	2.963(3)	2.220	127.59	x, y, z
	N1–H1•••O21	1.030	2.728(2)	1.698	179.84	-x,-y+1,-z
	N1’–H1’•••O21	1.030	2.686(3)	1.667	169.59	-x,+y+1/2,-z+1/2
	N3’–H3’•••O41’	1.030	2.836(2)	1.821	167.59	-x+1,-y,-z+1
	N41–H41B•••O21’	1.030	3.009(1)	1.986	172.18	-x+1,-y+1,-z+1

Source: By the author.